

UNCLASSIFIED



AD NUMBER

AD-904 853

NEW LIMITATION CHANGE

TO

DISTRIBUTION STATEMENT - A

Approved for public release;
distribution is unlimited.

LIMITATION CODE: 1

FROM

DISTRIBUTION STATEMENT - B

Distribution authorized to U.S.
Gov't. agencies only.

LIMITATION CODE: 3

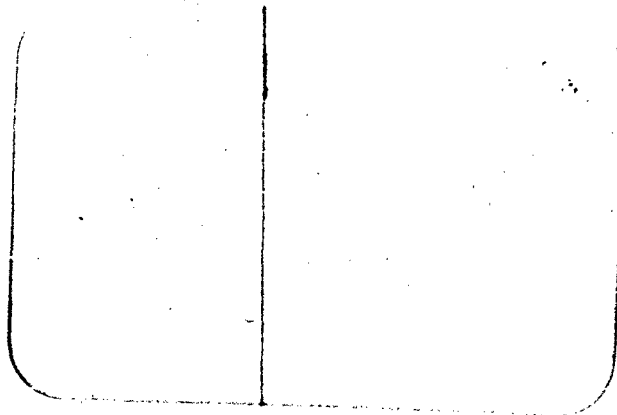
AUTHORITY

Cmdr., Naval Air Systems Command - NASC, via ltr dtd
Nov 27, 1973.

19990302122

THIS PAGE IS UNCLASSIFIED

AD904853



D D C
NOV 13 1972
RECEIVED
C

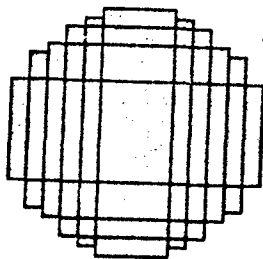
DISTRIBUTION LIMITED TO U.S.
GOVERNMENT AGENCIES ONLY;

- ☐ FOREIGN INFORMATION
- ☐ PROPRIETARY INFORMATION
- ☒ TEST AND EVALUATION
- ☐ CONTRACTOR PERFORMANCE EVALUATION

DATE: 11-7-72

OTHER REQUESTS FOR THIS DOCUMENT
MUST BE REFERRED TO COMMANDER,
NAVAL AIR SYSTEMS COMMAND, AAR-5017.4

Wash D. 90361



Technology Service Corporation

Technology Service Corporation

225 Santa Monica Boulevard
Santa Monica, California 90401
(213) 451-8778

ADAPTIVE FILTERING IN

AMTI RADAR

Final Report

TSC-PD-083-2

September 29, 1972

I. Bottlik
L. Brennan
G. Lank

DISSEMINATION LIMITED TO U.S.
GOVERNMENT AGENCIES ONLY;

EXCLUDED FROM AUTOMATIC
EXCLUDED FROM AUTOMATIC
X EXCLUDED FROM AUTOMATIC

EXCLUDED FROM AUTOMATIC EVALUATION

DATE: 11-7-72
EXCLUDED FROM THIS PROJECT
EXCLUDED FROM THIS PROJECT
EXCLUDED FROM THIS PROJECT

On

Contract N00019-72-C-0164

Submitted to

The NAVAL AIR SYSTEMS COMMAND

TABLE OF CONTENTS

	page
1. INTRODUCTION	1
2. ADAPTIVE FILTERS	3
3. AMTI PERFORMANCE OF ADAPTIVE FILTERS	8
3.1 PARAMETERS	9
3.2 TYPES OF PLOTS	12
3.3 DISCUSSION OF PERFORMANCE	13
4. SIMPLIFICATION OF ADAPTIVE FILTERS	74
5. SUGGESTED AREAS OF RESEARCH AND CONCLUSIONS	75
REFERENCES	77
APPENDICES:	
A. COMPUTATIONAL EQUATIONS	
B. GENERAL EFFECT OF ENVELOPE NORMALIZATION IN ADAPTIVE ARRAY CONTROL LOOPS	
C. MEAN STEADY-STATE OUTPUT CLUTTER - APPIEBAUM ARRAY	

1. INTRODUCTION

This final report presents the results of a 12-month study of adaptive filters for AMTI radar. The results are applicable to several types of radars, including AI and AEW systems. Adaptive systems, and adaptive filters in particular, sense the existing noise field and optimize a set of system parameters. In an adaptive filter, the filter weights and transfer functions are adjusted to maximize the output signal-to-clutter (plus receiver noise) ratio.

The clutter spectrum in an AMTI radar is a function of several variables including scan angle, radar velocity, antenna pattern, and angular distribution of clutter. Rain backscatter is an important component of clutter in higher frequency radars. Its location, mean radial velocity, and velocity spread due to wind shear are not generally known a priori. An adaptive filter senses all of these clutter properties and optimizes the filter response for detection of targets with a selected radial velocity. In most cases, a bank of adaptive filters will be required to cover the target doppler spectrum. The theory of adaptive filtering is discussed in Section 2 of this report.

During this study, a computer program was developed for the investigation of both the steady-state response and transient performance of adaptive AMTI filters. Provisions for both ground clutter and rain clutter were included. A variety of parameters are variables in this program, including: radar velocity, scan angle, target radial velocity, adaptive loop parameters, number of pulses processed coherently, and rain clutter properties (magnitude relative

to ground clutter, mean radial velocity, and spectral width). A large number of sample cases were run to develop some insight into the performance of adaptive filters and to uncover problem areas. Selected results are presented in Section 3 of this report.

The suitability of adaptive filters for future AMTI radars depends both on the performance of adaptive systems and on their complexity. Methods of reducing the complexity of adaptive control loops for filters (or adaptive array antennas) were also investigated during this study. A technique for reducing significantly the complexity of digital adaptive filters is discussed in Section 4 and in Appendix B of this report.

Suggested areas for further research on adaptive filters and conclusions of this study are presented in Section 5. A simplified and more accurate method of computing the control loop noise power in adaptive filters is contained in Appendix C.

2. ADAPTIVE FILTERS

Consider an airborne coherent pulsed radar designed to detect moving targets in a clutter background. Let V denote a column vector of the consecutive received signals from one range cell, $V_T = (v_1, v_2, \dots, v_K)$, where v_n is the complex video for the n^{th} sample and T denotes the transpose. An MTI filter output is obtained by forming the weighted sum of these v_n , $W_T V$, where W is a column vector of complex weights w_n . The filter response is determined by the w_n , which are chosen to maximize the output signal-to-interference ratio (S/C).

The interference (clutter plus receiver noise) power in the output is

$$C = E \left\{ |W_T V|^2 \right\} = W_T^* M W \quad (1)$$

where M is the covariance matrix of the interference process with elements

$$M_{mn} = E \left\{ v_m^* v_n \right\} \quad (2)$$

Both clutter and receiver noise (but not signal) are included in the computation of the covariance matrix. In these equations, $*$ denotes the complex conjugate and E the expectation or average. The output voltage samples v_n and weights w_n are complex quantities retaining both phase and amplitude information.

In designing a filter, some assumption must be made a priori concerning the target doppler frequency. Consider the case where a separate filter is synthesized for each of a set of target doppler frequencies, analogous to a

filter bank. Let S denote a column vector of signal phases for the K consecutive samples, $S_T = (1, e^{i\psi}, e^{i2\psi}, \dots, e^{i(K-1)\psi})$. A signal of amplitude A received from a target with doppler frequency f is represented by AS , with $\psi = 2\pi fT$, where T is the pulse repetition period. The corresponding signal voltage at the filter output is $AW_T S$ and the output S/C ratio is

$$\frac{S}{C} = \frac{|W_T S|^2}{W_T^* W_T} A^2 \quad (3)$$

In most cases of interest, the interference processes are Gaussian. The optimum detection algorithm for these cases is to form a maximum S/C filter and compare the signal amplitude at this filter output with a detection threshold [1]. The filter which maximizes S/C has weights [1] proportional to

$$W = M^{-1} S^* \quad (4)$$

An adaptive filter will now be described which senses the interference spectrum or covariance matrix M and generates a weight vector that approaches Eq. (4).

A K -pulse adaptive filter is implemented with K separate adaptive control loops, each generating one complex weight w_n , as illustrated in Figure 1. To cover all range cells in a pulsed radar, $K-1$ delay lines are required, each with a delay equal to the pulse repetition period. The operations indicated in Figure 1, and in the control loops illustrated in Figure 2, can be performed with either analog or digital circuitry. The control loops are identical except for the steering signals S_n^* , which are matched to the desired signal

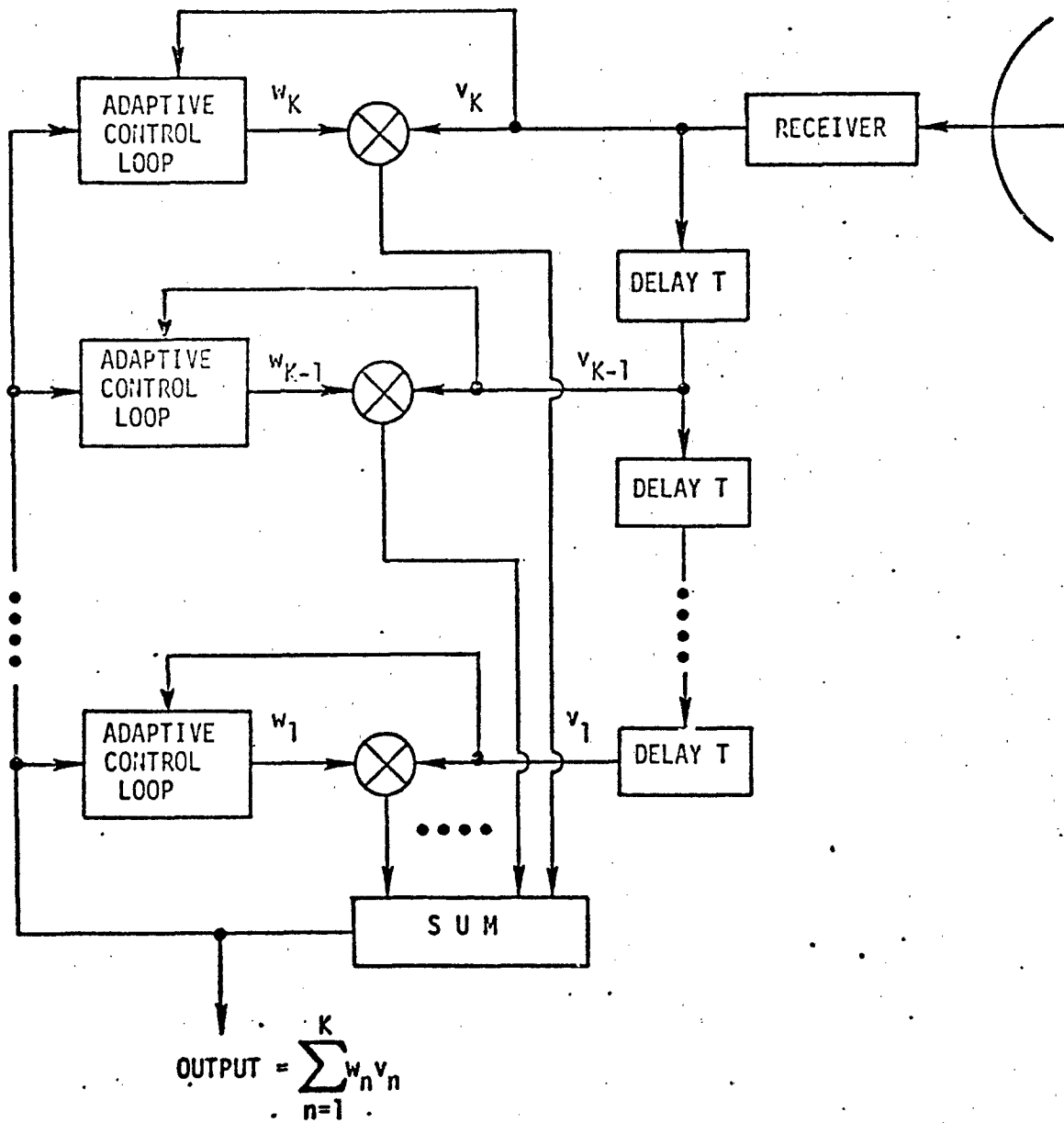


Figure 1. Block Diagram of Adaptive Filter

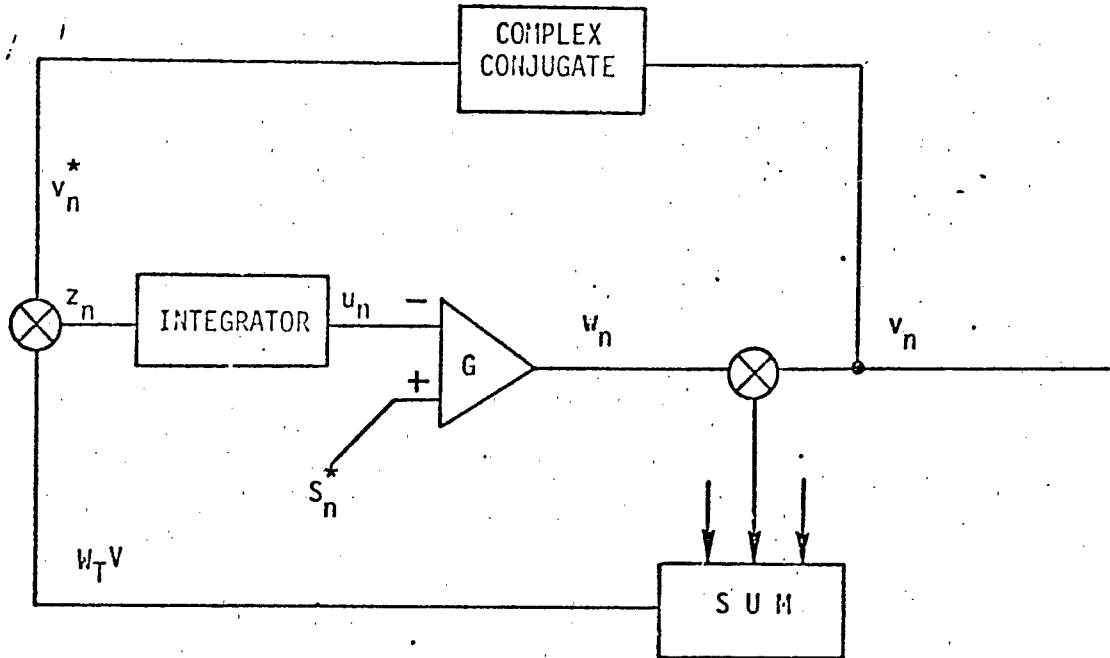


Figure 2. Adaptive Control Loop

doppler frequency. With low-pass filters employed as integrators in Figure 1, satisfying the equation

$$\tau \dot{u}_n + u_n = z_n \quad (5)$$

the weight vector satisfies the equation [2]

$$\frac{\tau}{G} \dot{W} + (M + I/G)W = S^* \quad (6)$$

where I is the identity matrix. When the gain G is large (relative to the eigenvalues of M), the weights approach the steady-state solution of Eq. (4).

The theory of adaptive filters is closely analogous to the theory of adaptive array antennas, which is detailed in [2]. Since the covariance matrix

M is Hermitian, the transient response of the system can be computed in normal coordinates. The effect of control loop noise in these systems has also been analyzed.^[2] A simplified and more exact derivation of the control loop noise equation is contained in Appendix C.

3. AMTI PERFORMANCE OF ADAPTIVE FILTERS

The basic criterion of performance used is the S/C (signal-to-clutter) ratio. Specifically we have set the input or unfiltered S/C ratio to one; hence our S/C ratio is actually the ratio of the output to the input S/C ratios. Some authors term this the MTI gain or improvement factor. The loop noise is not included in these calculations; however, it does not significantly affect them.

Another important criterion is the rate of convergence of the adaptive loops. To characterize this factor we have investigated the mean S/C ratio as a function of the number of independent samples, subject to the constraint that the time constant of the loops is chosen to give a constant loop noise factor ($\eta = 0.1$). The expected actual output under clutter conditions consists of two factors--one due to clutter and the other due to random variations in the filter weights (loop noise). The noise factor, η , is the ratio of the output due to loop noise to the output due to the clutter when the system has reached steady state. (For more detail see Appendices A and C.) The initial value of the weights has been chosen to be GS^* . This is independent of the clutter spectrum, optimum when only receiver noise is present, and is considered a reasonable design when the clutter is unknown.

There are many parameters which affect the performance of an adaptive system. We have chosen to keep some fixed (e.g., the antenna pattern) and have normalized others (see below). To depict the effect of all of these parameters, we have chosen a baseline set of values and then (for the most part) investigated the effect of varying just one of these parameters at one time.

The radar backscatter from rain has been modeled as a gaussian-shaped spectrum, its mean, variance, and power relative to the ground clutter being parameters. In the case of rain, the initial weights were not only chosen to be GS^* , but in some cases set equal to the mean steady-state value obtained under the corresponding no-rain condition. This latter initial value has been termed "rain onset." Interestingly (for the cases considered), only a slight improvement in the transient response takes place by using the latter initial values.

The maximum MTI gain shown in these curves is roughly 60 dB. This gain is limited by the sidelobe clutter spectrum. A sidelobe level of 29.6 dB, with a Dolph-Tschebycheff antenna pattern, was assumed in the model. The corresponding two-way sidelobe gain is roughly 60 dB below the maximum main beam antenna gain. This sidelobe level is representative of existing radar systems. Also, roughly 50 dB of MTI gain is adequate in most AMTI radars. In practice, the performance of an AMTI radar would typically be limited to 50 to 60 dB MTI gain by receiver noise. By assuming a lower sidelobe level, better MTI gain could be attributed to the adaptive filters. However, this would not be representative of typical radars.

3.1 PARAMETERS

V_R = mean rain velocity (relative to ground)

V_T = target velocity (relative to ground)

V_P = platform velocity (relative to ground)

λ = wavelength

f_r = pulse repetition frequency.

3.1.1 Antenna Pattern (Remains fixed throughout the plots depicted herein)

A Dolph-Tschebycheff design with elements spaced at $\lambda/2$. Identical receive and transmit patterns and zero gain in the reverse half-circle.

NEL = 30 = number of elements

SDLB = 29.6 dB = ratio of main beam peak to any sidelobe peak

BEAM(DEG) = 4.1 = beamwidth (in degrees) between 3 dB points.

3.1.2 Ground Clutter (Assumes independent gaussian stationary spatially homogeneous scatterers--clutter spectrum being caused by the moving radar platform)

NSC = 100 = number of equally spaced scatterers (over 180°) assumed in computing the covariance M

NP = 2,5,10,20 = number of pulses in the filter

ALFA = α = 1,2,10 = normalized platform velocity = $2V_p/\lambda f_r$

SCAN = ψ = 0(11.25)90°,45° = scan angle = angle between platform velocity and beam center (see Figure 3).

3.1.3 Rain Clutter (A gaussian-shaped spectrum)

RNM = μ = 0.1 = normalized mean = $2V_R/\lambda f_r$

RNS = σ = 0.01,0.05,0.1 = normalized standard deviation

RNP = ρ = 1,10 = ratio of total rain power to total clutter power. The total input power (rain + ground) is normalized to one.

3.1.4 Loop (Applebaum Array--see Figures 1 and 2)

GAIN = G = 10,10³,10⁶ = loop gain

ETA = η = 0.1 = noise factor = ratio of the output due to random variations in the weights to the output due to the clutter in the steady state. This and the gain determine the time constant of the loops.

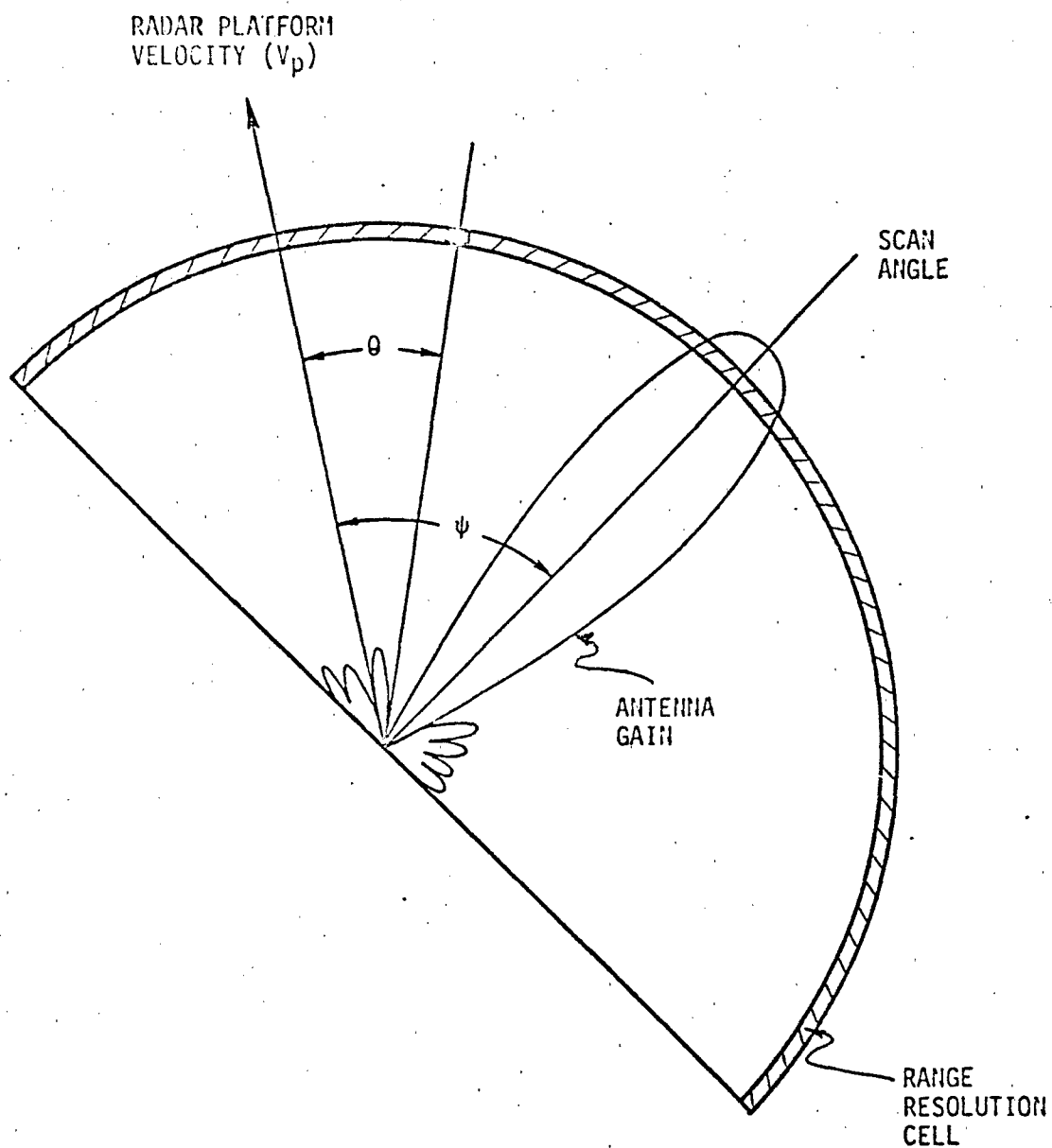


Figure 3. Coordinate System

3.1.5 Signal (Normalized to unit power, point source)

$$\begin{aligned} \text{BETA} = \beta &= 0(0.1)0.9, \underline{0.4} = \text{normalized target velocity (relative to} \\ &\quad \text{ground)} \\ &= 2V_T / \lambda f_r \text{ modulo } 1 \end{aligned}$$

$$\text{GAMMA} = \gamma = (\alpha \cos \psi + \beta) \text{ modulo } 1 = \text{design normalized doppler frequency for the filter.}$$

3.2 TYPES OF PLOTS

3.2.1 Transient Response

The S/C ratio (or MTI gain) is depicted vs. the number of independent samples. The initial value of the weights is chosen to be GS^* (where S^* is the steering signal which is independent of the clutter), which is considered a reasonable design when the clutter is unknown. The response at this initial value is shown by a small dash. Both the steady-state and optimum performance are depicted as straight lines. Due to the high base-line gain of 10^6 on most plots, the steady state and optimum merge into a single line. Since the noise factor, η , is kept fixed, these plots show the convergence rate of the loops at the same relative loop noise level. Please note the logarithmic "number of samples" scale.

3.2.2 Transient Response (Rain Onset)

Same as "Transient Response" except that the initial value of the weights is chosen to be the mean steady-state value for the corresponding no-rain condition. The small dash indicates the response at this initial value. Another small dash labeled "NO RAIN SS" is the steady-state response under the corresponding no-rain condition.

3.2.3 Clutter Spectrum

The "folded" (due to the pulse repetition frequency, f_r) spectrum of the clutter is depicted. When rain is present, it includes the contribution to the spectrum by the rain. It is normalized to unity (0 dB) total power.

3.2.4 Spectra-Filter, Clutter

Depicts two folded spectra on the same grid. One is the spectral response of the filter formed by the weights (easily distinguishable since it has one less peak than the number of pulses). It is normalized to 0 dB at the desired design frequency of γ . The other is the clutter spectrum as specified above.

3.2.5 Optimum Performance

Depicts the optimum S/C ratio (MTI gain) vs. the normalized target velocity (β). A number of curves are shown at various scan angles, ψ .

3.3 DISCUSSION OF PERFORMANCE

Very good steady-state performance (S/C ratio in the 50 to 60 dB range) is obtainable for all but extreme parameter values (just what these extreme values are is discernible from the detailed discussion below).

Reasonable convergence rate of the loops is also obtainable for most parameter values, i.e., in about 10^3 to 10^4 samples the mean response is within a few decibels of the steady state which is negligibly close to the optimum. This is for a noise factor of 0.1; hence the additional degradation of performance due to random fluctuations in the weights at this point is negligible.

Since the mean weights during adaptation are not equal to the steady-state weights, the loops form a biased estimate of the weights. This causes

rather slow convergence in some cases. The staircase-like convergence of the mean response (even on a logarithmic scale) indicates that there are long intervals of sampling when no significant improvement in the mean response takes place (whether the variance of the weights at this time is being significantly reduced has not yet been investigated). For example, for the baseline case (Figure 4) from 100 to 1000 samples, there is only about a 2 dB improvement.

For some extreme cases (very heavy rain) (Figure 44), the mean response even diverges (after almost achieving the steady-state value) to a value even less than the initial value (after about 30,000 samples) before again converging to the steady-state. This occurs when the average magnitude of the initial weights differs widely from the magnitude of the steady-state weights. The steady-state weights, $M^{-1}S^*$, tend to be large when the covariance matrix contains one or more very small eigenvalues. It might be preferable to have an unbiased estimator, i.e., one in which the mean magnitudes of the weights would always be comparable to the steady-state weights. In this case the effect of additional samples would be to adjust the relative magnitudes and phases of the weights, which would improve the response. Such estimators can be found--the problem is that they markedly increase the complexity of the calculations.

It is felt that better estimators than the investigated loops are possible; however, probably at an increased complexity. The investigated loops do however give a sufficiently good performance that is probably satisfactory for many applications. The simplicity of the loops then makes them a good overall design for some systems.

3.3.1 Base Line

The base line has those parameter values which are underlined in Section 3. Figure 4 shows the mean transient response with its characteristic staircase-like (even with a logarithmic abscissa) approach to the steady-state value. About 10^4 samples are seen to be required to complete adaptation. The duration of one sample is the radar (compressed) pulse length, typically around 1 microsecond.

Figures 5 through 10 show the filter response (of the mean value of the weights) as adaptation takes place. The clutter spectrum is superimposed on all of these figures. Initially (samples = 0) no specific attempt at suppressing the broad peak of the clutter spectrum is evident. As the number of samples increases, two main effects are discernible. The lobe peaks of the filter in the region of the clutter spectrum maximum are decreasing and more filter lobes are being squeezed into the extent of the clutter lobe (from 2 to 4 lobes). The main filter lobe which includes the selected target doppler frequency also widens a bit. This is believed to be a necessary consequence of narrowing the other lobes. A very slight shift in the peak of the main filter lobe may also be noted. This effect is more pronounced under more extreme conditions (e.g., see Figure 51).

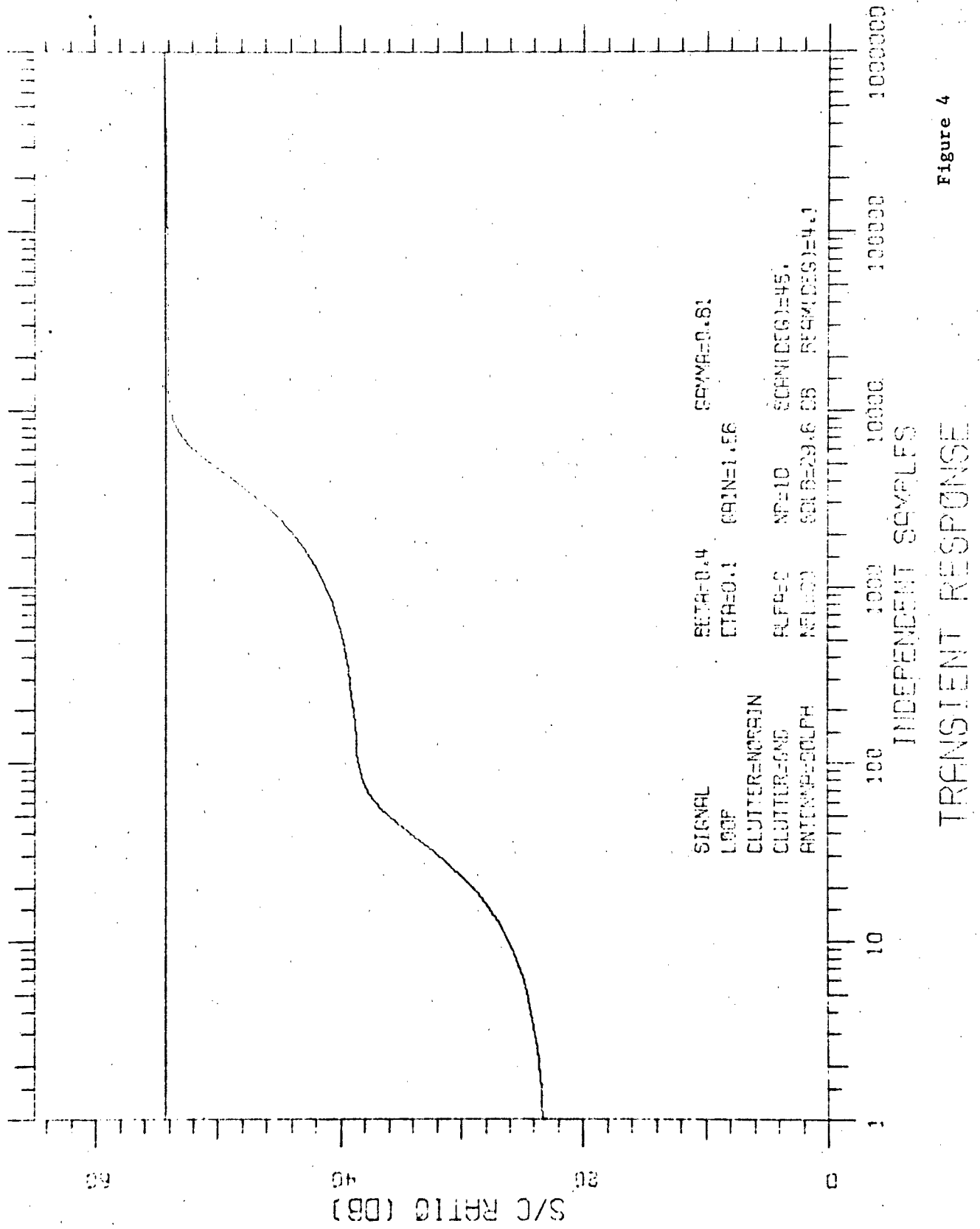


Figure 4

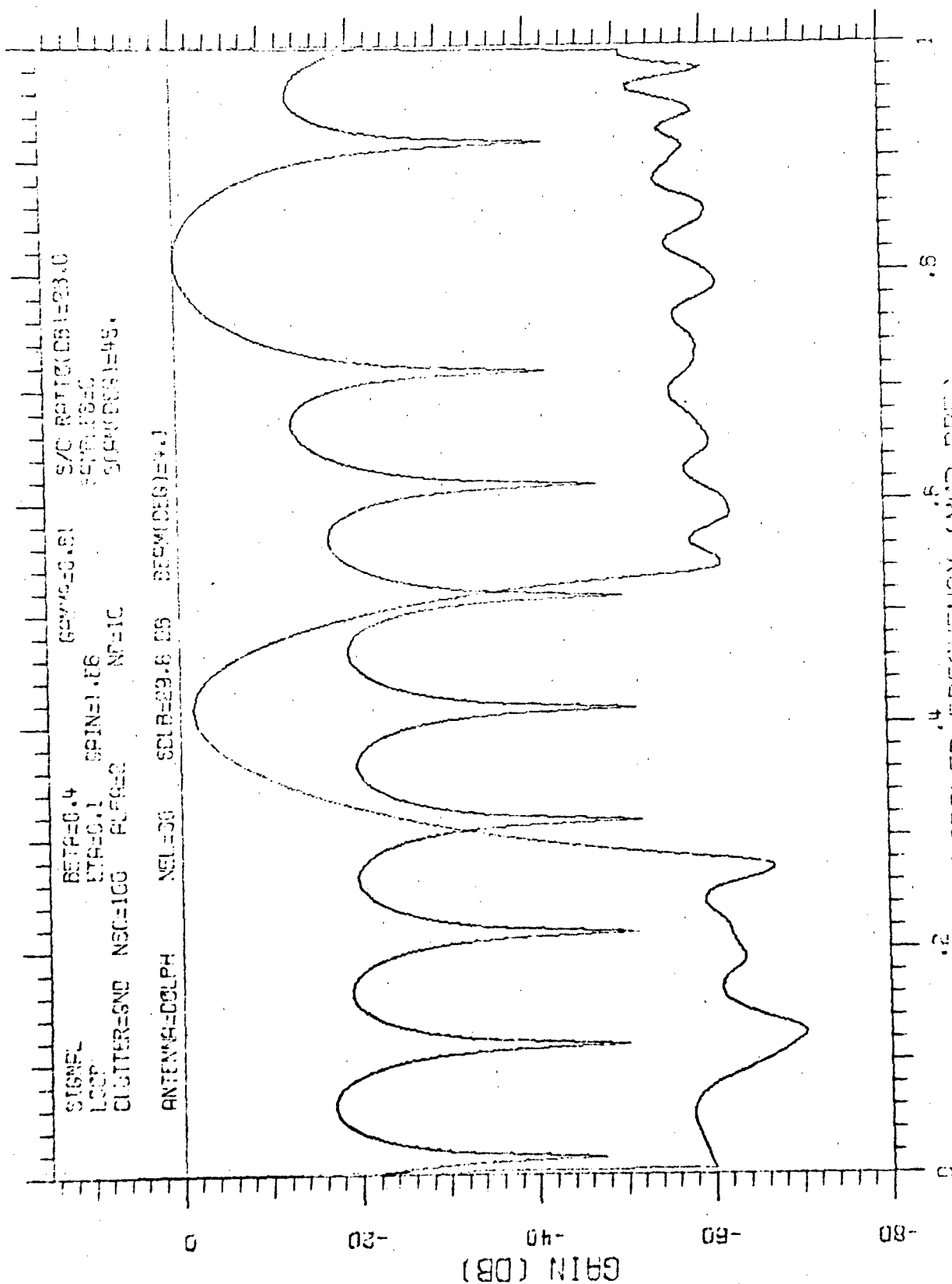


Figure 5

SPECTRA-FILTER, CLUTTER

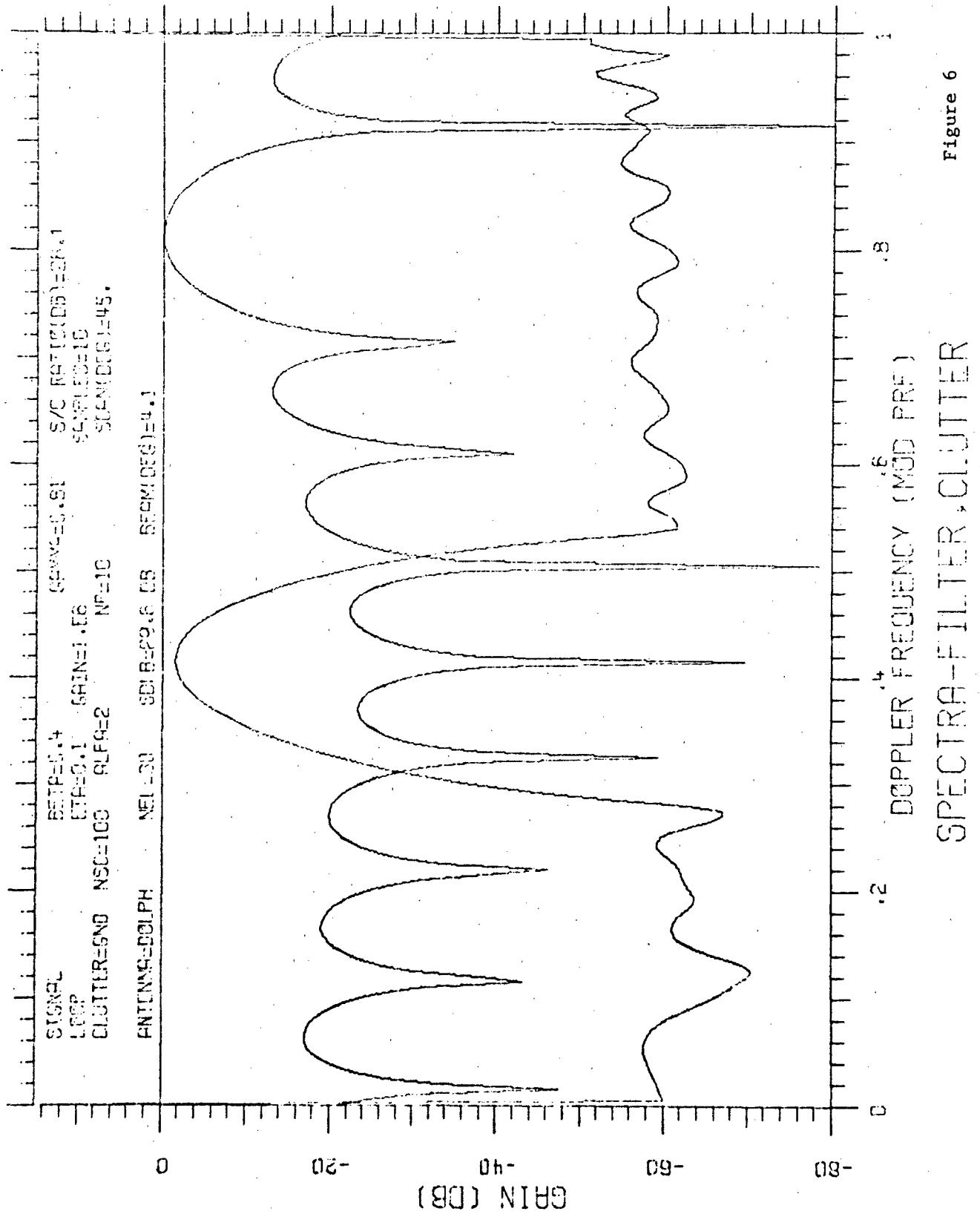


Figure 6

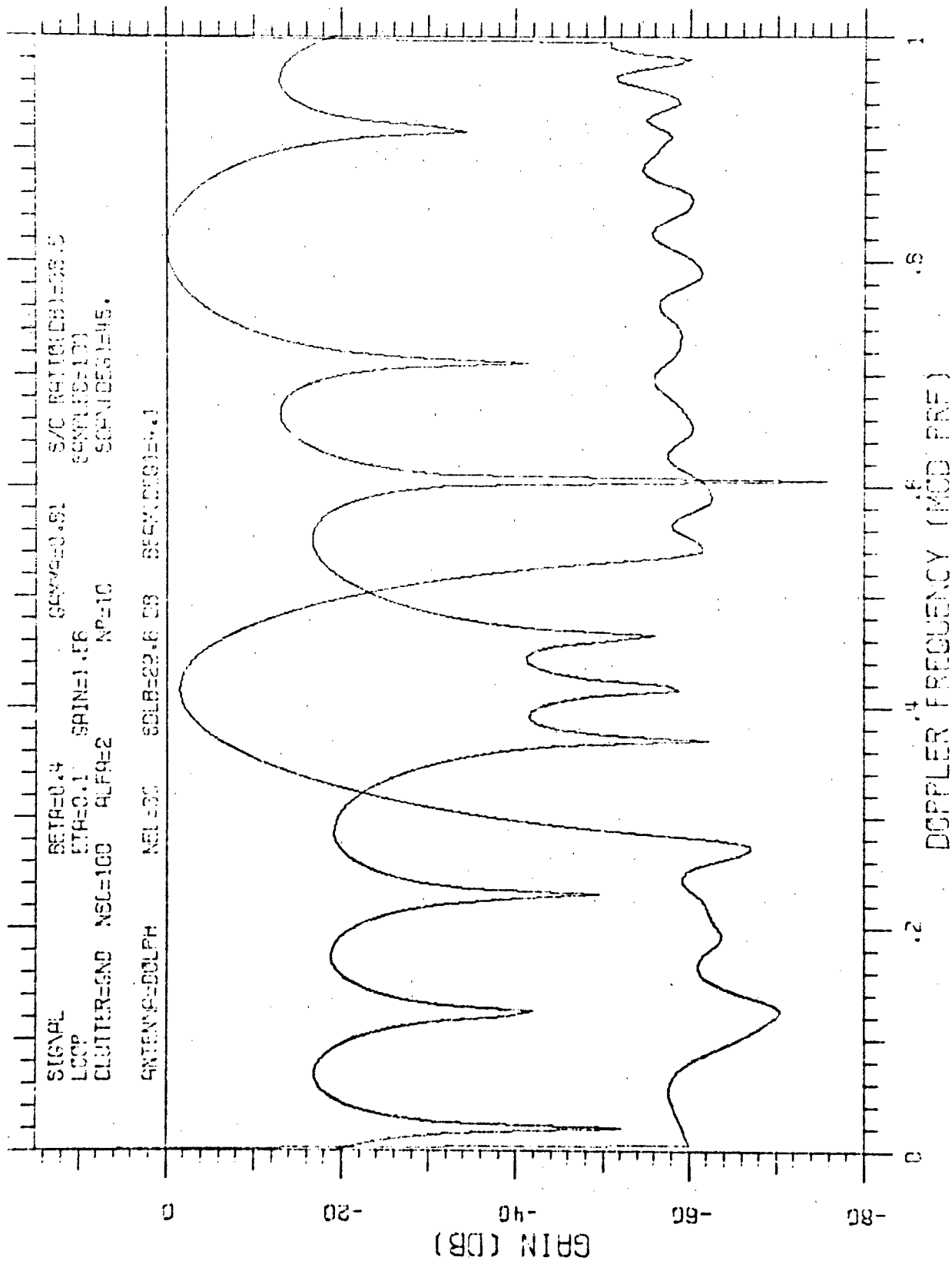


Figure 7

SPECTRA-FILTER CLUTTER

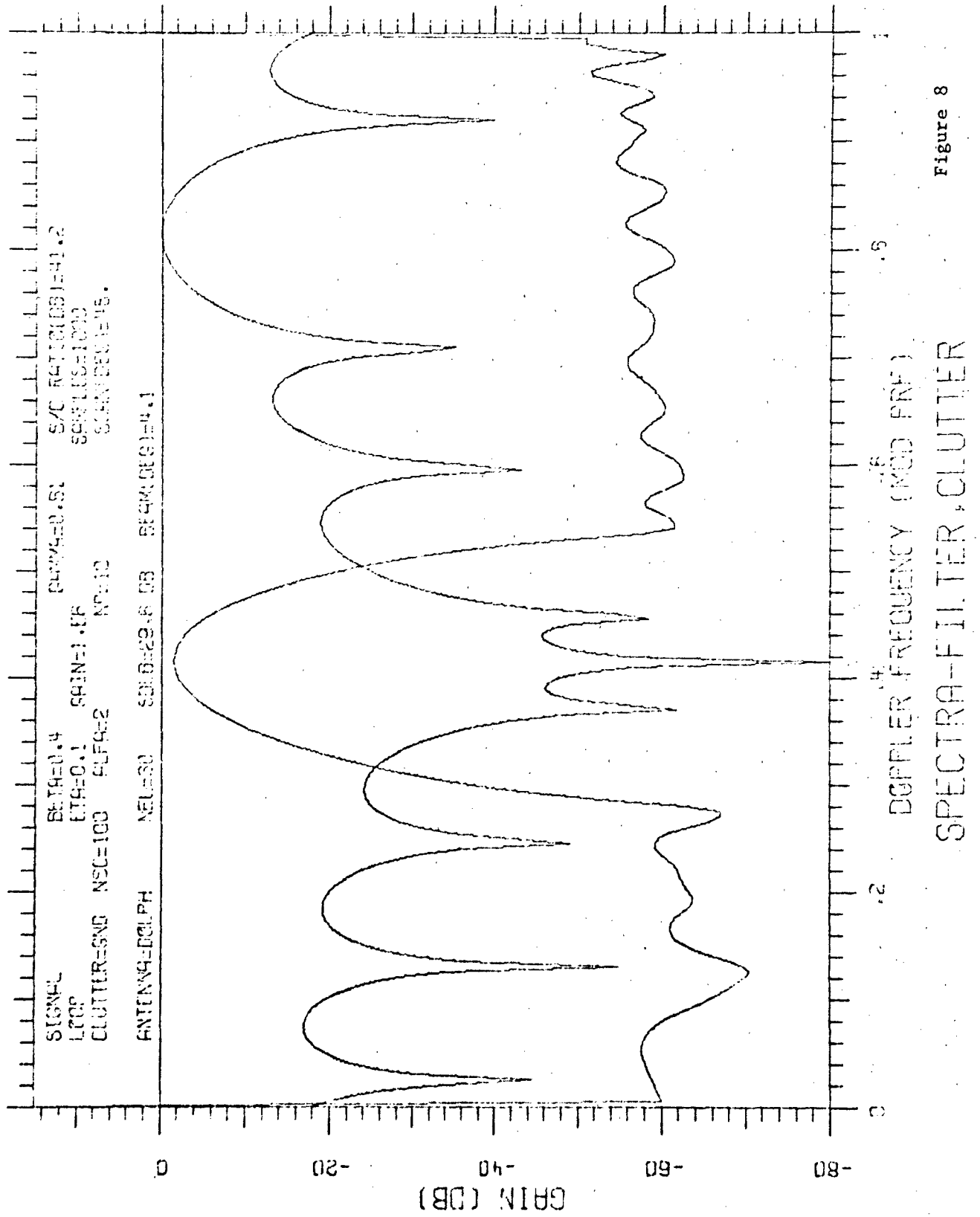


Figure 8

Figure 9.

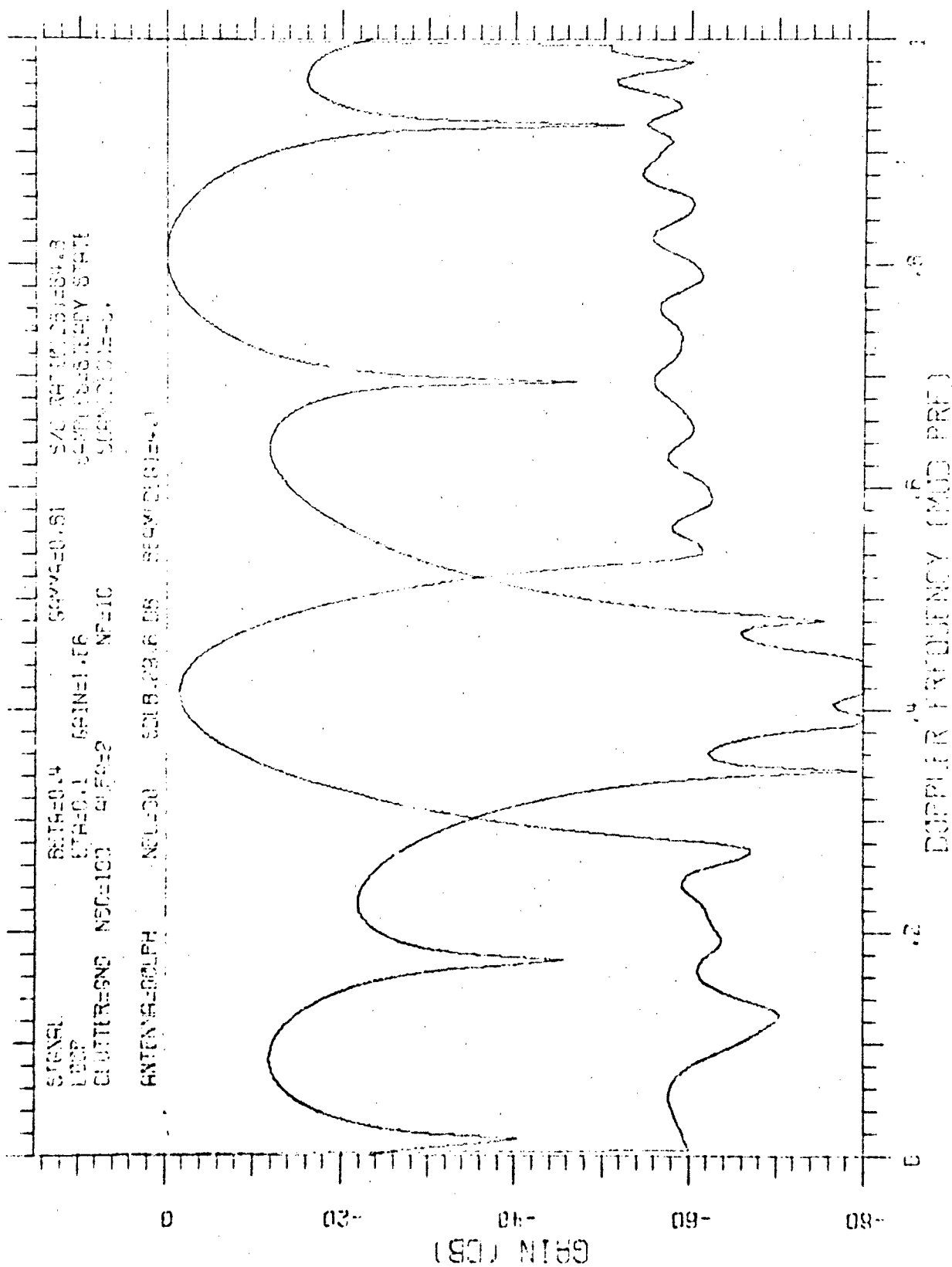


Figure 10

3.3.2 Optimum Performance

Figure 11 investigates the variation of performance with target doppler velocity (β) and scan angle (ψ). The optimum S/C ratio is shown. However, for a loop gain of 10^6 this is practically (within 0.1 dB) the same as the steady-state performance.

As expected, performance drops sharply as the target doppler approaches 0 (or 1) since in this limiting case the target is spatially stationary (or appears so due to the doppler ambiguity). It is interesting to note that performance in this case is worst at 0 scan angle. This occurs because the platform motion clutter spectrum becomes more spread out with increasing scan angle (see Figures 12 through 16), thus making discrimination possible. However, as the target doppler moves away from 0 (or 1), this same increased clutter spread causes decreased performance since it is more difficult to place a broad null in the filter spectrum. The erratic behavior of the performance with scan angle in the target doppler midrange is believed to be due to the relative difficulty of achieving specific separations between the filter main peak and predominant broad null. In the midrange of target doppler the adapted performance is seen to be relatively insensitive to scan angle, showing that the adaptation manages to compensate for the disparate clutter spectra (Figures 12 to 16).

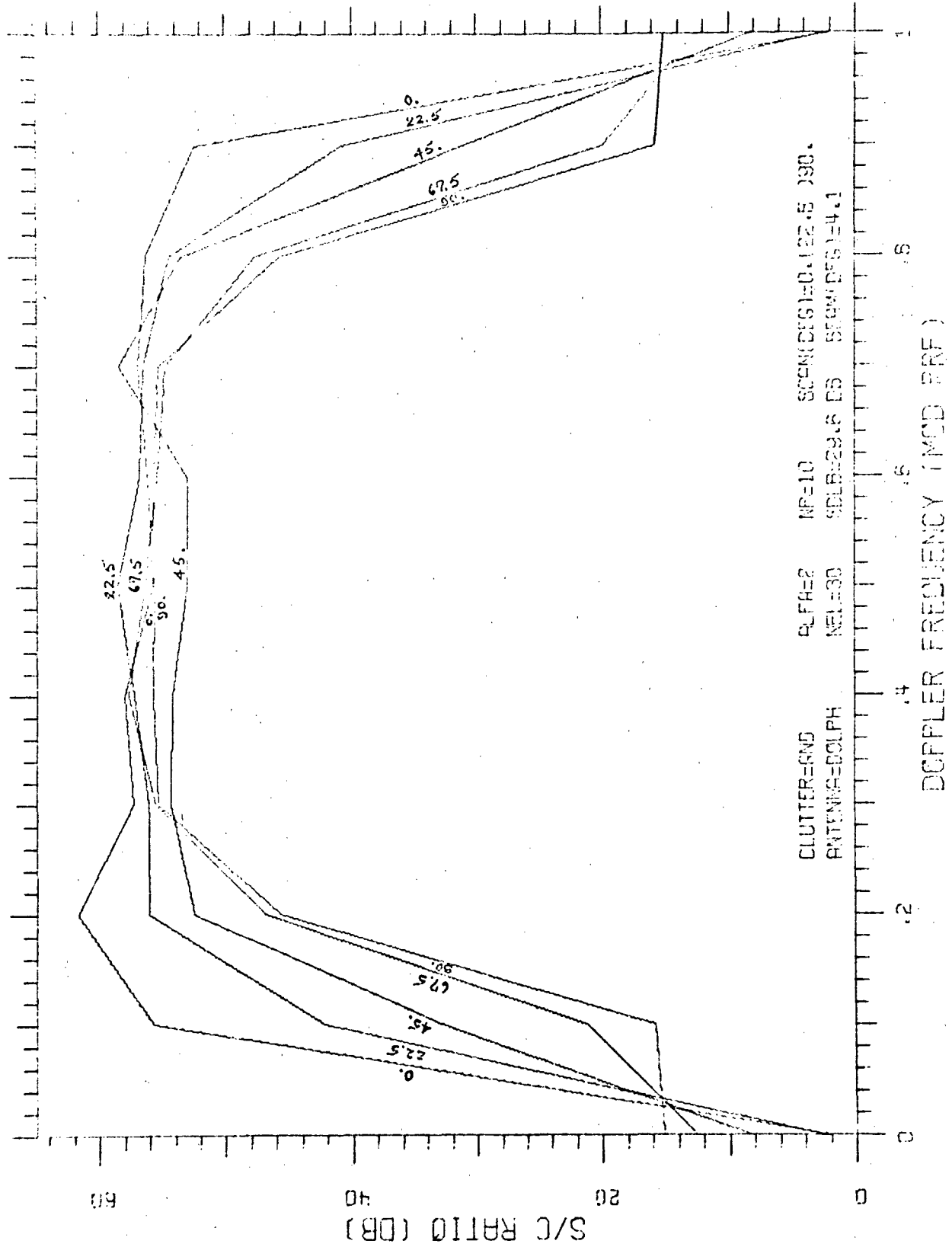


Figure 11

3.3.3 Variation with Scan Angle

3.3.3.1 Clutter Spectra. Figures 12 through 16 depict the variation of the clutter spectrum with scan angle. Two main effects are to be noted. The primary peak broadens with increasing scan angle and the location of this peak moves towards decreasing normalized doppler frequency, making two complete circuits for the 90° variation in the scan angle. These two circuits are specifically due to α being 2. The spike at 0 (or 1) is due to α being an integer which is also the cause of the spike and the main lobe being superimposed at 0 scan angle (refer to Appendix A, Equation 7).

3.3.3.2 Transient Response. Figures 17, 18, 4, and 19 show the transient response variation with scan angle. Note that at 0° scan angle the initial filter does extremely well since the clutter spectrum has only a very narrow peak; however, considerable samples are required to improve upon it since the loops find it difficult to place a very deep null at this specific point. However, even at a slight scan angle (11.25°), the initial filter is seen to be rather poor and rapid improvement ensues under adaptation. At 90° the initial response is even worse, yet the adapted response is only slightly worse than at 0° scan angle. With increasing scan angle, the transient response becomes more and more step-like.

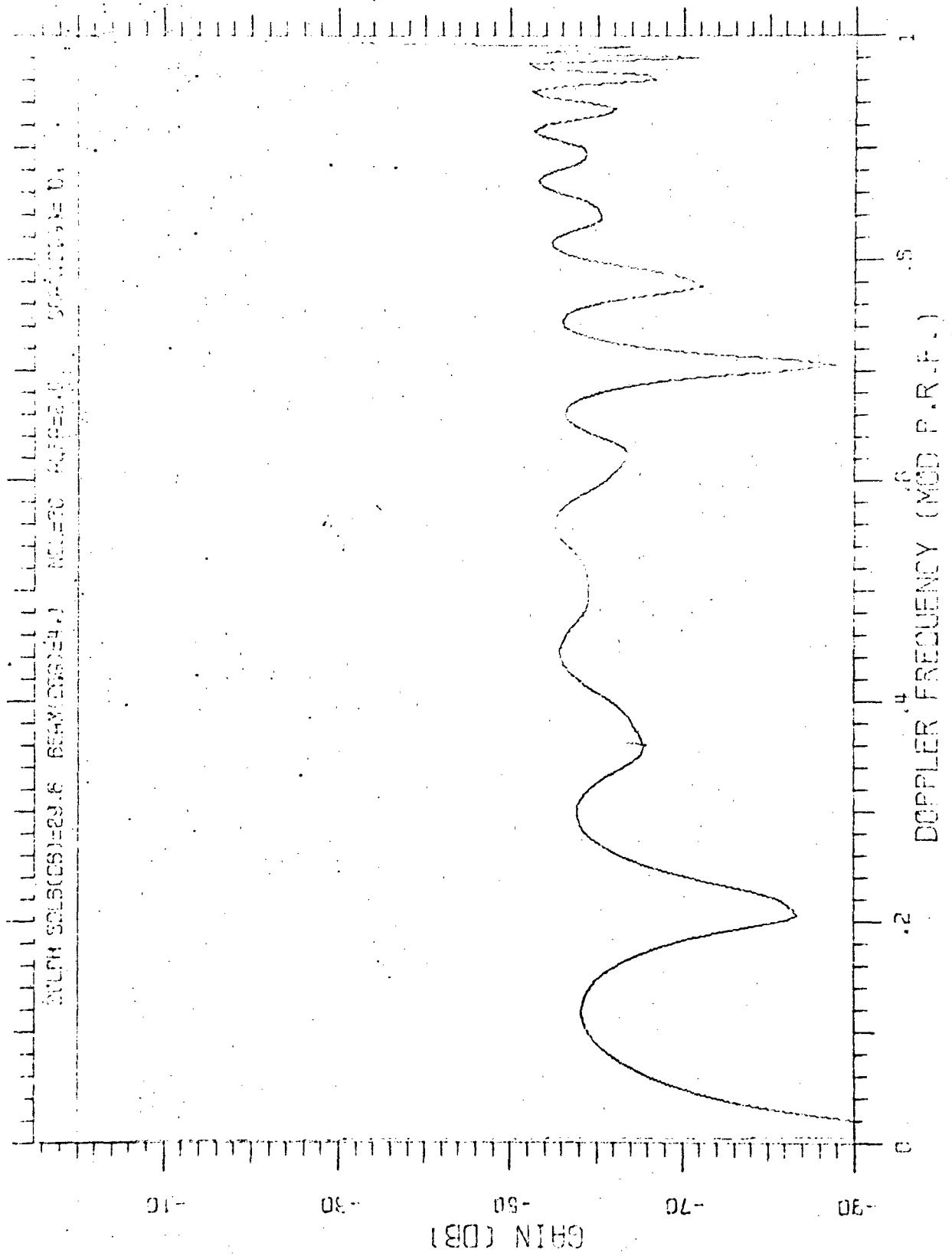


Figure 12

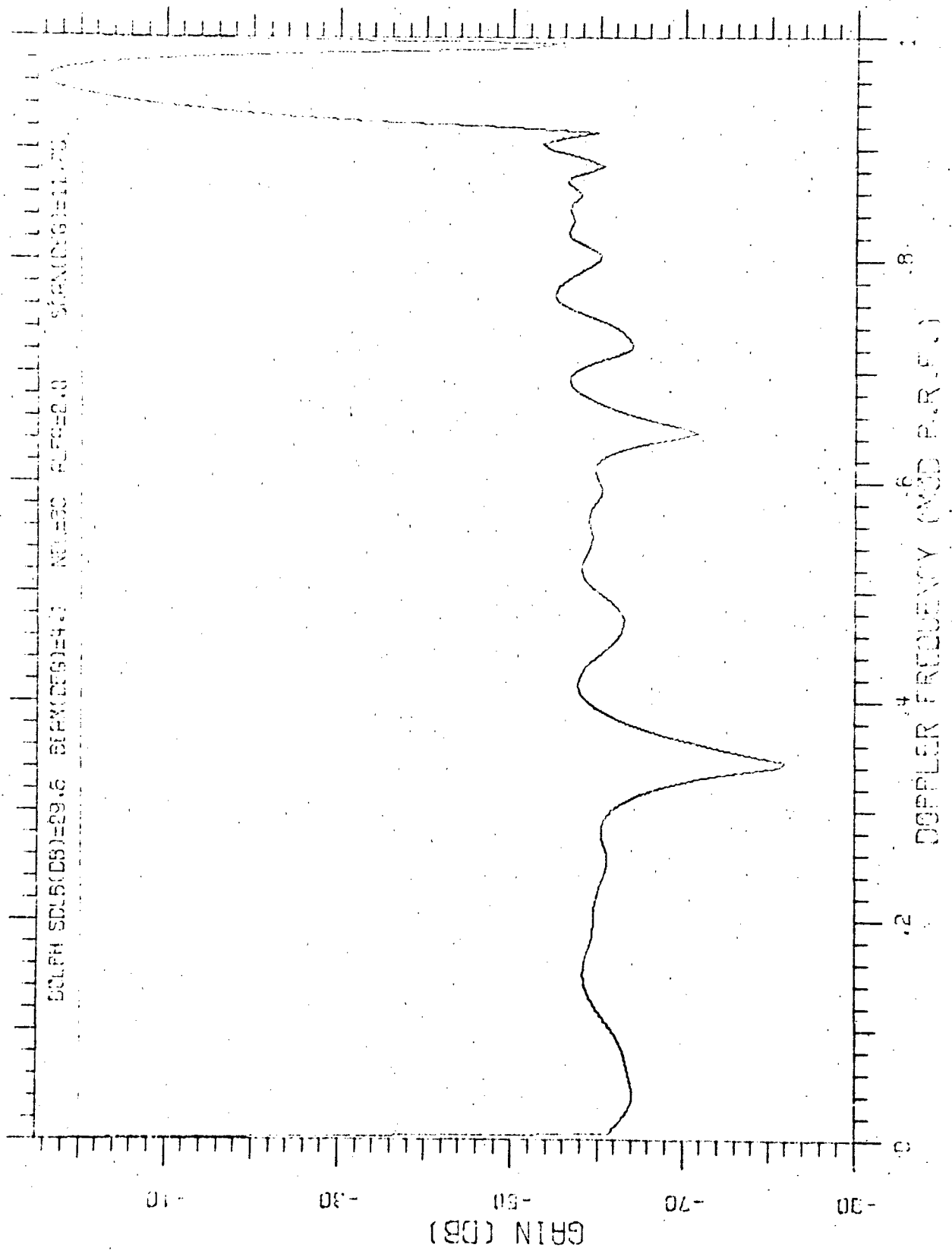
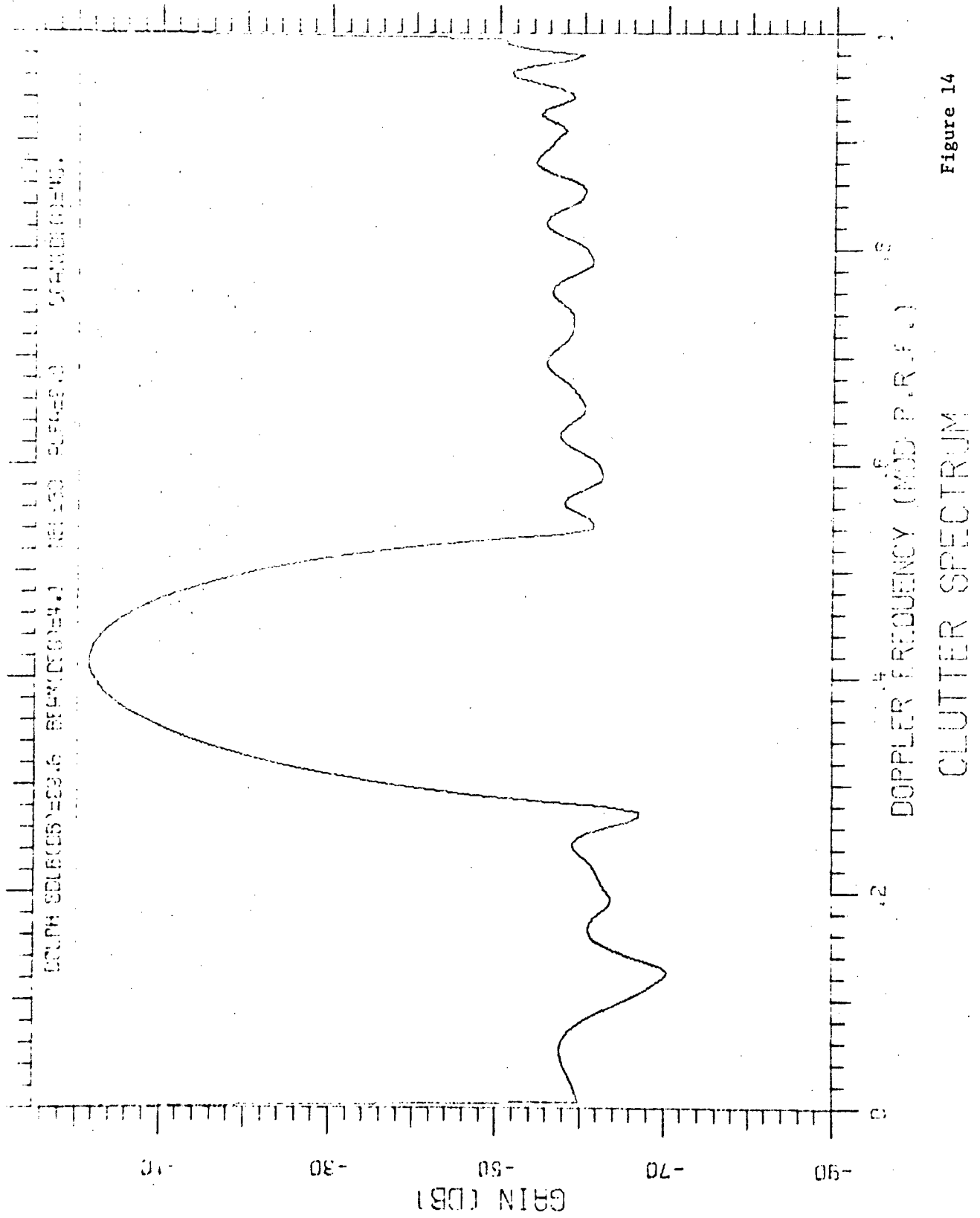


Figure 13



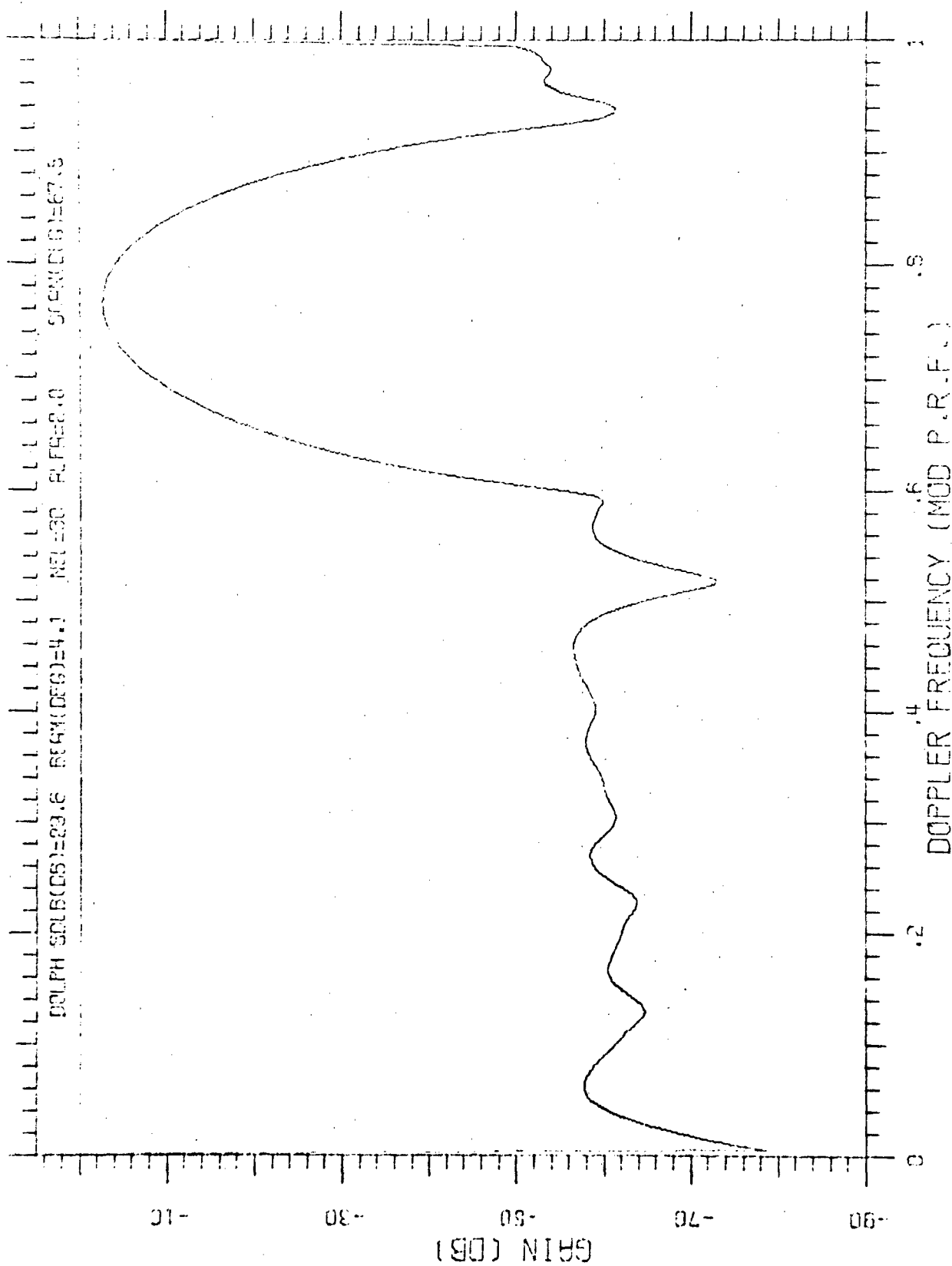


Figure 15

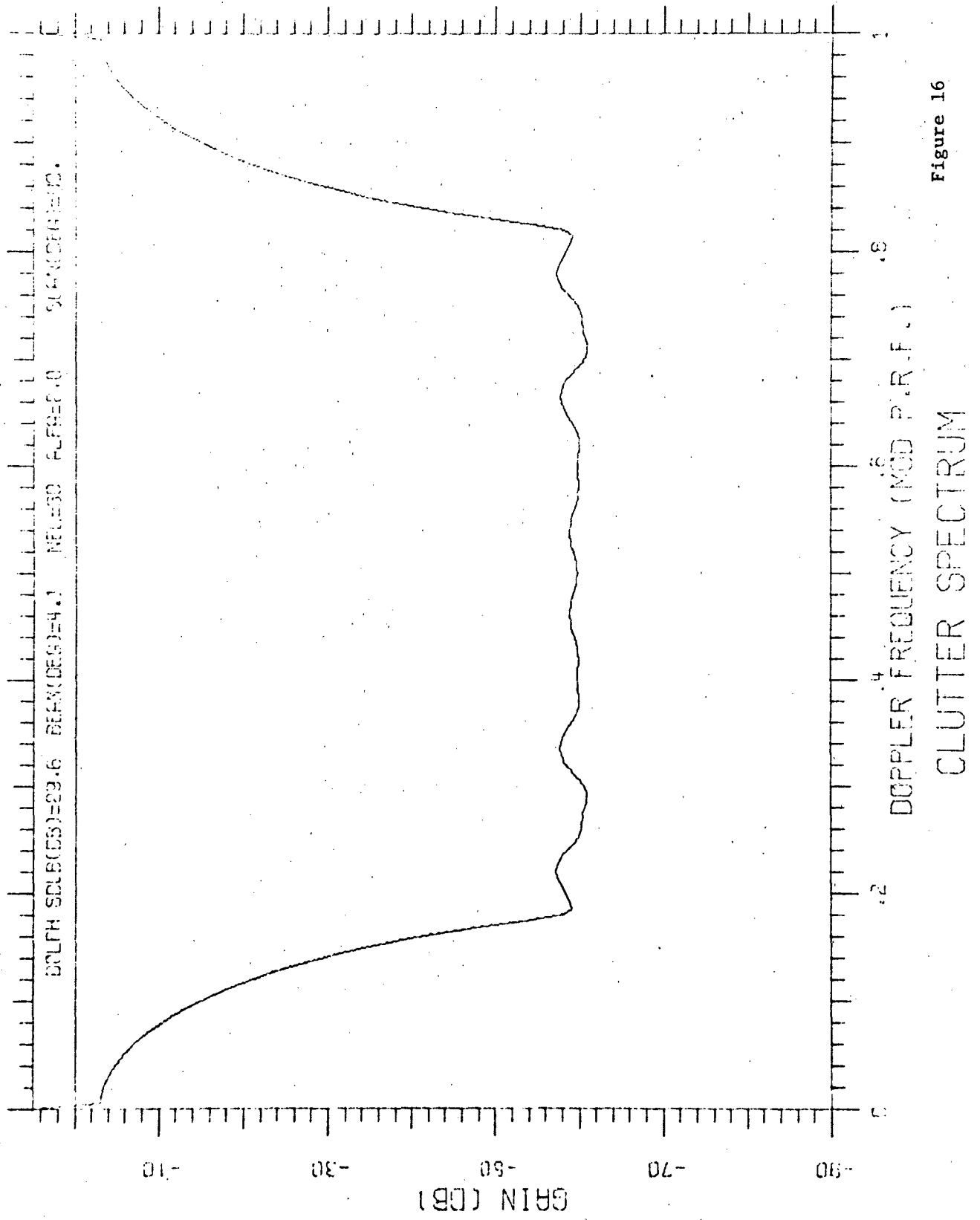


Figure 16

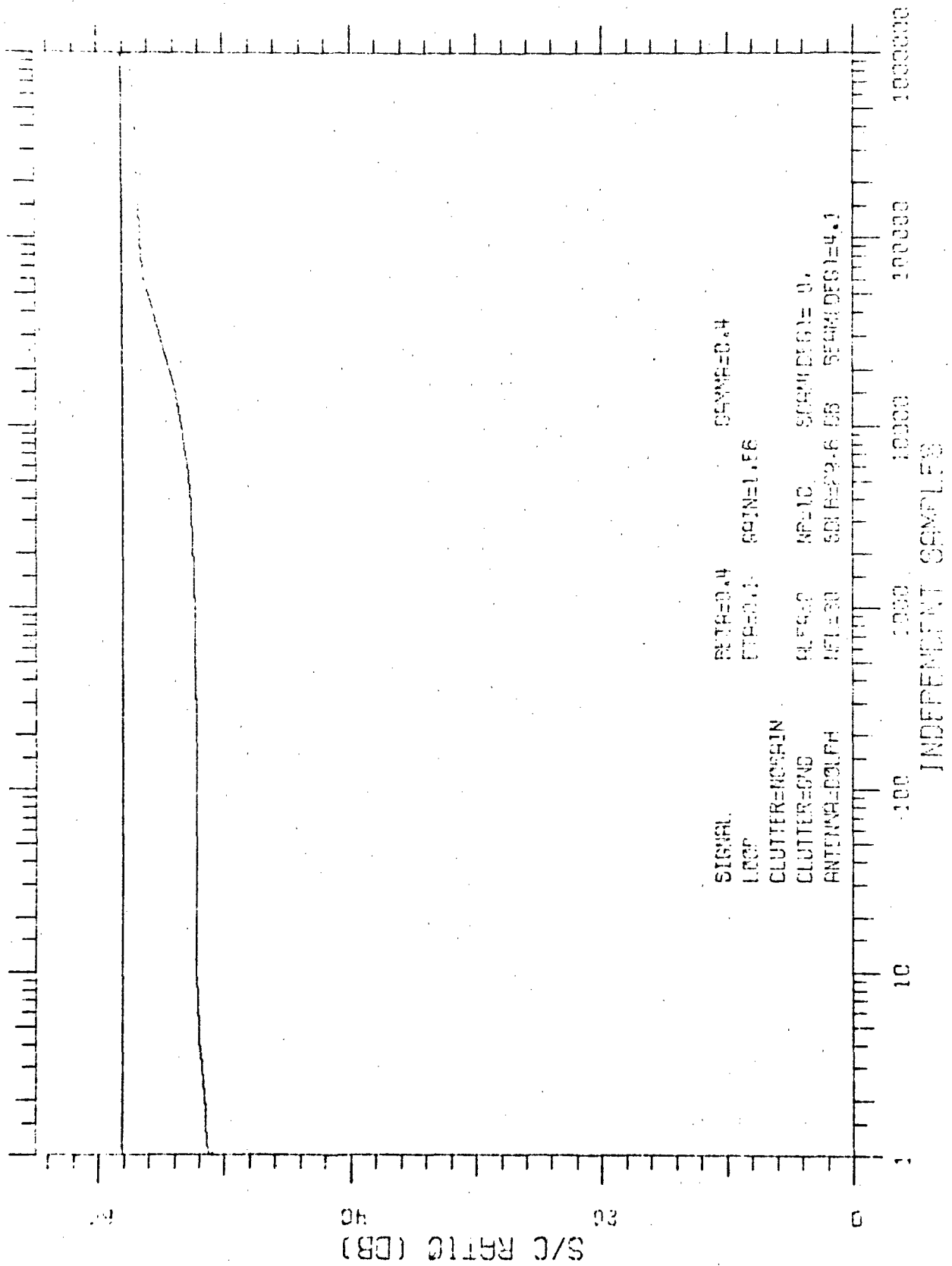
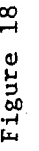


Figure 17



11
12
13
14
15
16
17
18
19
20
21
22
23
24
25
26
27
28
29
30
31
32
33
34
35
36
37
38
39
40
41
42
43
44
45
46
47
48
49
50
51
52
53
54
55
56
57
58
59
60
61
62
63
64
65
66
67
68
69
70
71
72
73
74
75
76
77
78
79
80
81
82
83
84
85
86
87
88
89
90
91
92
93
94
95
96
97
98
99
100
101
102
103
104
105
106
107
108
109
110
111
112
113
114
115
116
117
118
119
120
121
122
123
124
125
126
127
128
129
130
131
132
133
134
135
136
137
138
139
140
141
142
143
144
145
146
147
148
149
150
151
152
153
154
155
156
157
158
159
160
161
162
163
164
165
166
167
168
169
170
171
172
173
174
175
176
177
178
179
180
181
182
183
184
185
186
187
188
189
190
191
192
193
194
195
196
197
198
199
200
201
202
203
204
205
206
207
208
209
210
211
212
213
214
215
216
217
218
219
220
221
222
223
224
225
226
227
228
229
230
231
232
233
234
235
236
237
238
239
240
241
242
243
244
245
246
247
248
249
250
251
252
253
254
255
256
257
258
259
260
261
262
263
264
265
266
267
268
269
270
271
272
273
274
275
276
277
278
279
280
281
282
283
284
285
286
287
288
289
290
291
292
293
294
295
296
297
298
299
300
301
302
303
304
305
306
307
308
309
310
311
312
313
314
315
316
317
318
319
320
321
322
323
324
325
326
327
328
329
330
331
332
333
334
335
336
337
338
339
340
341
342
343
344
345
346
347
348
349
350
351
352
353
354
355
356
357
358
359
360
361
362
363
364
365
366
367
368
369
370
371
372
373
374
375
376
377
378
379
380
381
382
383
384
385
386
387
388
389
390
391
392
393
394
395
396
397
398
399
400
401
402
403
404
405
406
407
408
409
410
411
412
413
414
415
416
417
418
419
420
421
422
423
424
425
426
427
428
429
430
431
432
433
434
435
436
437
438
439
440
441
442
443
444
445
446
447
448
449
450
451
452
453
454
455
456
457
458
459
460
461
462
463
464
465
466
467
468
469
470
471
472
473
474
475
476
477
478
479
480
481
482
483
484
485
486
487
488
489
490
491
492
493
494
495
496
497
498
499
500
501
502
503
504
505
506
507
508
509
510
511
512
513
514
515
516
517
518
519
520
521
522
523
524
525
526
527
528
529
530
531
532
533
534
535
536
537
538
539
540
541
542
543
544
545
546
547
548
549
550
551
552
553
554
555
556
557
558
559
560
561
562
563
564
565
566
567
568
569
570
571
572
573
574
575
576
577
578
579
580
581
582
583
584
585
586
587
588
589
590
591
592
593
594
595
596
597
598
599
600
601
602
603
604
605
606
607
608
609
610
611
612
613
614
615
616
617
618
619
620
621
622
623
624
625
626
627
628
629
630
631
632
633
634
635
636
637
638
639
640
641
642
643
644
645
646
647
648
649
650
651
652
653
654
655
656
657
658
659
660
661
662
663
664
665
666
667
668
669
670
671
672
673
674
675
676
677
678
679
680
681
682
683
684
685
686
687
688
689
690
691
692
693
694
695
696
697
698
699
700
701
702
703
704
705
706
707
708
709
710
711
712
713
714
715
716
717
718
719
720
721
722
723
724
725
726
727
728
729
730
731
732
733
734
735
736
737
738
739
740
741
742
743
744
745
746
747
748
749
750
751
752
753
754
755
756
757
758
759
760
761
762
763
764
765
766
767
768
769
770
771
772
773
774
775
776
777
778
779
780
781
782
783
784
785
786
787
788
789
790
791
792
793
794
795
796
797
798
799
800
801
802
803
804
805
806
807
808
809
810
811
812
813
814
815
816
817
818
819
820
821
822
823
824
825
826
827
828
829
830
831
832
833
834
835
836
837
838
839
840
841
842
843
844
845
846
847

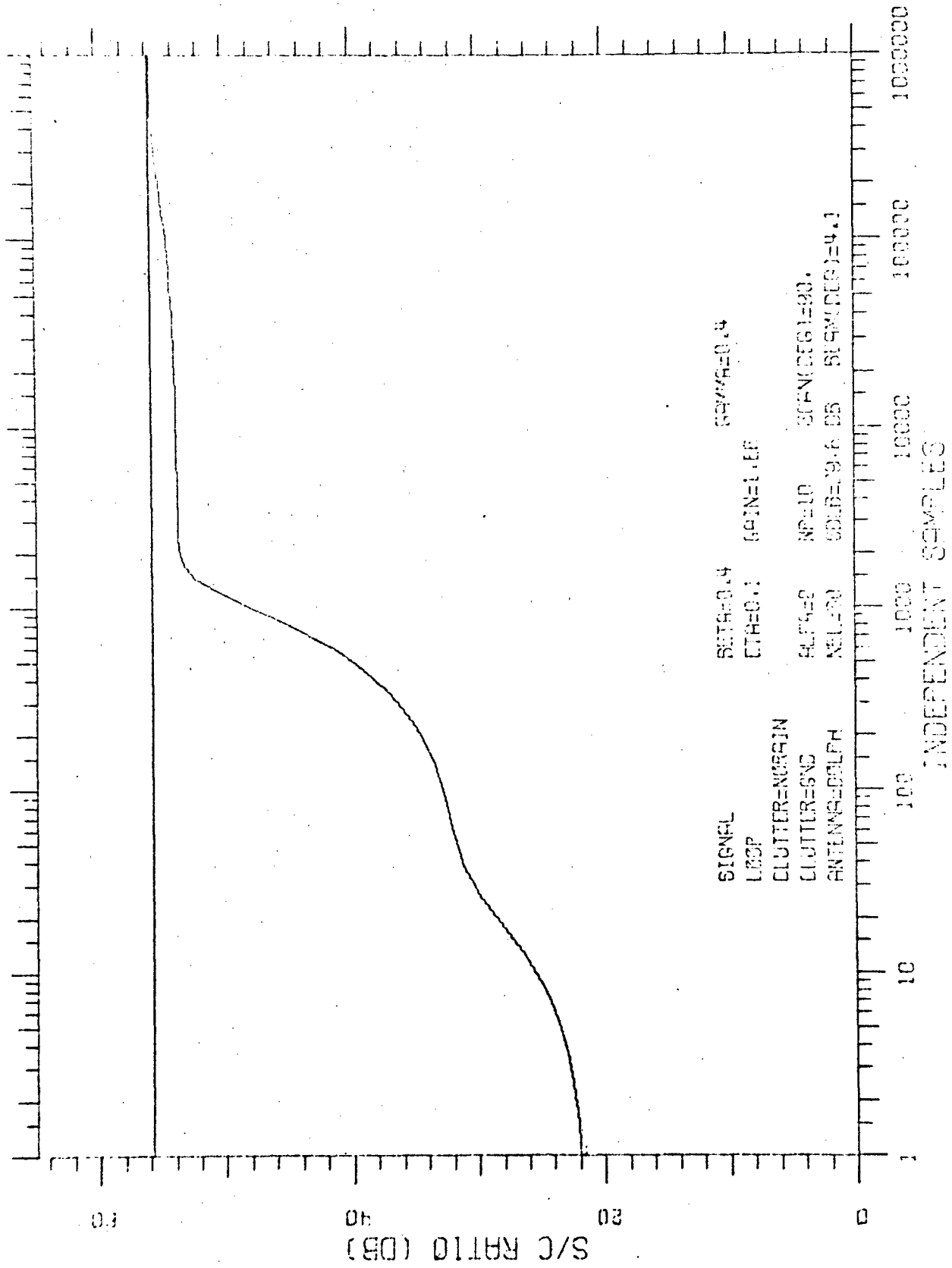


Figure 19

TRANSIENT RESPONSE

3.3.4 Variation with Target Velocity (β)

(Figures 20, 21, 4, 22, and 23) It is interesting to note that, though the steady-state performance changes significantly with target doppler (as discussed above), the number of samples required to achieve this steady-state response remains essentially 10^4 samples. A more and more pronounced staircase-like transient response is evident with worsening steady-state performance.

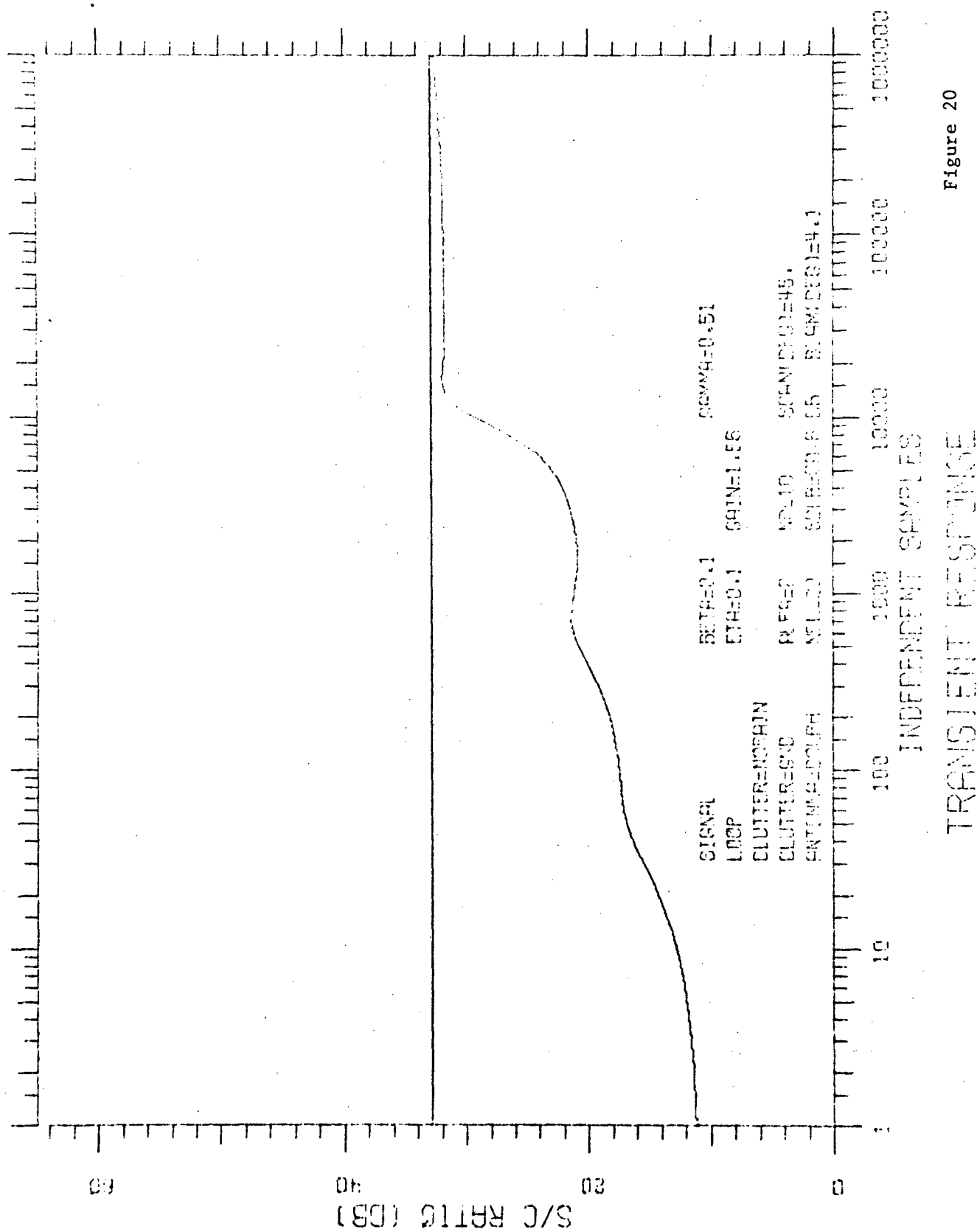


Figure 20

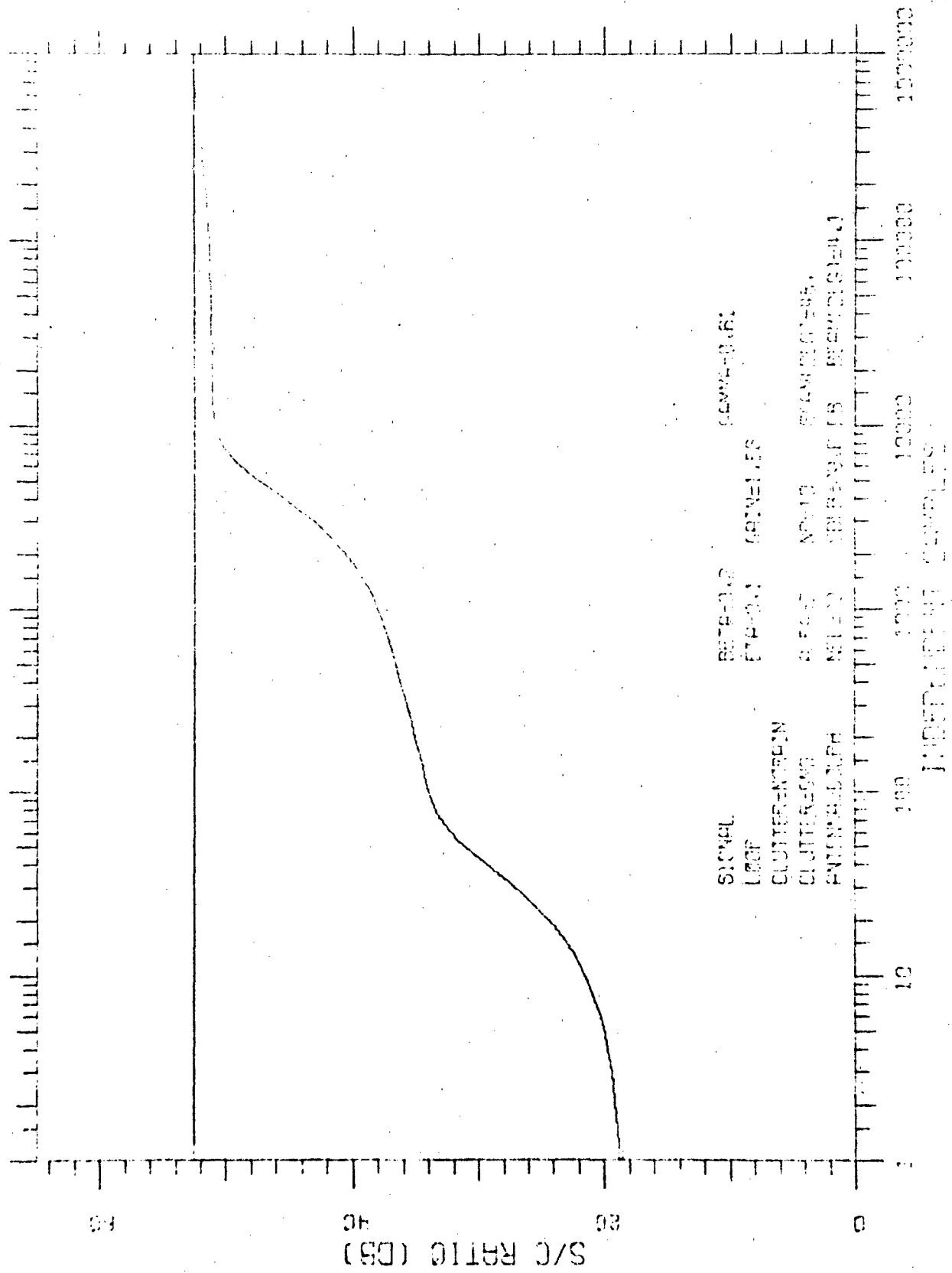


Figure 21

TRANSIENT RESPONSE

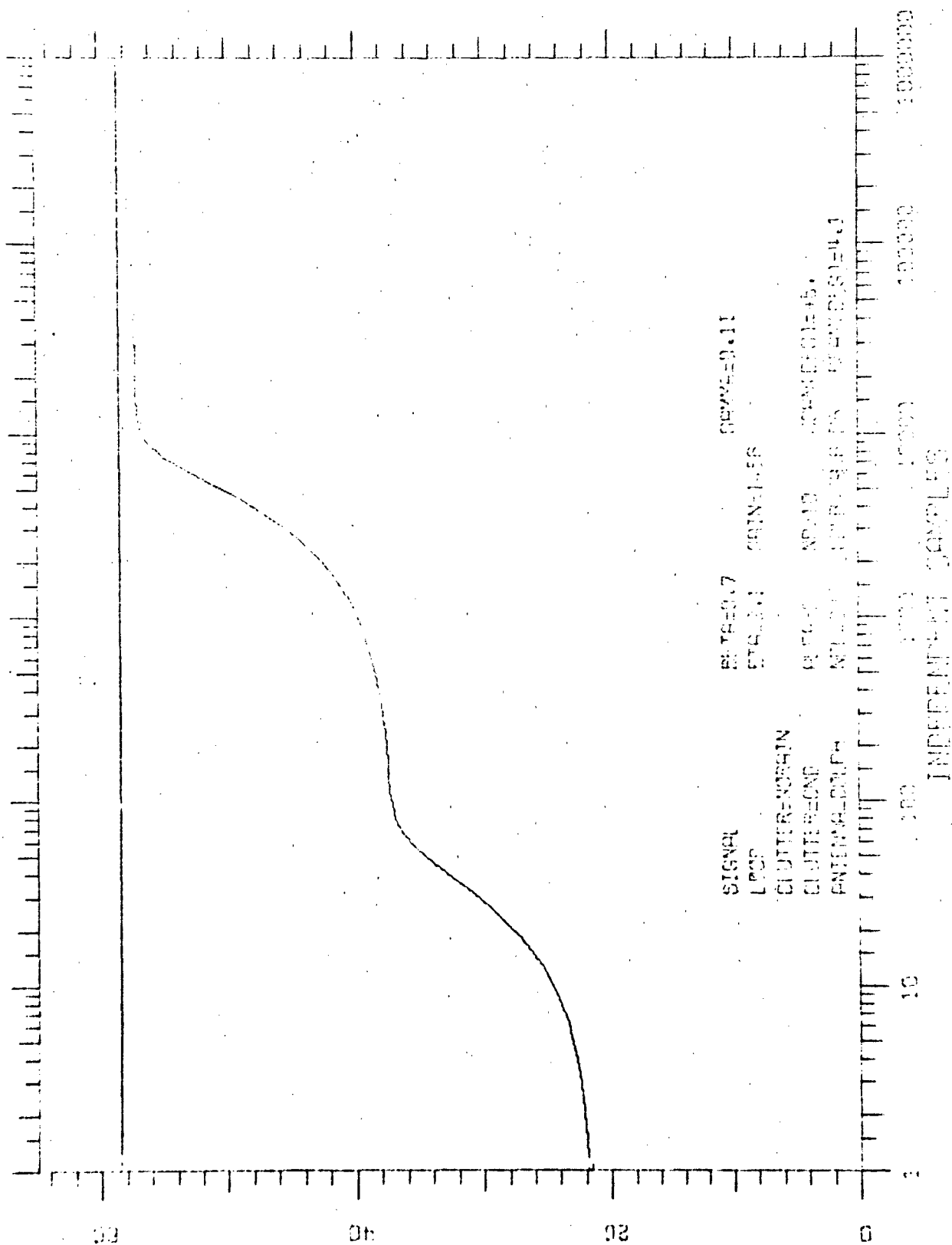


Figure 22

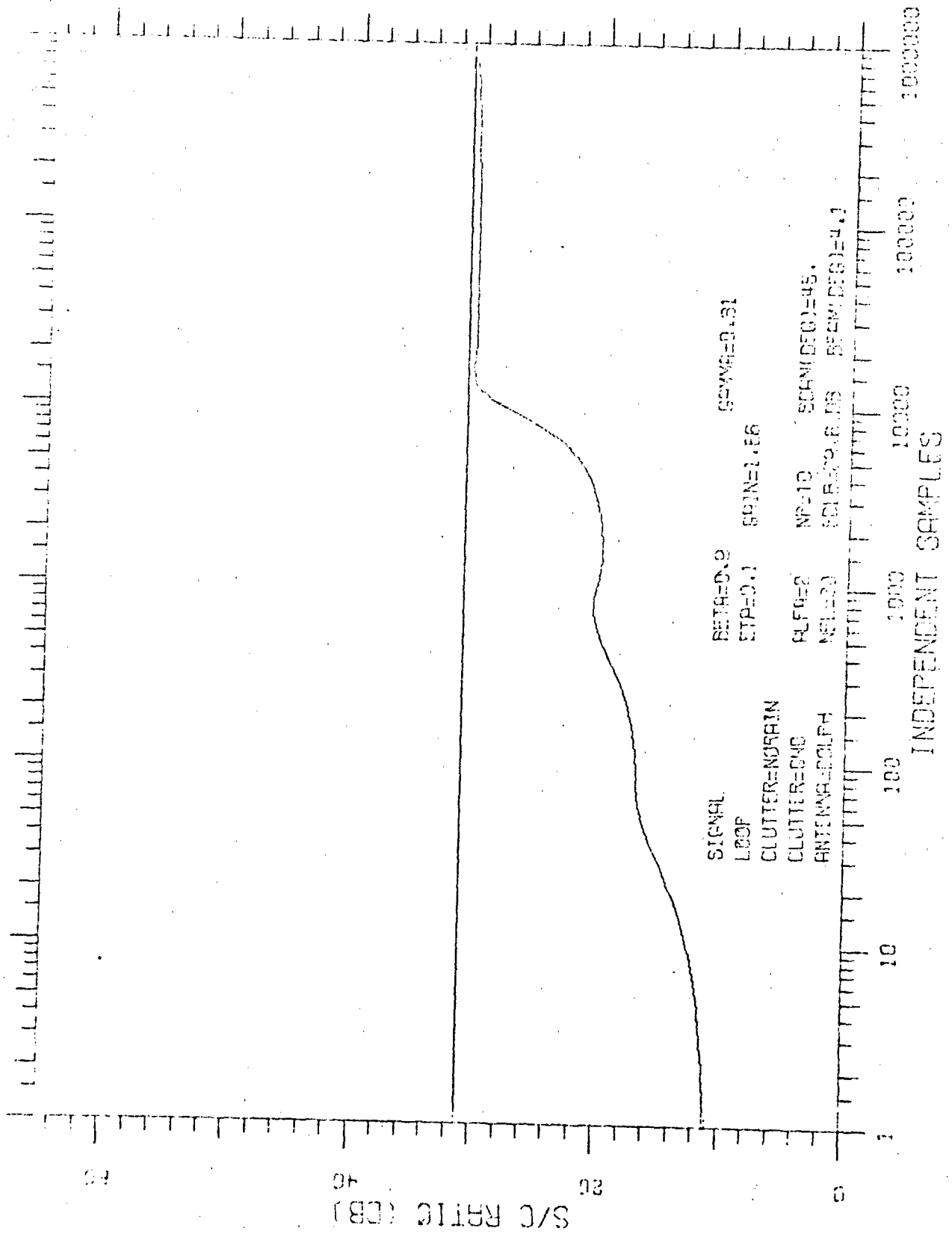


Figure 23

3.3.5 Variation with Number of Pulses

(Figures 24, 25, 4, and 26) With increasing number of pulses, the variety of filters possible increases rapidly, so it is not surprising that the steady-state performance improves. However, the complexity of the system also increases markedly so that by 20 pulses the additional gain in performance probably does not warrant the increased complexity.

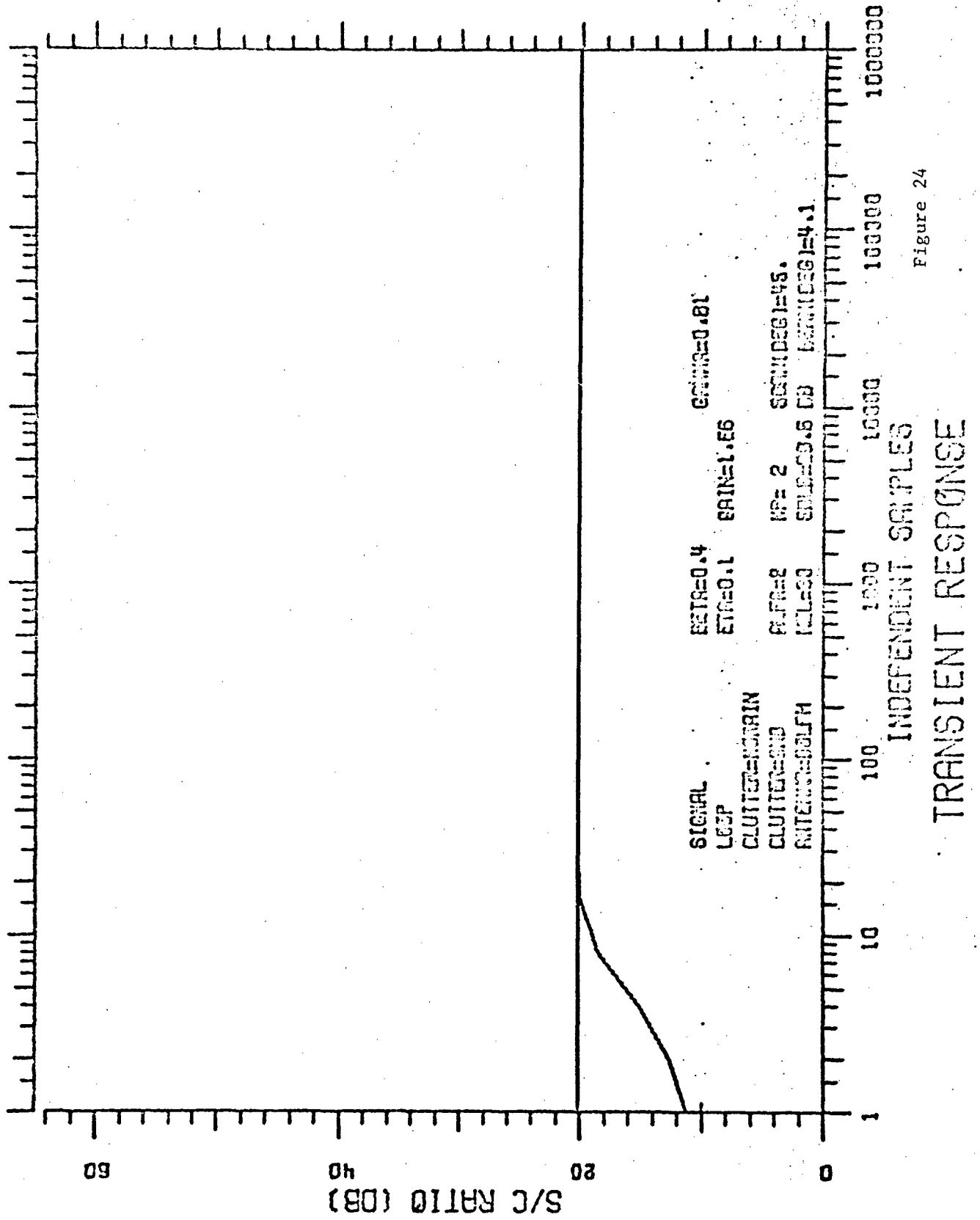


Figure 24

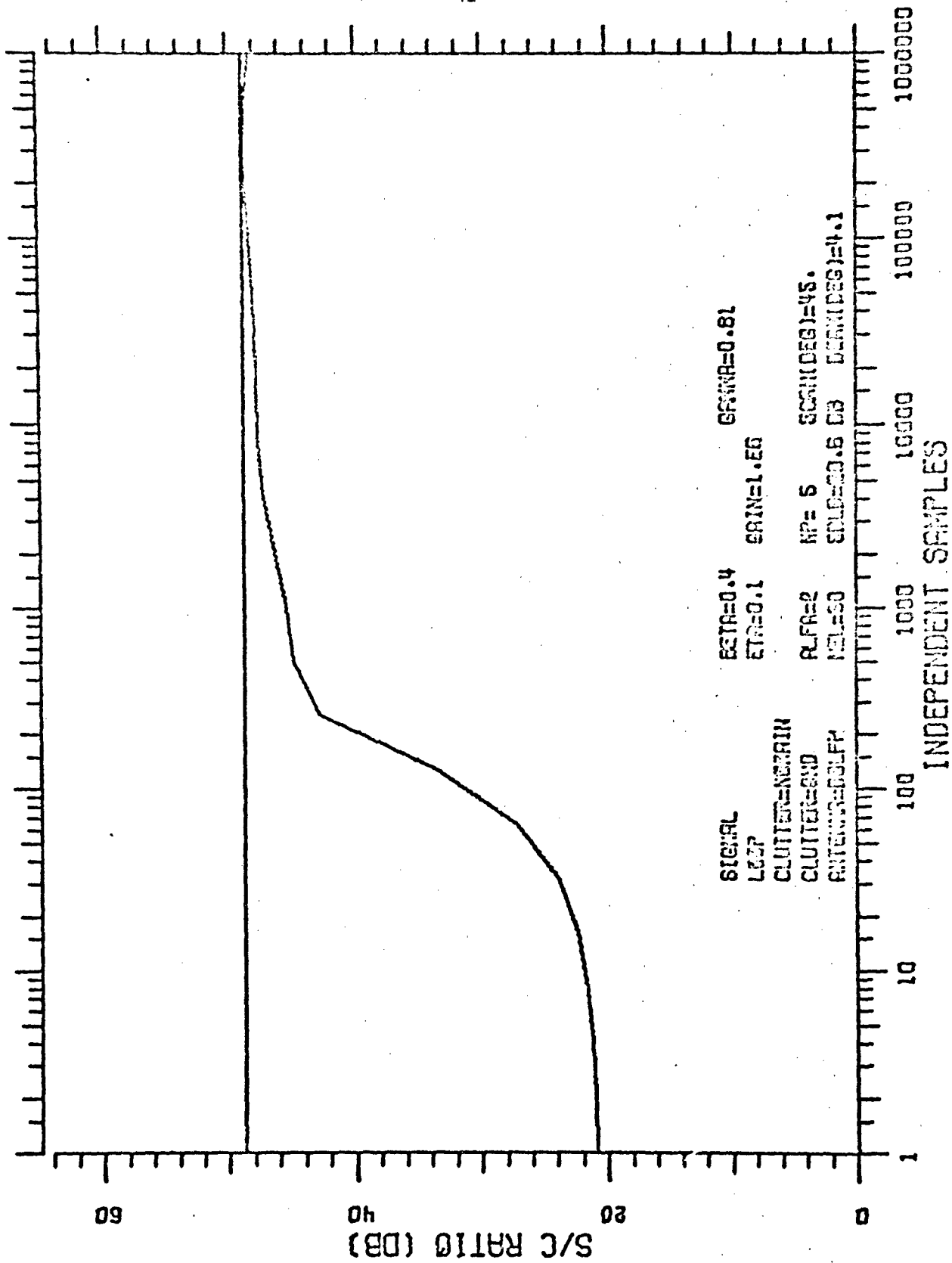


Figure 25

TRANSIENT RESPONSE

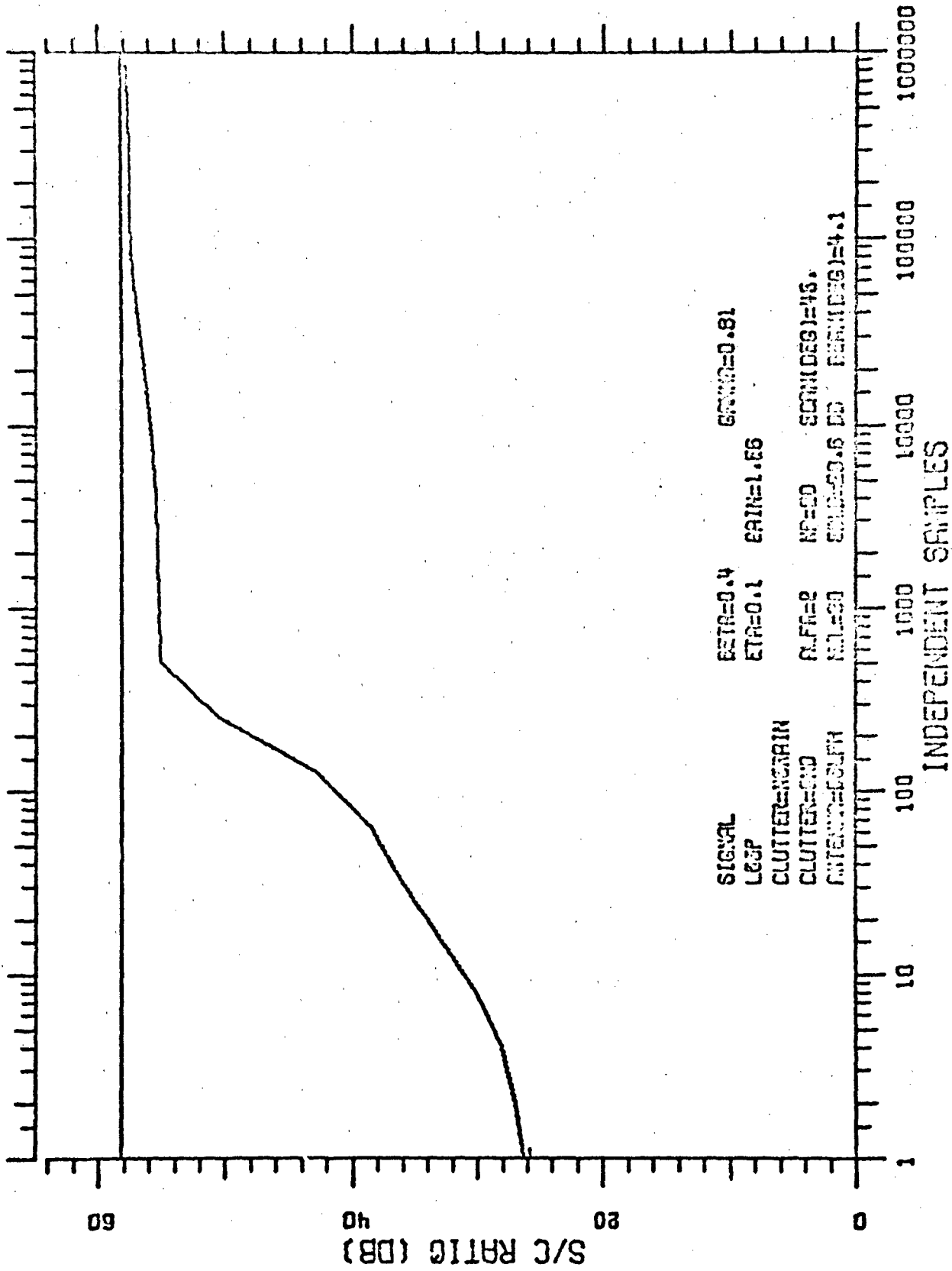


Figure 26

TRANSIENT RESPONSE

3.3.6 Variation with Platform Velocity (α)

(Figures 27, 4, and 28) Small α is seen to give better steady-state performance. However, it is to be noted that after 10^4 samples, essentially the same performance results for $\alpha = 1$ and $\alpha = 2$. Since $\alpha = 2V_p/\lambda f_r$, small α requires a low platform velocity, high pulse repetition rate, or a long wavelength. These parameters are usually decided on the basis of other system requirements than filter performance, e.g., the PRF may be selected to avoid second-time-around returns and range ambiguities.

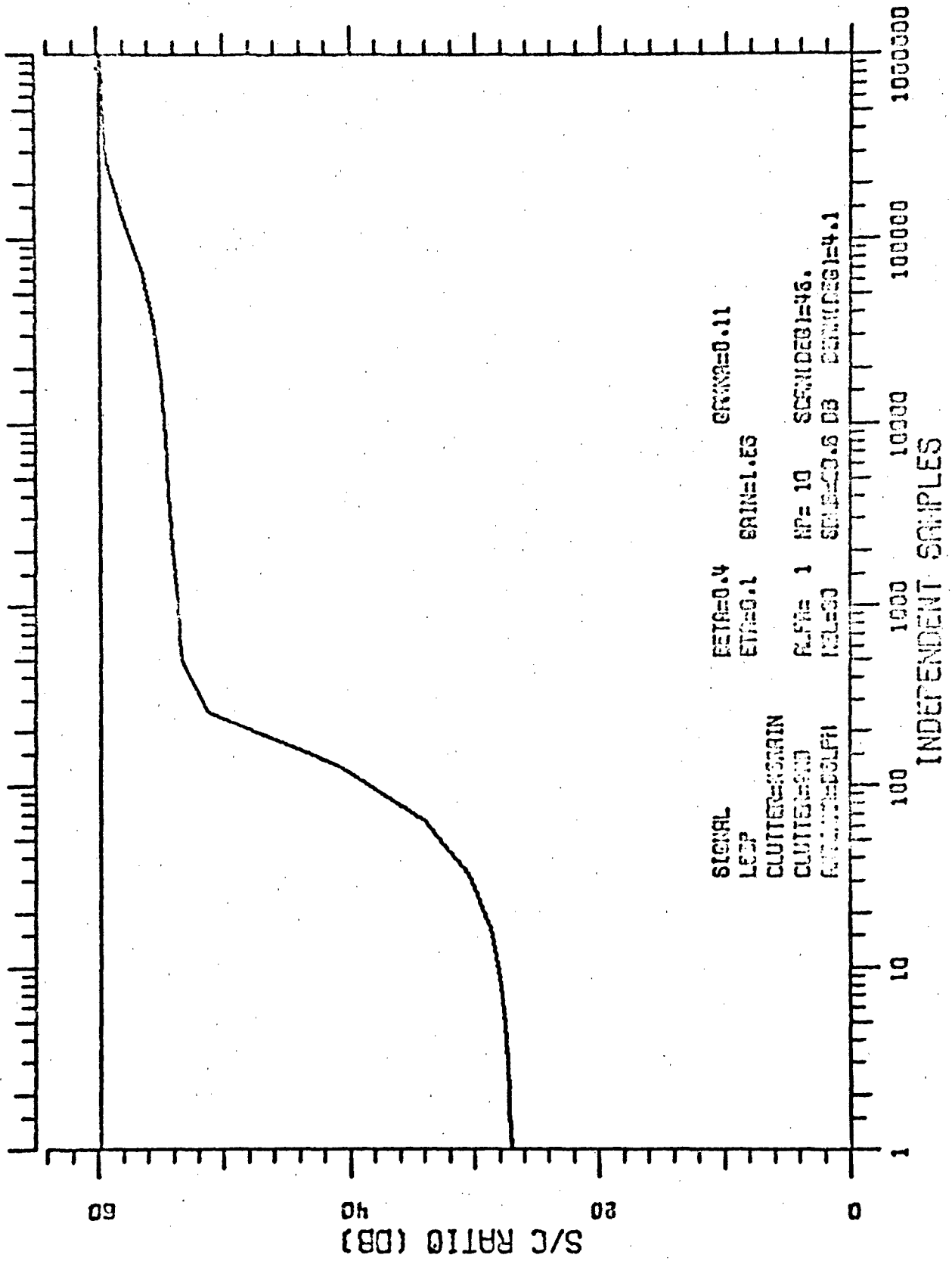


Figure 27

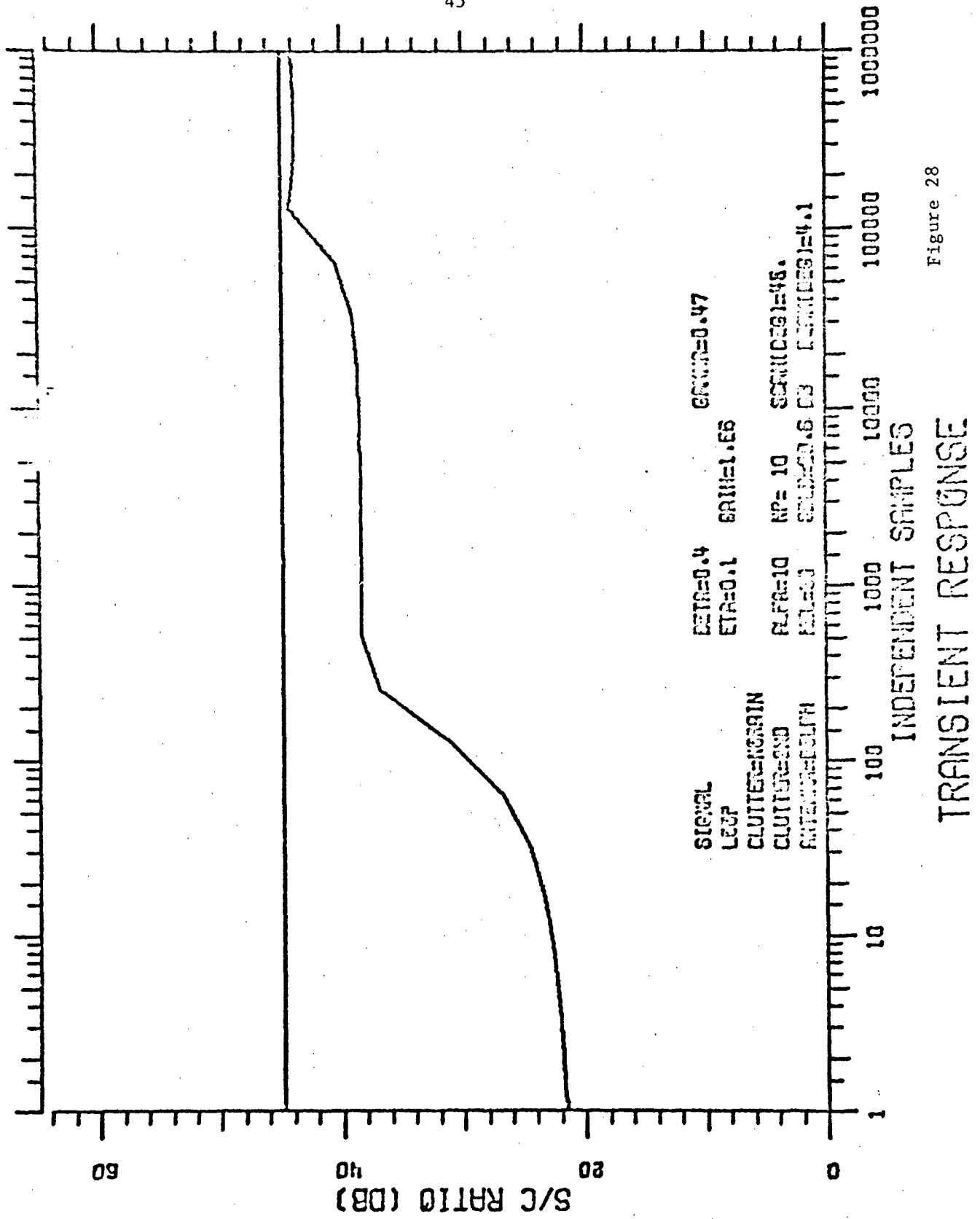


Figure 28

3.3.7 Variation with Loop Gain

(Figures 29, 30, and 4) Note that the time constant of the loops is changed so as to maintain a constant noise factor (η) of 0.1. It is seen that low loop gain causes a steady-state performance considerably less than the optimum performance. The transient response is identical for the various gains except that with lower gain the asymptote is reached sooner. At low loop gains, the weights approach values $([M+(I/G)]^{-1}S^*)$ which are different than the optimum $(M^{-1}S^*)$. This bias in the steady-state solution is negligible when $1/G$ is small compared to the smallest eigenvalue of M .

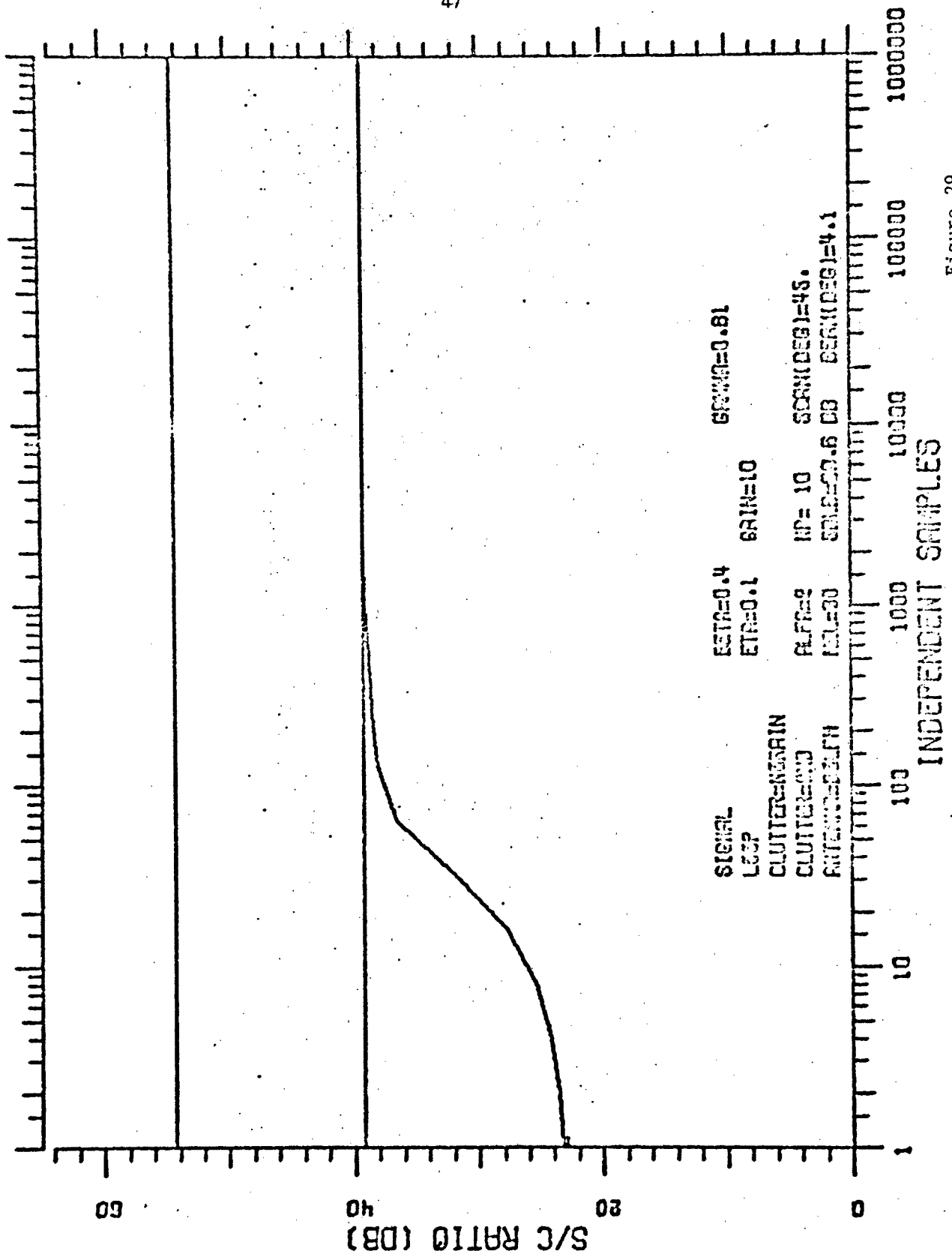


Figure 29

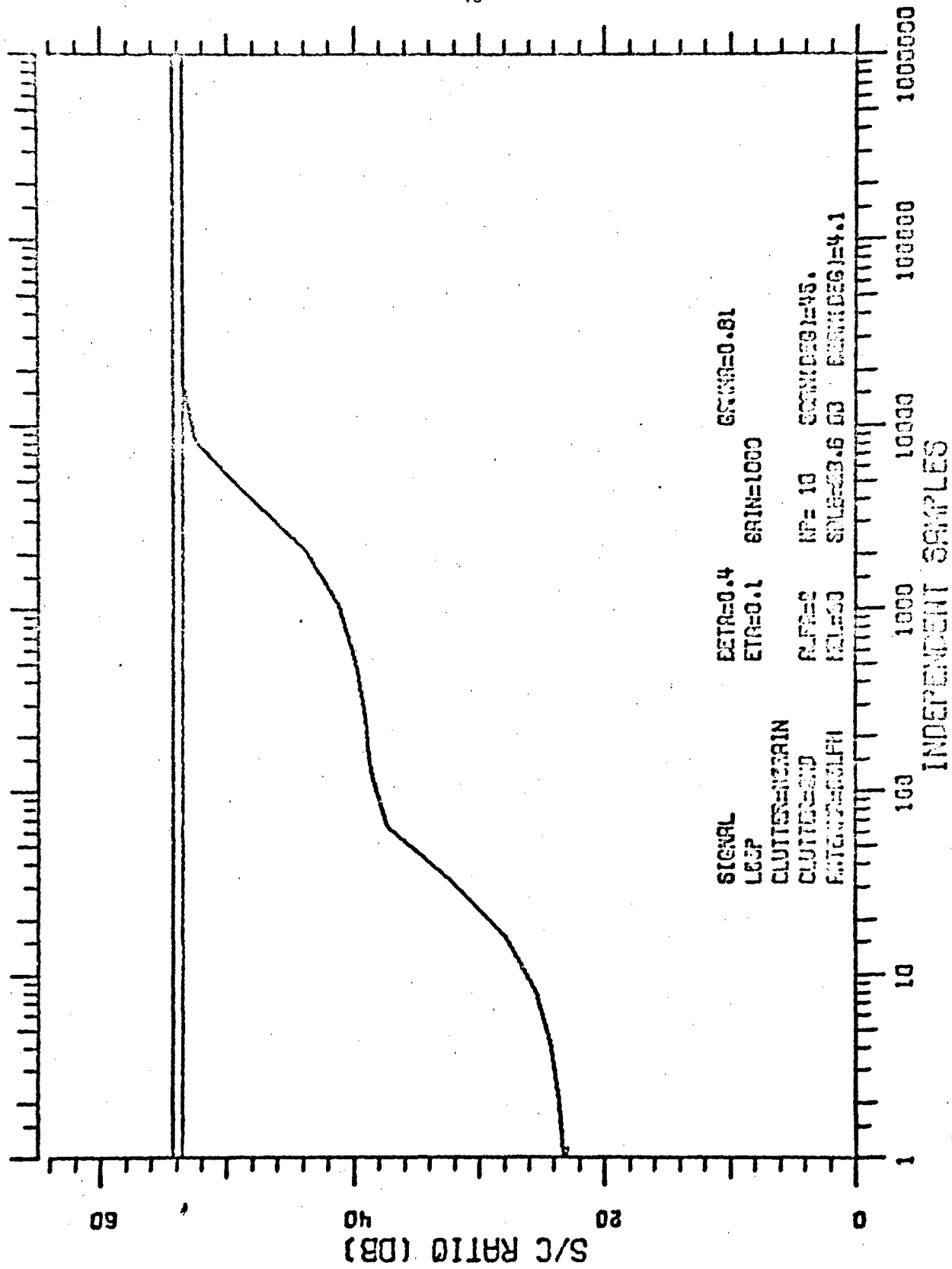


Figure 30

TRANSIENT RESPONSE

3.3.8 Rain Base Line

(Figures 31 through 36) A gaussian-shaped rain spectrum with mean of 0.1, standard deviation of 0.05, and with total power equal to the total clutter power is added to the baseline clutter spectrum. Note that the total power is then normalized to one so that the S/C ratio depicted is still the ratio of output to input S/C ratio (MTI gain). In practice, there would be an increase in total clutter power so that the input S/C ratio would decrease. Thus to maintain the output S/C ratio, the MTI gain would actually have to increase. Specifically, with a relative rain power of one, the MTI gain would have to increase 3 dB to maintain the output S/C ratio at the pre-rain level.

Some improvement (about 4 dB maximum) in transient response results from initializing the weights at the pre-rain steady-state values (Figure 32). However, as the number of samples increases, this improvement diminishes and disappears before the steady state is approached. The baseline rain is rather severe (compare Figures 5 and 33); hence the adaptation is governed mostly by the rain--not the ground clutter.

Note in particular that even for this relatively severe rain the adapted MTI gain is essentially the same as for the no-rain case. As shown below, for lighter rains the MTI gain may actually improve.

Figures 33 through 36 show the filter spectra during adaptation; the clutter (rain and ground) spectrum is superimposed to show how the filter nulls out the broad clutter spectrum peak.

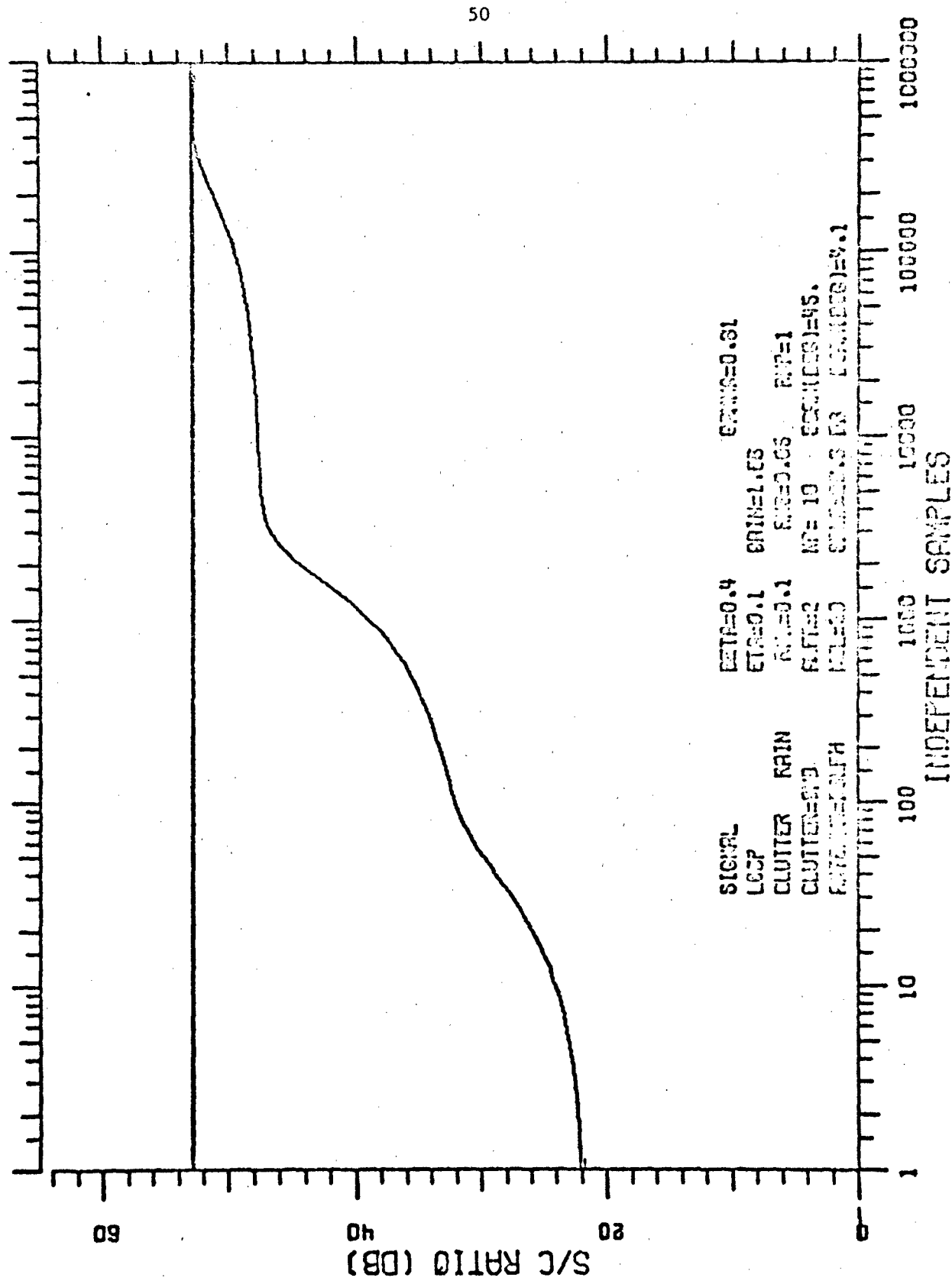
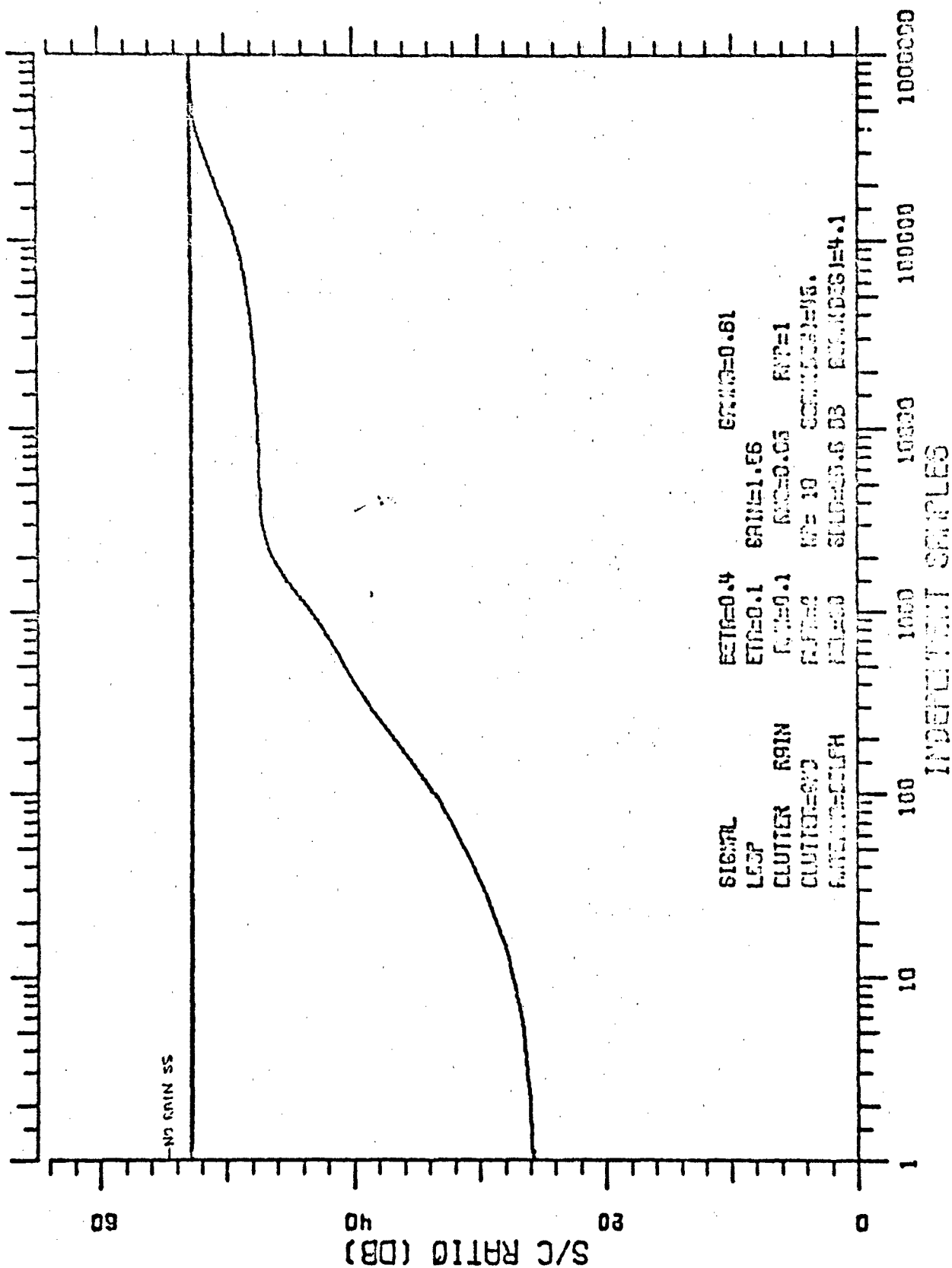


Figure 31



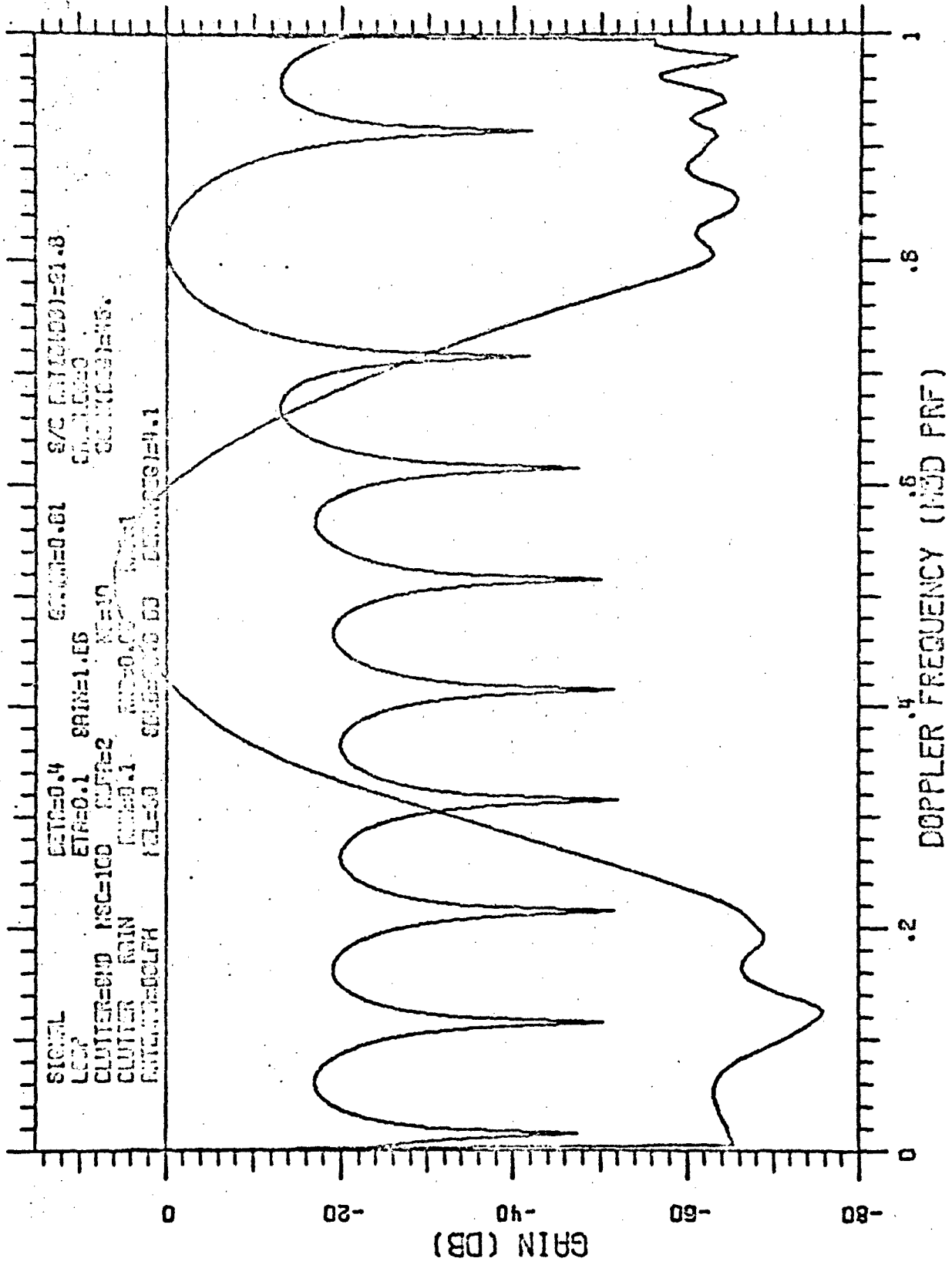


Figure 33

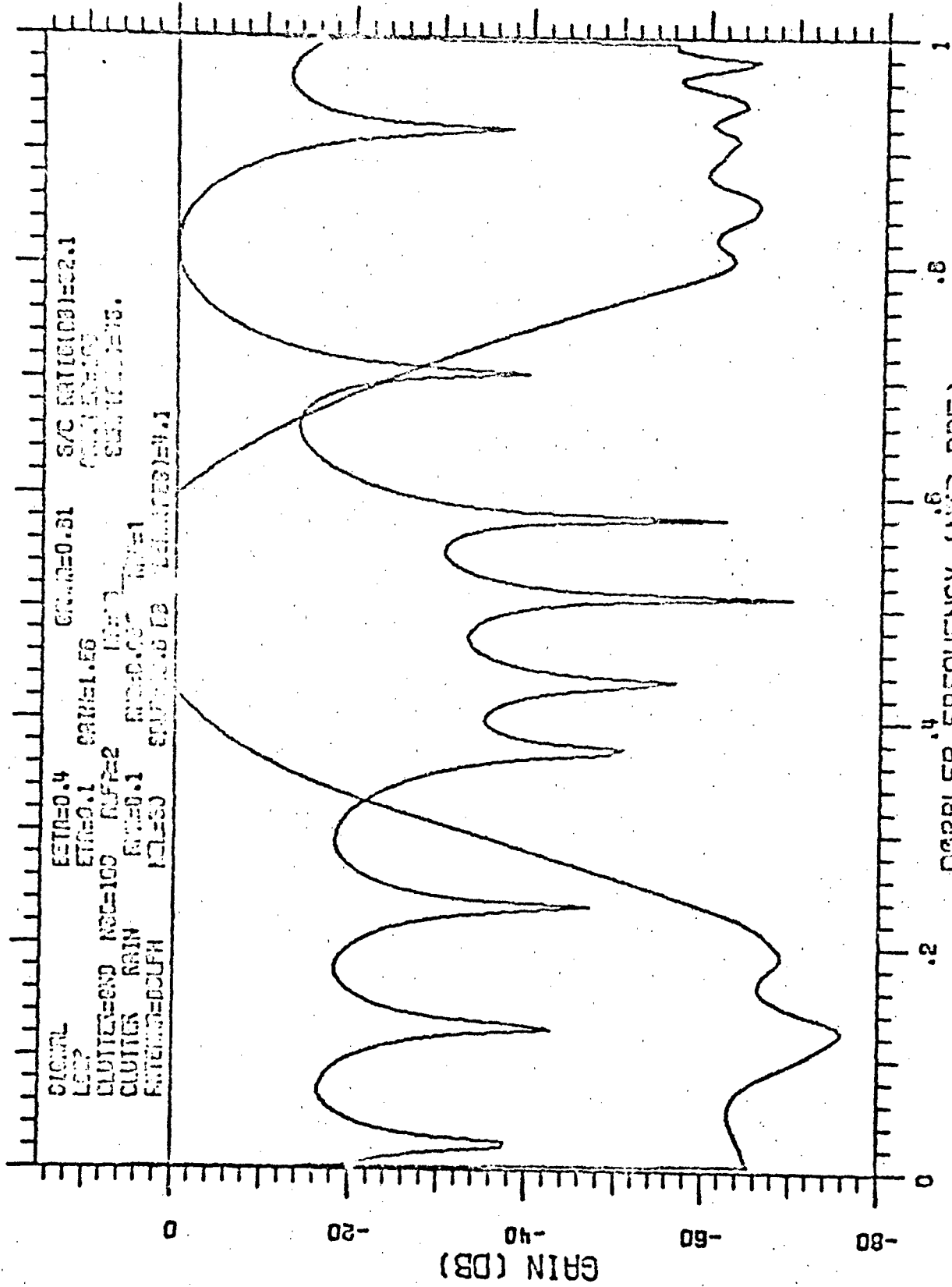


Figure 34

SPECTRA-FILTER, CLUTTER

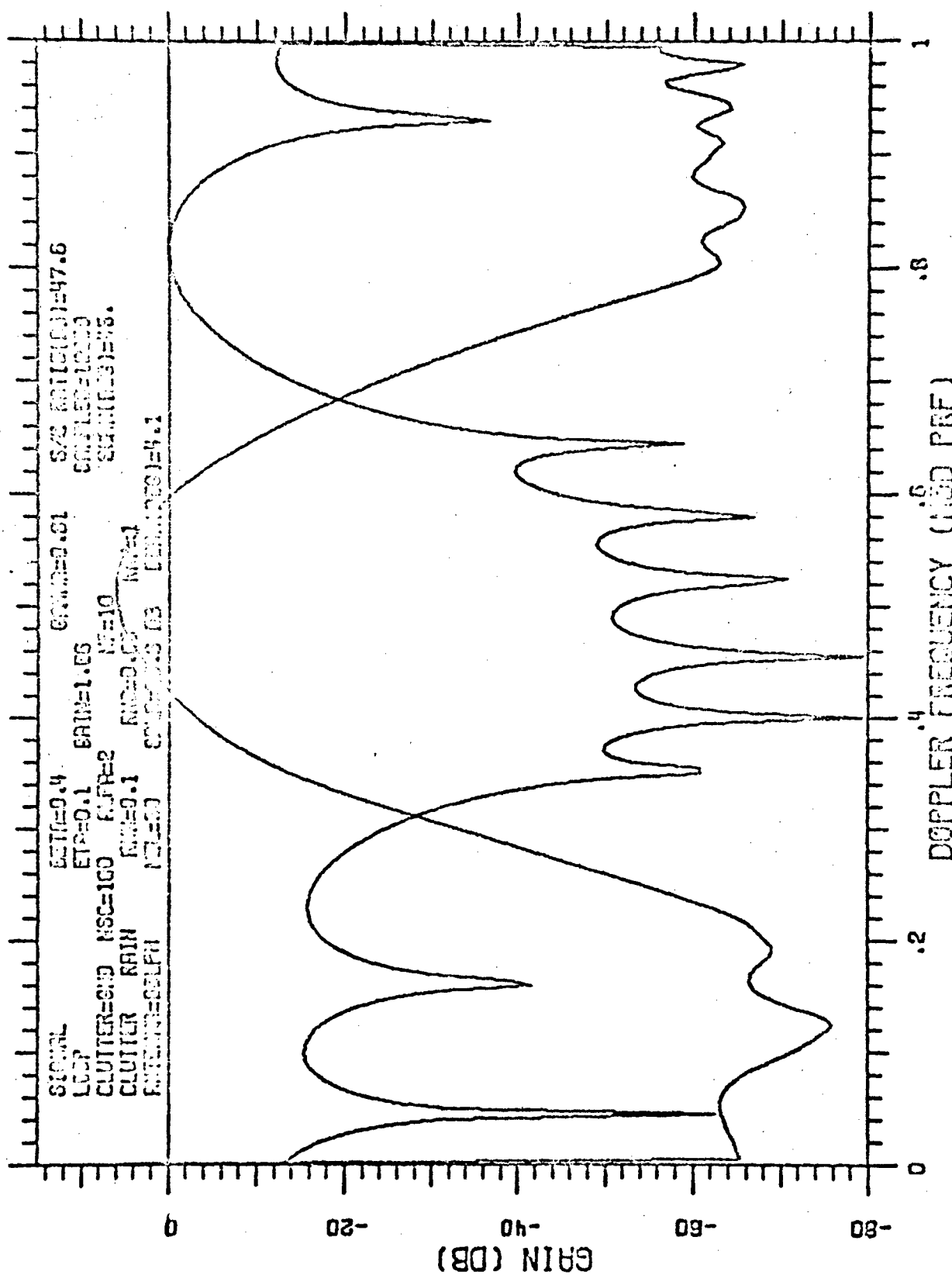


Figure 35

3.3.9 Rain at 0° Scan Angle

(Figures 37 through 40) The broadness of the rain spectrum (compare Figures 12 and 38) can clearly be seen in this case. Of particular interest is the tremendous drop in performance when the initial filter is used (recall that in the no-rain case at 0° scan angle, the initial filter was very good, as shown in Figure 17). There is a slight (2 dB) drop in the MTI gain at steady state.

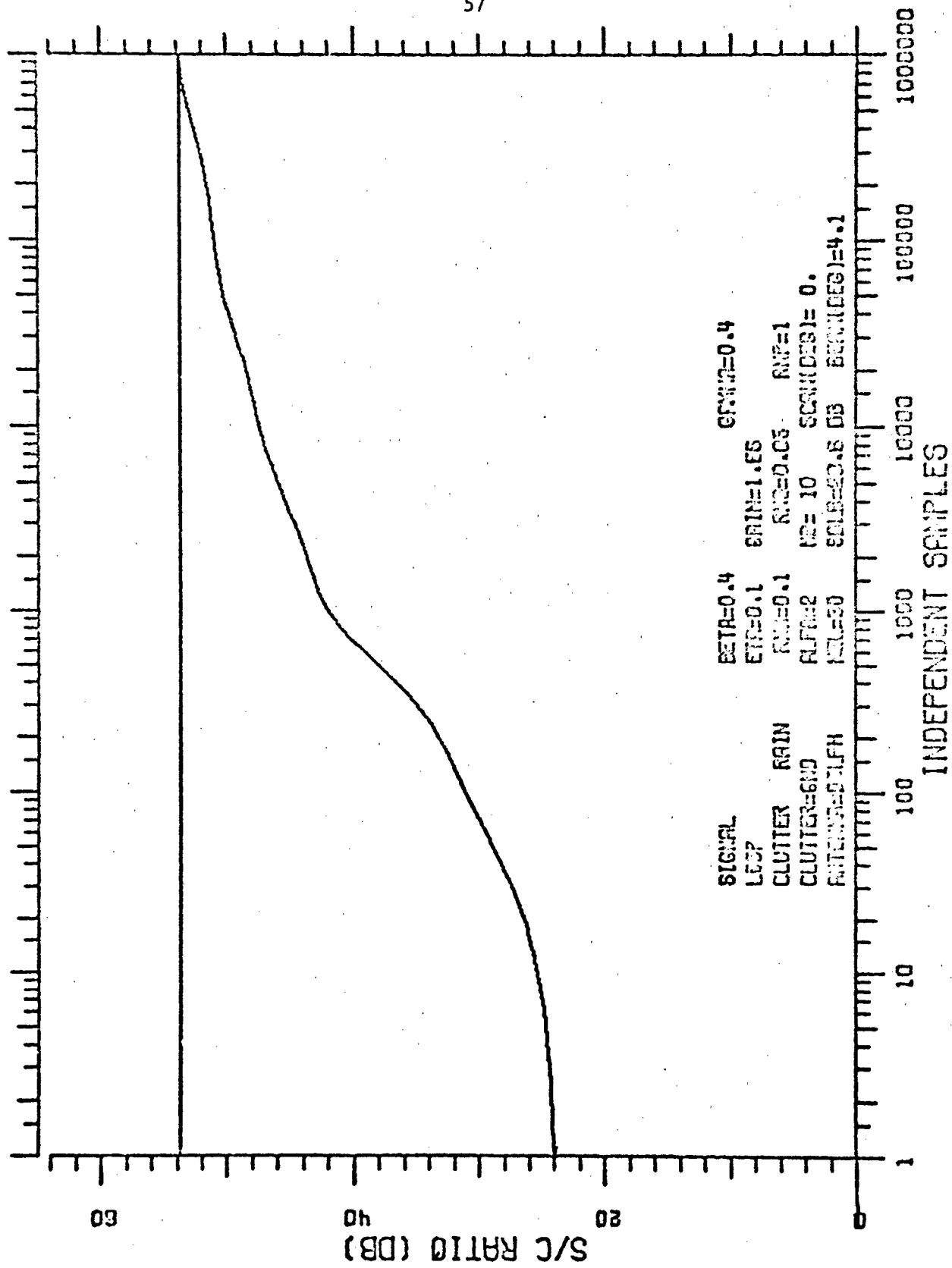


Figure 37

Figure 38

SPECTRA-FILTER, CLUTTER

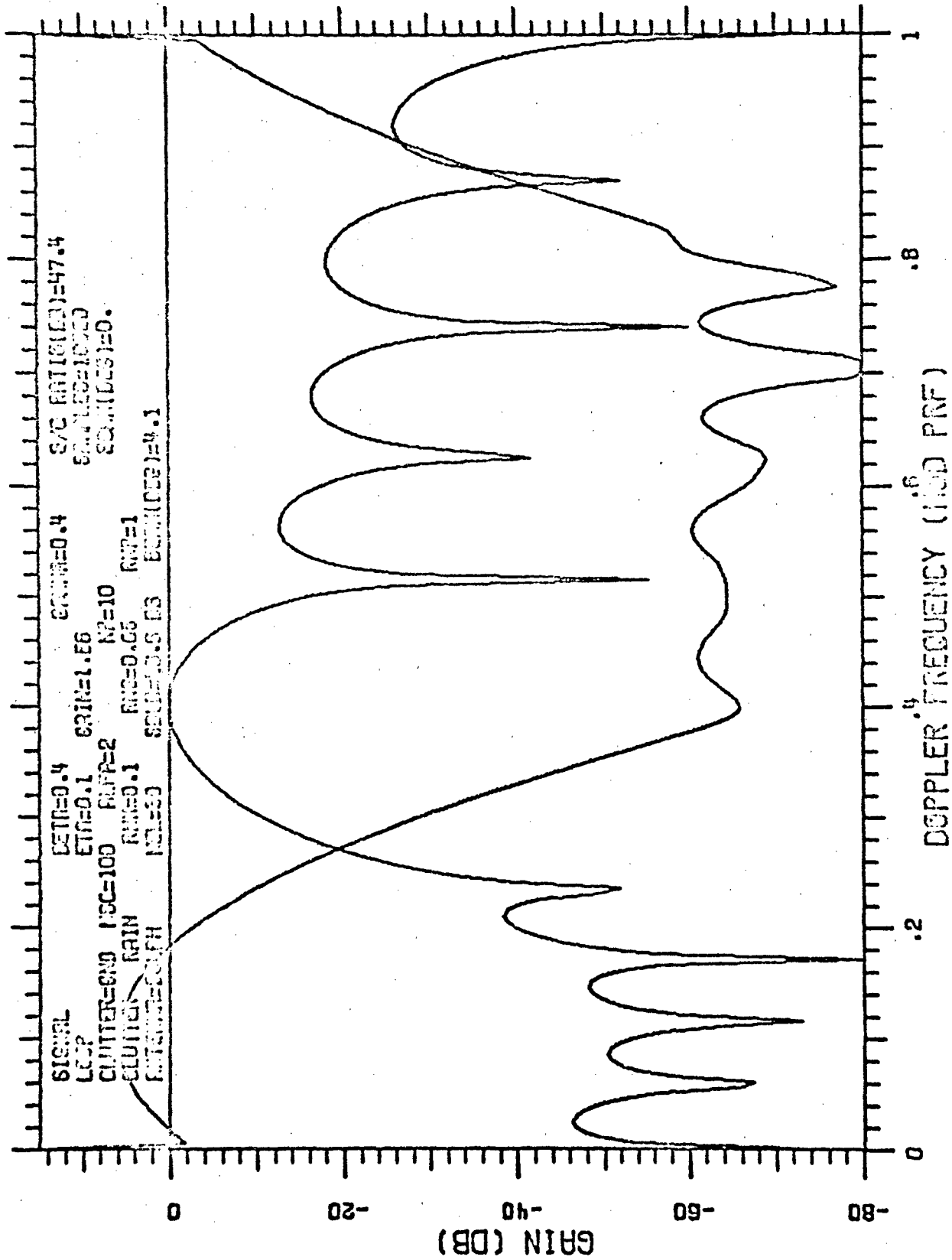


Figure 39

SPECTRA-FILTER, CLUTTER

3.3.10 Increased Rain Power

(Figures 31, 37, 41, and 42) Increasing the rain power relative to the clutter power has the curious effect of increasing the adapted MTI gain. Note however that the input S/C ratio would now drop 11 dB; hence the output S/C ratio would actually be worse. Figures 31 and 41 show the comparison at 45° scan angle; Figures 37 and 42 illustrate the effect of increasing rain clutter power at 0° scan angle.

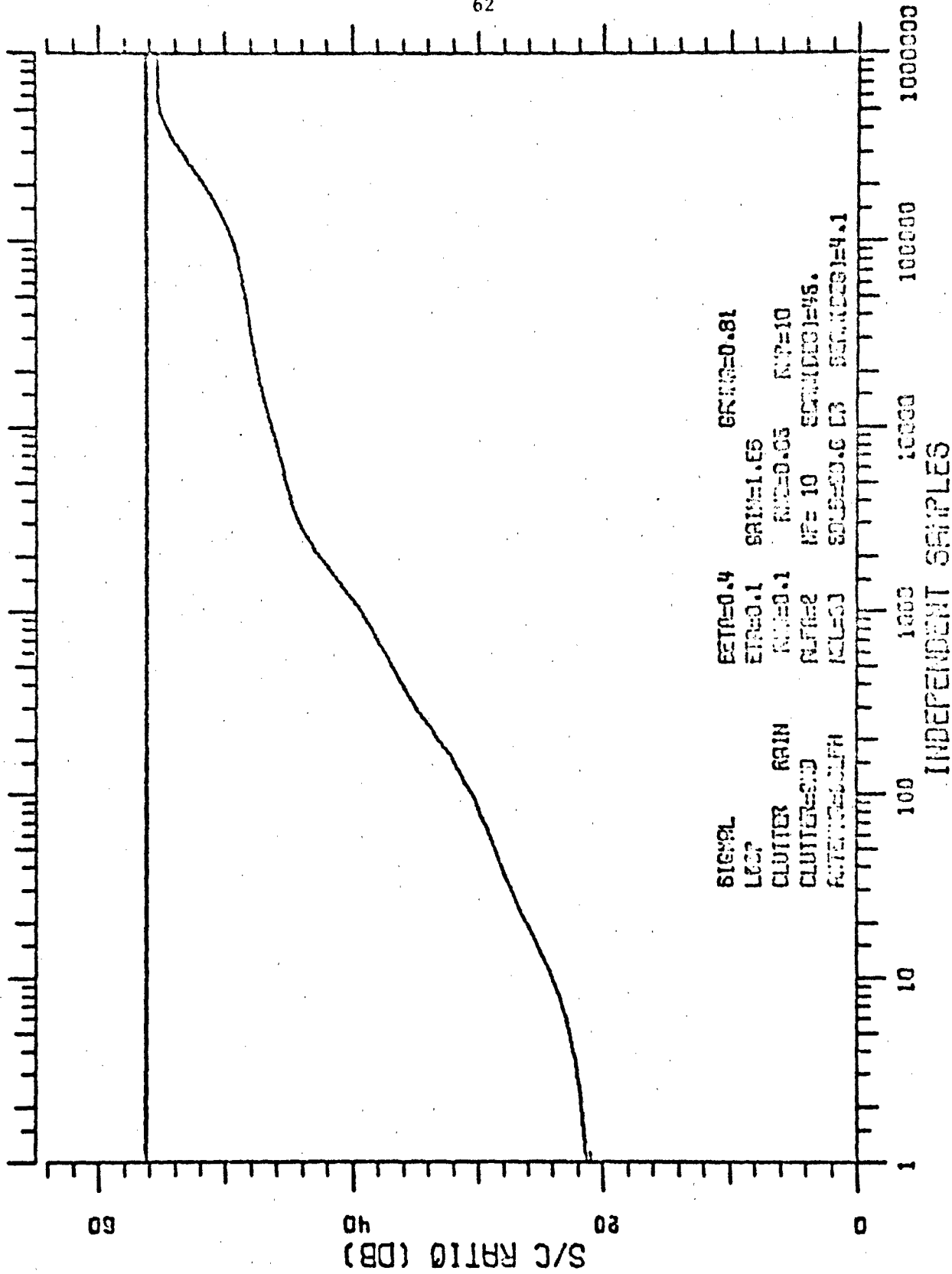
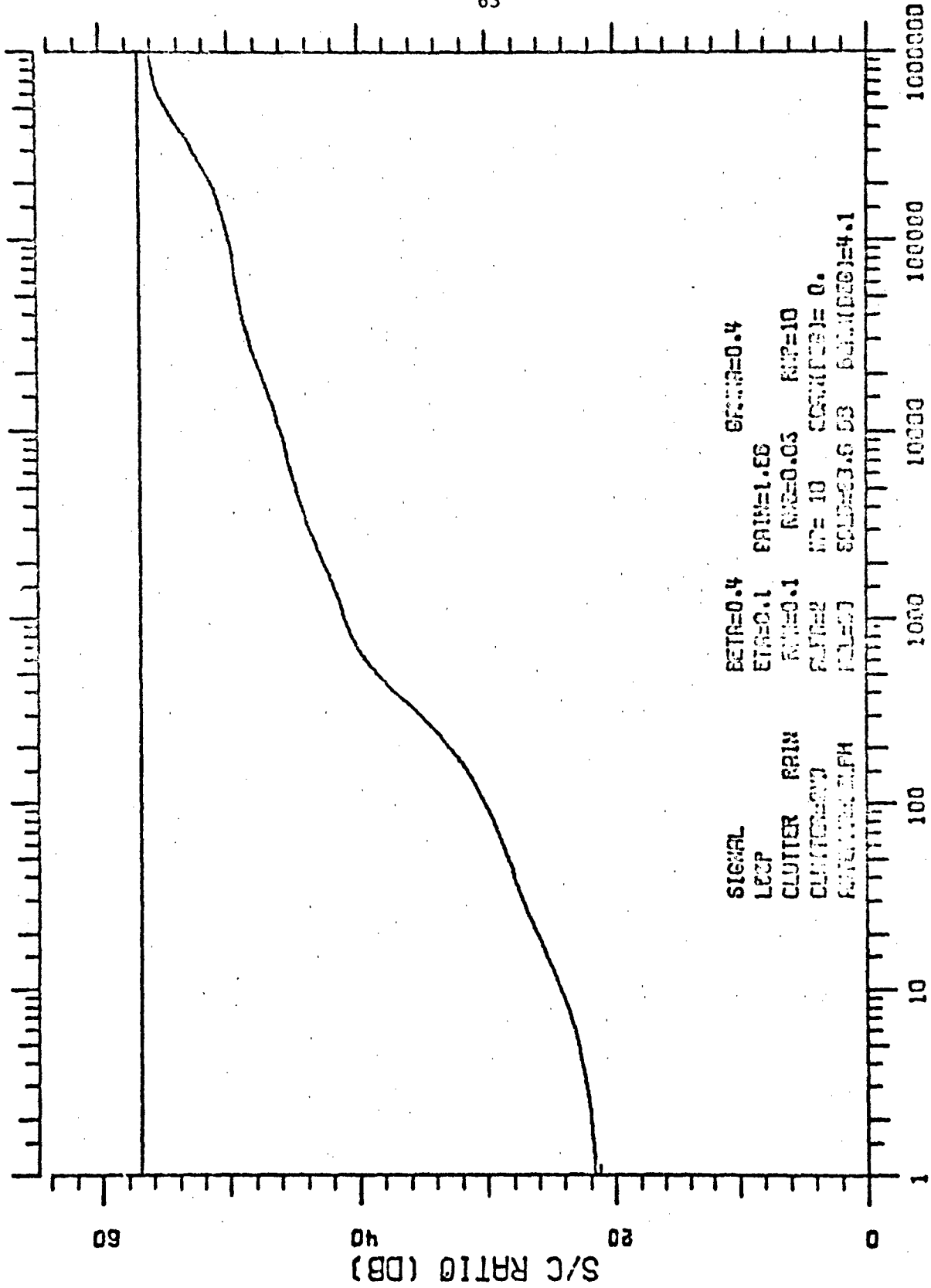


Figure 41

TRANSIENT RESPONSE



INDEPENDENT SAMPLES
 TRANSIENT RESPONSE

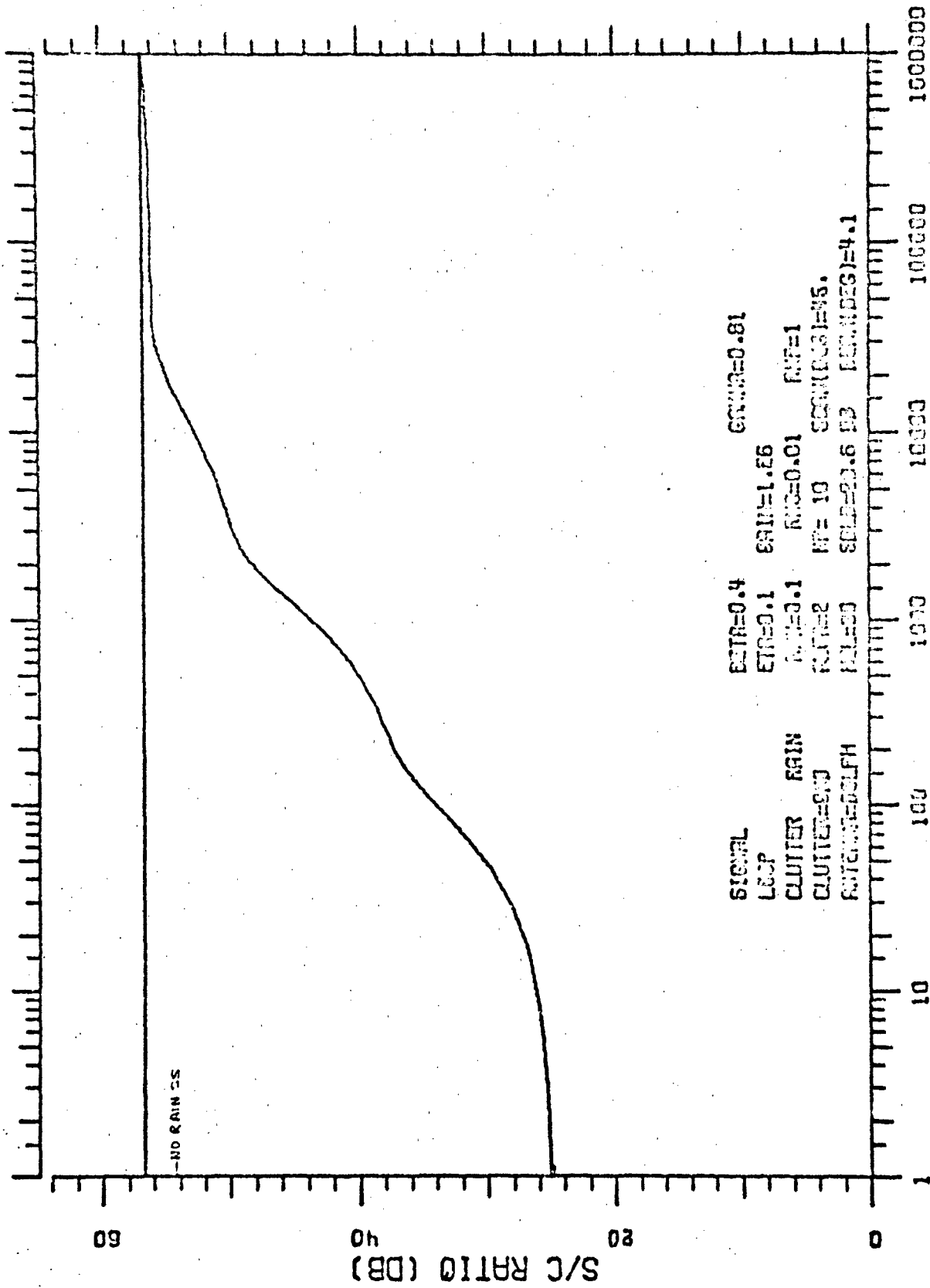
Figure 42

3.3.11 Variation with Rain Spectral Width

(Figures 31 and 43 through 51) When the rain spectral width is reduced to 0.01, the MTI gain increases by about 2 dB over the no-rain case, which is almost enough to compensate the 3 dB drop in input S/C ratio. Thus the effect of this narrow spectrum rain is almost compensated for by adaptation and the actual output S/C ratio drops only 1 dB.

Under extreme rain spectral width ($RNS = 0.1$), a very curious phenomenon occurs in the mean transient response. Adaptation proceeds reasonably well until 4000 samples (Figure 44), but thereafter it diverges most significantly before converging again. Setting the initial weights to their no-rain steady-state mean values (Figure 45), though having a slightly better initial performance and achieving the final steady-state value a little sooner, also has a more serious interim drop in performance. Of particular note is that after 30,000 (after initial weights of GS^*), the performance is worse than initially.

Figures 46 through 51 show the filter response during adaptation for this extreme rain case. The dip in performance is seen to be due to a large filter lobe at other than the design frequency, γ . This is believed to be caused by the relative changes caused in the transformed weights (see Appendix A) as each transformed weight in succession (determined by its corresponding eigenvalue) approaches its asymptotic value. The latter is also believed to be the cause of the staircase-like transient response. We have not yet found a simple way of compensating for this effect.



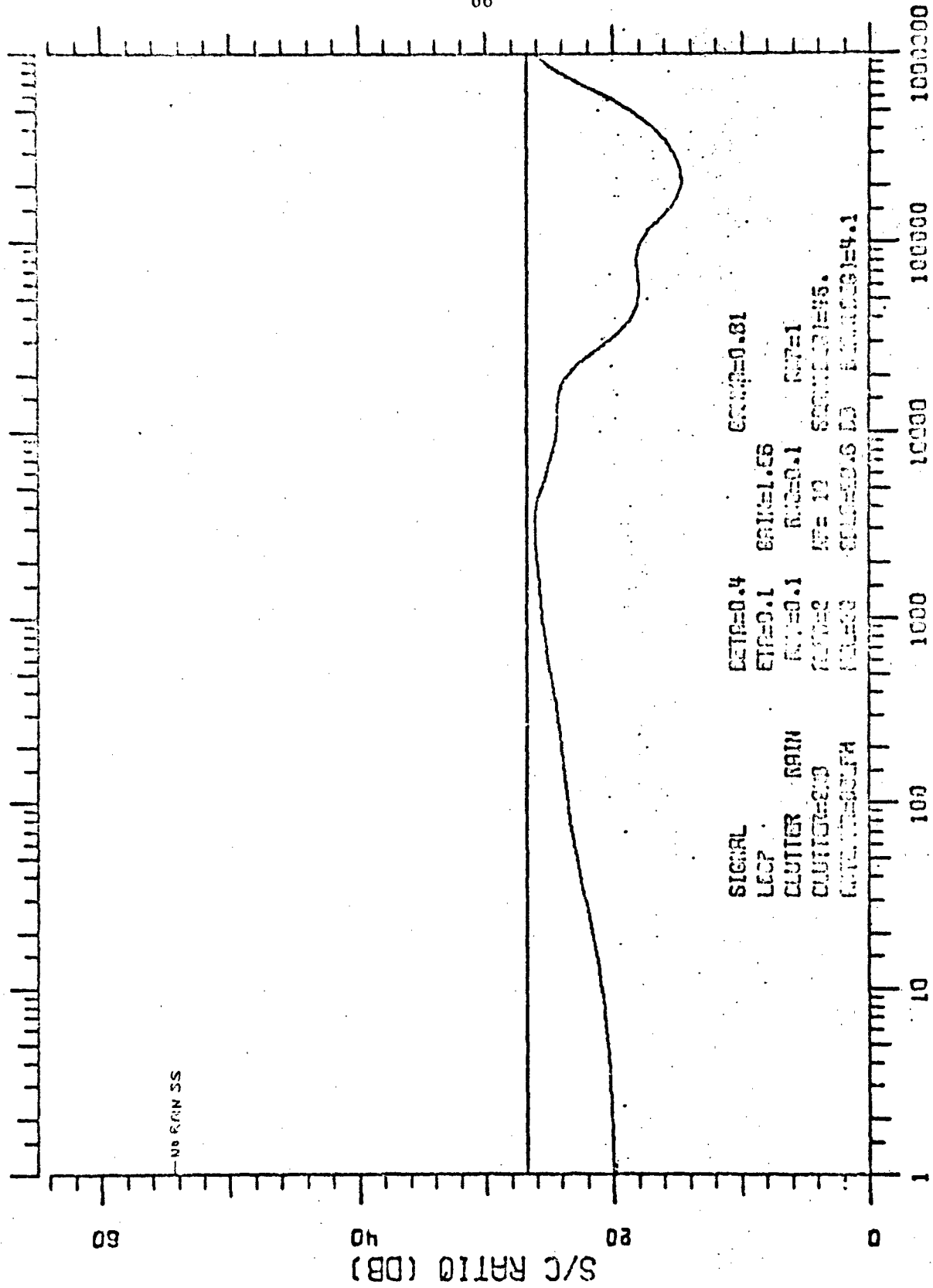


Figure 44

TRANSIENT RESPONSE

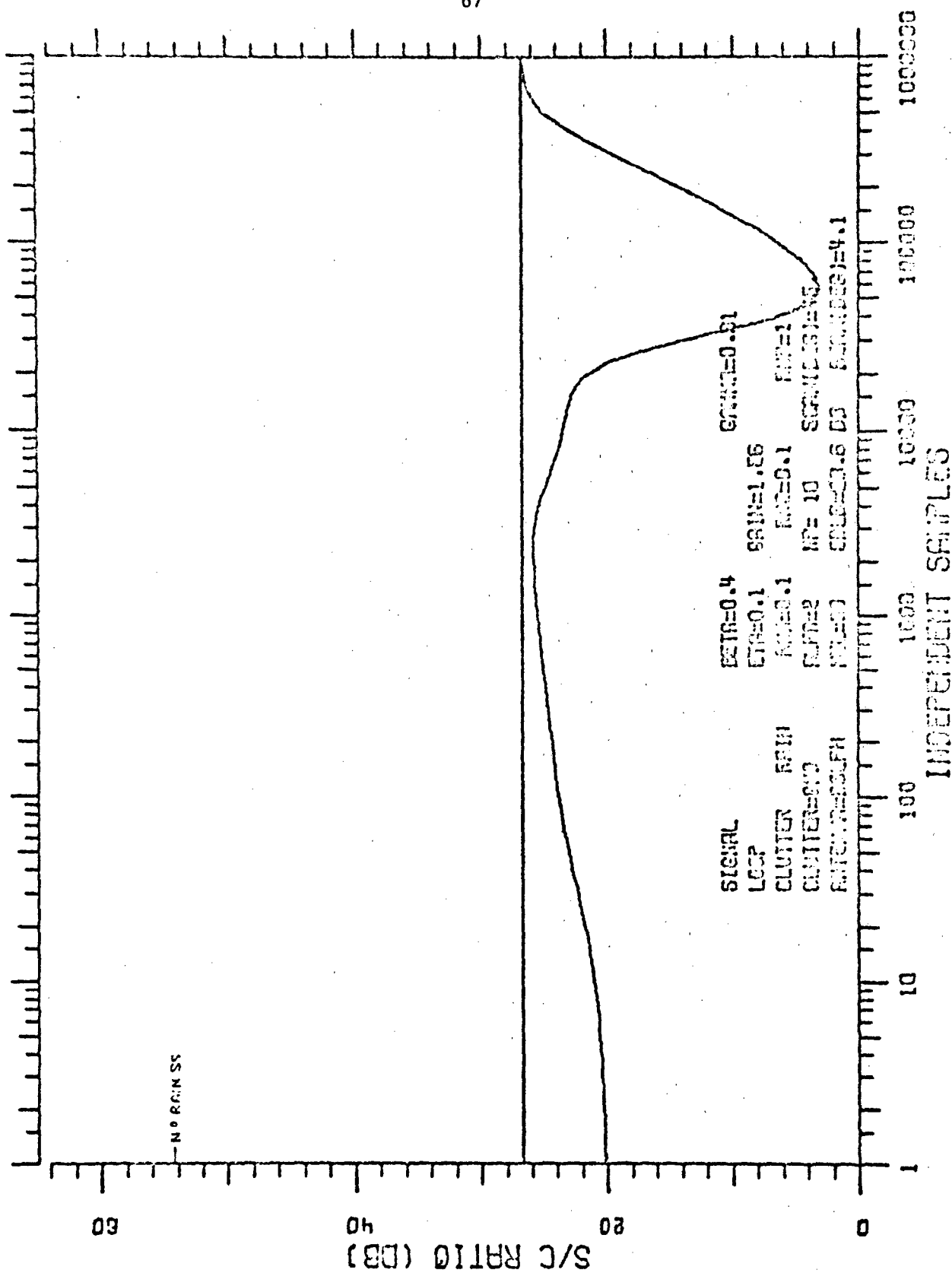


Figure 45

TRANSIENT RESPONSE (RAIN ONSET)

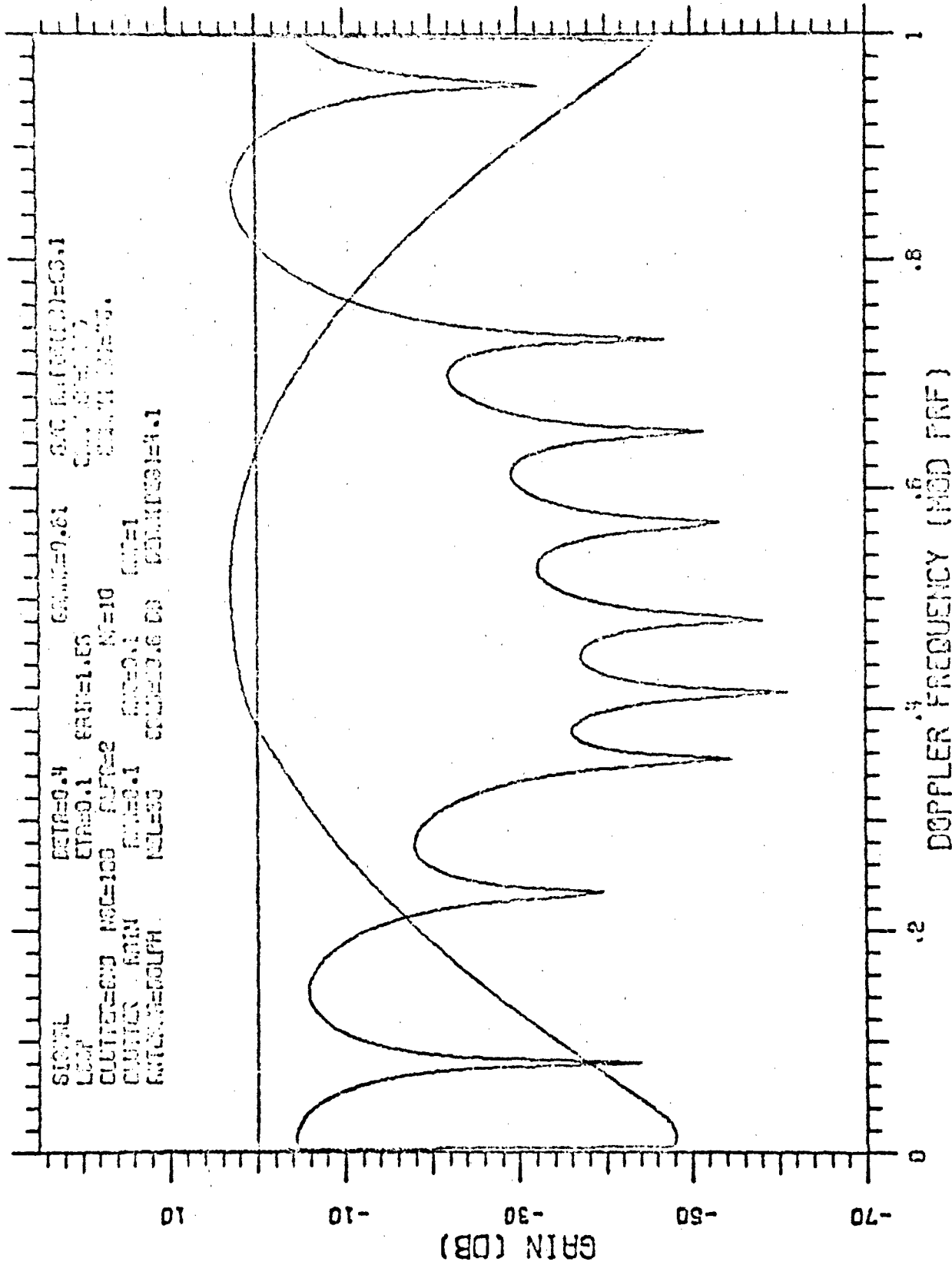


Figure 47

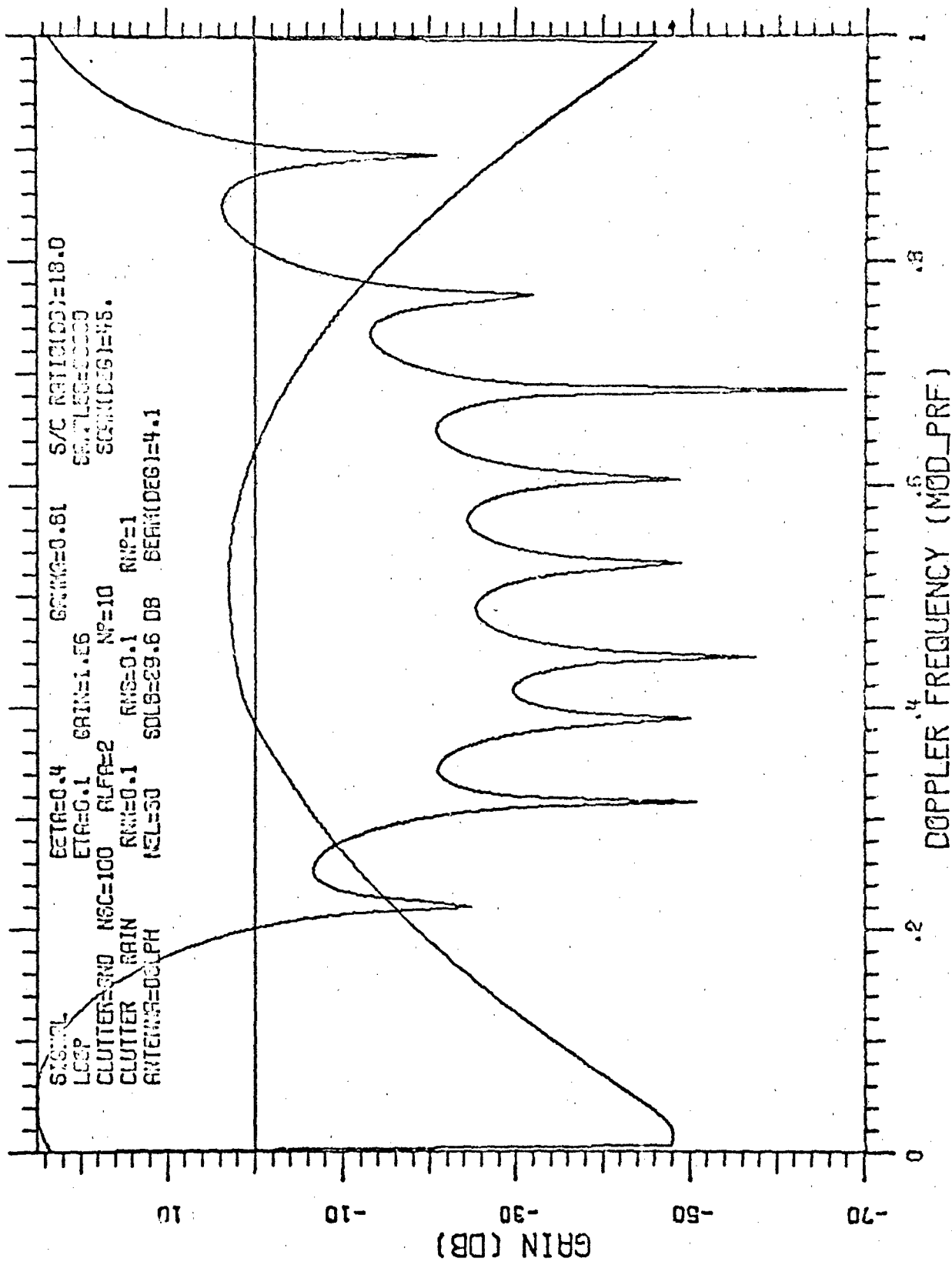


Figure 48

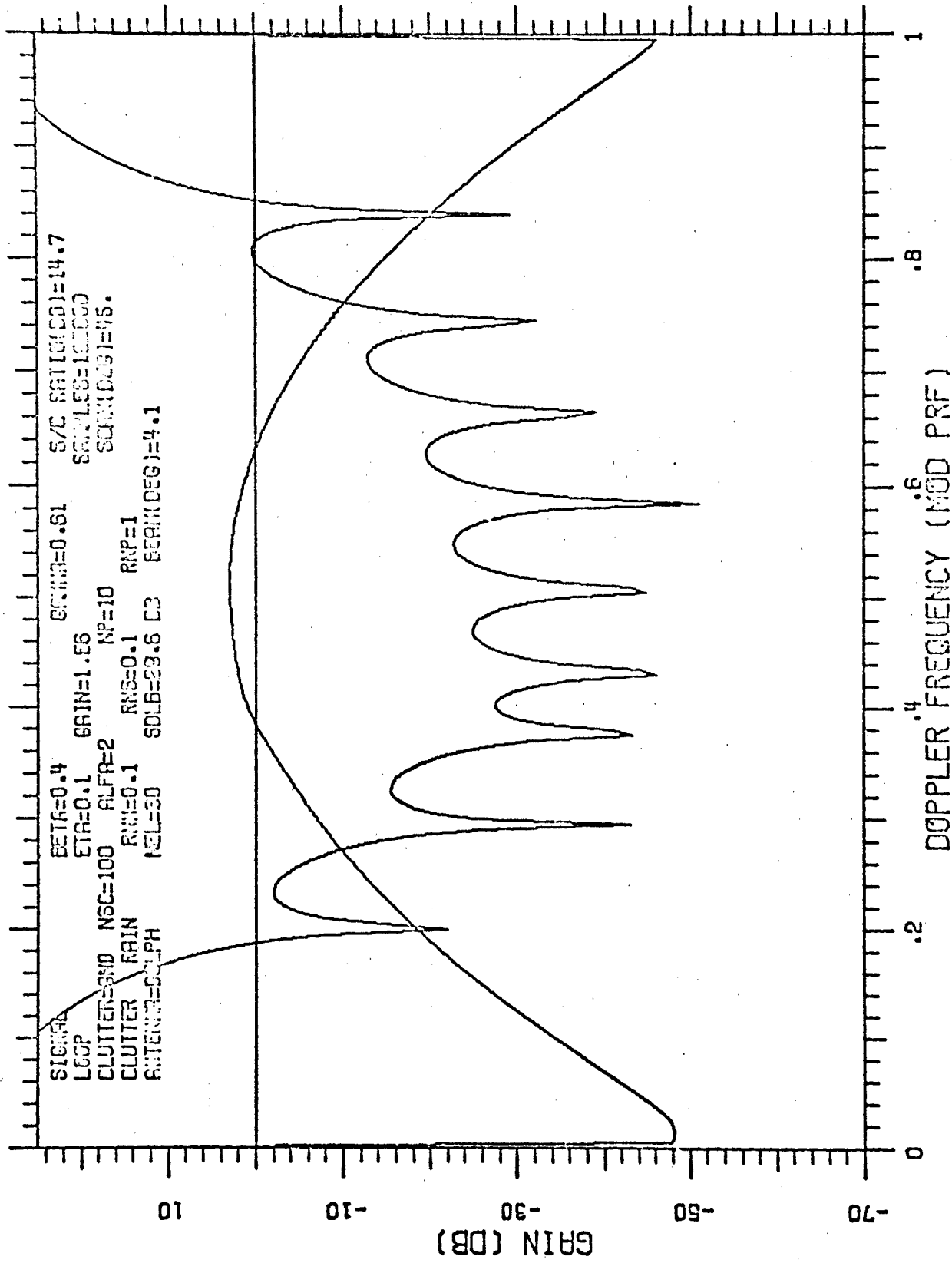


Figure 49

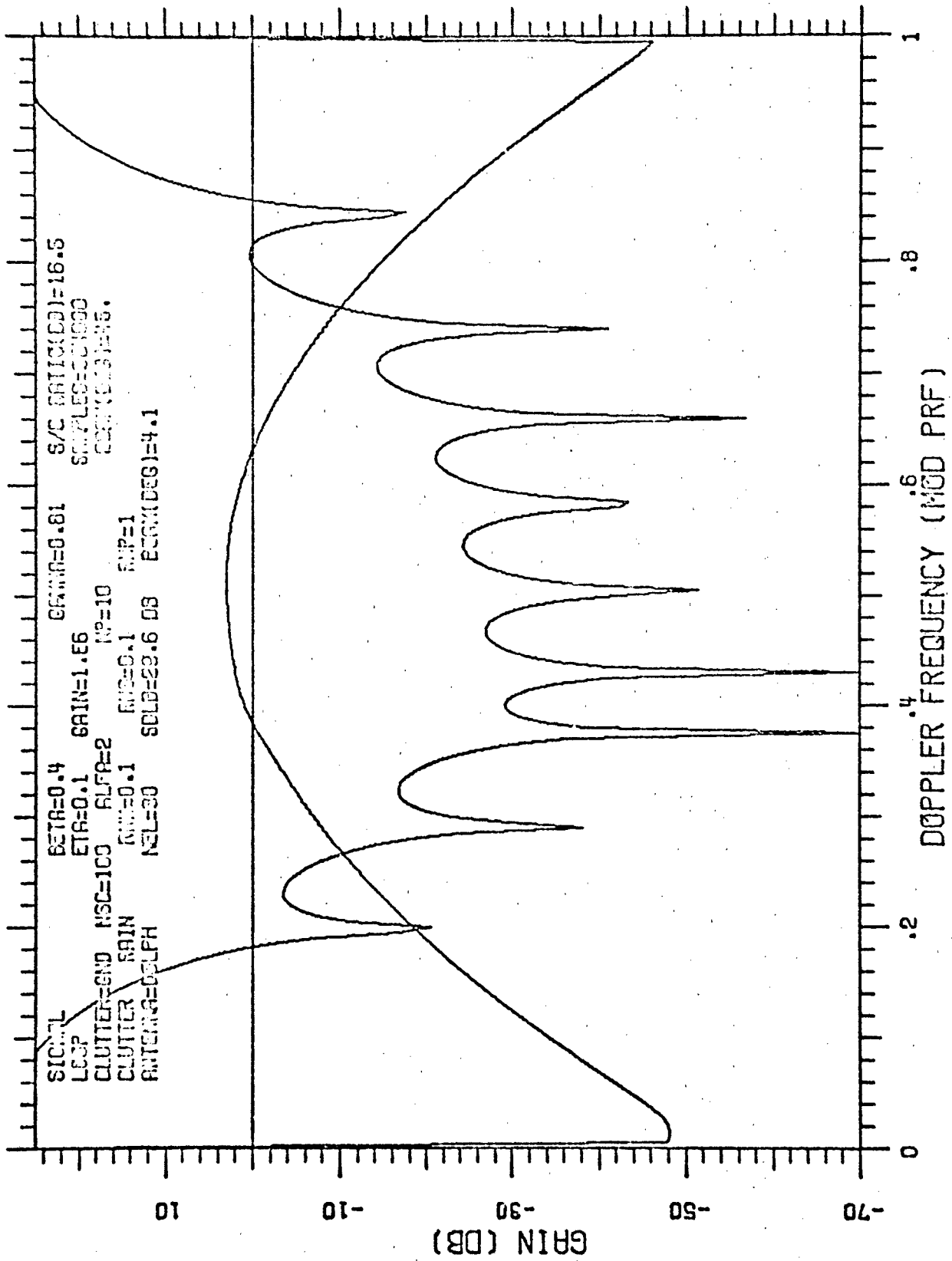


Figure 50

4. SIMPLIFICATION OF ADAPTIVE FILTERS

The complexity of adaptive filters which are implemented digitally depends strongly on the number of bits required at various points in the system. Both the data storage requirements and the amount of computation depend on number of bits. Under earlier contracts, TSC has investigated the effects of quantization noise at various points in the adaptive control loops. These studies were performed for adaptive array antennas, but the results apply directly to the closely analogous case of adaptive filters. It was found by introducing the effects of quantization in an adaptive array simulation that a single bit (one bit in-phase, one bit quadrature) is sufficient at the v_n^* input to the cross-correlator (see Figure 2). An analysis of this simplification was performed under this contract which verifies the simulation results. This analysis appeared in the July 1972 issue of IEEE Trans. AES, and was included in the interim report^[8] on this contract. It is shown that the estimated covariance matrix differs only by a scale factor when this v_n^* input is represented by a single bit per quadrature component. This result permits a major simplification of adaptive filters.

Further study of this problem has shown that a single-bit representation of the v_n^* input to the cross-correlator can be used, i.e., one-bit representation of just one quadrature component. The analysis supporting this conclusion is contained in Appendix B.

5. SUGGESTED AREAS OF RESEARCH AND CONCLUSIONS

As discussed in Section 3 of this report, the Applebaum type of adaptive array gives very good performance for its relatively simple implementation. One way to obtain considerable improved performance would be to estimate the covariance matrix directly, to invert it, and to calculate the weights by $W = \hat{M}^{-1} S^*$. This procedure is not as complex as it first appears since the estimation and inversion only have to be done once for the whole bank of filters (each filter requires its own set of loops), the different filters being obtained by a matrix multiplication. The inversion of the matrix would be the most complicated portion of this procedure. However, the covariance matrix has a peculiar nature (i.e., M_{mn} is a function only of $m-n$ --see Appendix A), which allows it to be inverted in a particularly simple manner (see [6] and [7]). The promise of a considerable improvement in performance at a modest increase in complexity makes this procedure worthy of investigation. Such an investigation may also shed some light on what minor (in complexity) modifications of adaptive loops would yield the most improvement in performance.

The sometimes aberrant behavior (i.e., temporary divergence of the S/C ratio during adaptation) of the loops considered does raise the question of whether variations of adaptive loops (e.g., the Widrow array) also exhibit this behavior.

The effect of the loop noise on the S/C ratio has been determined for the steady-state condition; however, its transient variation during adaptation remains to be investigated.

An important area for further research is AMTI radars with adaptivity in both space and time, i.e., adaptive control of both the antenna pattern and doppler filter response. One important optimization study in space-time adaptive systems is related to the choice of degrees of freedom. For example, a system with 12 degrees of freedom could use a single antenna output with 12-pulse adaptive filtering, three separate antenna outputs on four consecutive pulses, etc. Antenna outputs could be obtained from sub-arrays or separate beams, e.g., sum and difference beams in a reflector antenna with multiple feeds. Methods of speeding convergence in these systems and of simplifying the implementation are important areas for study.

The results reported here show that adaptive filters can provide important improvements in AMTI radars. One advantage of adaptive systems is the ability to sense the presence of rain clutter and re-optimize the filter response. The convergence rates of the adaptive filters are adequate for some applications--the typical convergence times of 1000 to 10^4 samples correspond to 1 to 10 milliseconds in a radar with a 1 microsecond compressed pulse length. The change in clutter due to antenna scan is usually small in this time interval. In other cases, more rapid convergence may be required, e.g., to follow changes in clutter spectrum with range.

REFERENCES

1. L. Brennan and I. Reed, "Optimum Processing of Unequally Spaced Radar Pulse Trains for Clutter Rejection," IEEE Trans. AES, May 1968.
2. L. Brennan, I. Reed, and E. Pugh, "Control Loop Noise in Adaptive Array Antennas," IEEE Trans. AES, March 1971.
3. C. Dolph, "A Current Distribution for Broadside Arrays which Optimizes the Relationship between Beam Width and Side Lobe Level," Proc. IRE and Waves and Electrons, June 1946.
4. F. Nathanson, Radar Design Principles, McGraw-Hill, 1969, p. 206 ff.
5. A. Papoulis, The Fourier Integral and Its Applications, McGraw-Hill, 1962, p. 25, 246.
6. S. Zohar, "Toeplitz Matrix Inversion: The Algorithm of W. F. Trench," J. Assoc. Computing Machinery, Vol. 16, No. 4, October 1969, pp. 592-601.
7. S. Zohar, "Propagation Studies: The Solution of a Toeplitz Set of Linear Equations," JPL Space Programs Summary 37-61, Vol. III, Part K.
8. I. Bottlik, L. Brennan, and G. Lank, "Adaptive Filtering in AMTI Radar," Technology Service Corporation Report TSC-PD-083-1, 28 April 1972.

APPENDIX A

COMPUTATIONAL EQUATIONS

1.0 INTRODUCTION

The equations used in computing the clutter spectrum (ground and rain), covariance matrix, filter weights (optimum, steady-state, and mean transient), and the resulting S/C ratio are outlined in this Appendix. We consider the azimuthal antenna pattern with sidelobes and homogeneous spatially stationary clutter both in azimuth and range. We neglect considerations of the variation of antenna pattern due to radome and near field scatterers, clutter inhomogeneities due to terrain type and incidence angle, elevation antenna pattern, and depression angle. The coordinate system is shown in Figure 3.

2.0 NORMALIZED PARAMETERS

It is convenient to measure the platform velocity V_P , and the target radial velocity (relative to ground), V_T , in terms of the wavelength, λ , and the pulse repetition frequency, f_r .

$$\alpha = 2 V_P / \lambda f_r$$

$$\beta = 2 V_T / \lambda f_r \pmod{1}$$

$$\gamma = \alpha \cos(\psi) + \beta \pmod{1}$$

γ is the target doppler frequency modulo the pulse repetition frequency.

3.0 EQUATIONS

3.1 ANTENNA GAIN

A Dolph-Tschebycheff antenna pattern (see Ref. 3) is used. The two-way antenna power pattern is given by (identical receive and transmit patterns are assumed):

$$g(\sin\phi) = G^4(\phi) = \begin{cases} T_M \left[Z_0 \cos\left(\frac{\pi d}{\lambda} \sin\phi\right) \right] / T_M(0) & -\frac{\pi}{2} \leq \phi \leq \frac{\pi}{2} \\ 0 & \text{otherwise} \end{cases} \quad (1)$$

where

$T_M = M^{\text{th}}$ order Tschebycheff polynomial

$M = \text{NEL} - 1 = 29$

$\text{NEL} = 30 = \text{number of elements}$

$d = \lambda/2 = \text{spacing between elements}$

$Z_0 = 1.01 = \text{parameter determining sidelobe level and beamwidth}$

All cases considered herein use the same antenna pattern with parameter values as shown above, which yield a main beam 3 dB width of 4.1 degrees and a sidelobe level (ratio of mainbeam peak to any sidelobe peak) of 29.6 dB.

3.2. CLUTTER SPECTRUM

We assume spatially stationary homogeneous clutter. The doppler frequency due to a stationary scatterer at angle θ relative to the platform velocity (Fig. 3) is

$$f_d = 2 v_p \cos\theta / \lambda . \quad (2)$$

However, the doppler frequency "folds over" at the pulse repetition frequency, f_r , hence

$$f_d / f_r = \frac{2 v_p \cos\theta}{\lambda f_r} = \alpha \cos\theta \pmod{1}. \quad (3)$$

The clutter spectral density is thus

$$S(f) df = \sum_{\theta \ni \text{mod}(\alpha \cos\theta, 1) = f} G^4(\theta - \psi) \left| \frac{d\theta}{df} \right| df . \quad (4)$$

Let n be an integer, Arccos be the principal $[0, \pi]$ inverse function. Then

$$S(f) = \sum_{\phi = \text{Arccos}\left(\frac{f+n}{\alpha}\right) - \psi} G^4(\phi) \left| \frac{d\phi}{df} \right| + \sum_{\phi = \text{Arccos}\left(\frac{f+n}{\alpha}\right) + \psi} G^4(-\phi) \left| \frac{d\phi}{df} \right| \quad (5)$$

$$-\sin\psi \leq \frac{f+n}{\alpha} < 1 \quad \sin\psi \leq \frac{f+n}{\alpha} \leq 1$$

Let
$$T_1 = \sqrt{1 - \left(\frac{f+n}{\alpha}\right)^2}$$

$$T_2 = \frac{f+n}{\alpha} \quad . \quad \text{Then}$$

$$\sin\theta = T_1 \cos\psi - T_2 \sin\psi \quad (\text{for the 1}^{\text{st}} \text{ summation})$$

(6)

$$= T_2 \cos\psi + T_1 \sin\psi \quad (\text{for the 2}^{\text{nd}} \text{ summation}) .$$

Noting that $\left|\frac{d\phi}{df}\right| = 1/\alpha T_1$ for either summation and recalling that $G^4(\phi) = g(\sin\phi)$ we obtain

$$S(f) = \sum_{n \in N_1} g(T_1 \cos\psi - T_2 \sin\psi)/\alpha T_1 + \sum_{n \in N_2} g(-T_1 \cos\psi - T_2 \sin\psi)/\alpha T_1 \quad (7)$$

where

$$N_1 = \left\{ n \mid -\sin\psi \leq \frac{f+n}{\alpha} \leq 1 \right\}$$

$$N_2 = \left\{ n \mid \sin\psi \leq \frac{f+n}{\alpha} \leq 1 \right\}$$

$$T_1 = \sqrt{1 - \left(\frac{f+n}{\alpha}\right)^2}$$

$$T_2 = \frac{f+n}{\alpha}$$

$g(\sin\phi)$ is defined in Eq. 1.

3.3 GROUND CLUTTER COVARIANCE

Let N be the number of pulses to be processed coherently. The n^{th} pulse voltage return from a scatterer at angle θ is given by (normalized to the first pulse):

$$a_n = e^{12\pi\alpha(n-1) \cos\theta} G^2(\theta-\psi) \quad (8)$$

The contribution of this clutter element to the clutter covariance is given by:

$$M_G = A^* A^T \quad (9)$$

where A is column vector of the a_n .

$$\begin{aligned} \text{Thus } M_G(m,n) &= \int e^{-12\pi(m-1)\alpha\cos\theta} G^2(\theta-\psi) \\ &\quad \times e^{12\pi(n-1)\alpha\cos\theta} G^2(\theta-\psi) d\theta \\ &= \int G^4(\theta-\psi) e^{-12\pi(m-n)\alpha\cos\theta} d\theta \end{aligned} \quad (10)$$

Since $G^4(\phi) = G^4(-\phi)$, $G(\phi) = 0$ for $|\phi| > \pi/2$

$$M_G(m,n) = \int_0^{\pi/2} G^4(\phi) \left[e^{-12\pi(m-n)\alpha\cos(\phi-\psi)} + e^{-12\pi(m-n)\alpha\cos(\phi+\psi)} \right] d\phi \quad (11)$$

The preceding integral is approximated by a sum of $NSC/2$ equally spaced angles over the region $(0, \pi/2)$. This matrix is scaled so that the diagonal terms (which are all equal) have the value of which corresponds to unity input clutter power. Note that the covariance matrix is really only a function of $m-n$.

3.4 RAIN CLUTTER SPECTRUM

Following Nathanson [Ref. 4], we assume that the rain spectrum is Gaussian. It is again convenient to introduce normalized parameters for the mean rain velocity (relative to ground), V_R , and the standard deviation of the spectrum (mainly due to wind shear effects), σ_R . Thus let

$$\mu = RNM = 2 V_R / \lambda f_r$$

$$\sigma = RNS = 2 \sigma_R / \lambda f_r .$$

Due to platform motion, the normalized mean relative to the radar is $\mu + \alpha \cos \psi$. The rain clutter spectrum (normalized to unit power) is hence

$$S_R(f) = \frac{1}{\sqrt{2\pi} \sigma} e^{-\frac{(f - \mu - \alpha \cos \psi)^2}{2\sigma^2}} \quad (12)$$

The above analysis ignores the "fold over" of the doppler frequency due to the pulse repetition frequency, however, it is an excellent approximation as long as σ is say less than 0.1.

3.5 RAIN CLUTTER COVARIANCE

The rain clutter correlation function is the inverse Fourier transform of its spectrum, i.e.

$$R(\tau) = \mathcal{F}^{-1} S_R(f) = \int S_R(f) e^{j2\pi f\tau} df. \quad (13)$$

From Reference 5

$$\mathcal{F} e^{-at^2} = \sqrt{\frac{\pi}{a}} e^{-\omega^2/4a}$$

hence,

$$R(\tau) = e^{j2\pi(\mu + a\cos\psi)f_r\tau} e^{-2(\pi\sigma f_r\tau)^2}, \quad (14)$$

and the clutter covariance matrix is

$$M_R(m,n) = e^{j2\pi(\mu + a\cos\psi)(m-n)f_r} e^{-2(\pi\sigma(m-n))^2} \quad (15)$$

3.6 COMBINING RAIN AND GROUND CLUTTER

Let $\rho = RNP$ be the ratio of the total rain power to the total ground power. The rain and ground covariances and spectra have been normalized to unit power. Hence, since the rain and ground clutter are assumed statistically independent, the total covariance (also normalized to unit power) is given by

$$M(m,n) = \frac{1}{1+\rho} M_G(m,n) + \frac{\rho}{1+\rho} M_R(m,n) \quad (16)$$

Note again that all the covariances are really only functions of $m-n$.

The total spectrum is given by

$$S(f) = \frac{1}{1+\rho} S_G(f) + \frac{\rho}{1+\rho} S_R(f) \quad (17)$$

3.7 OPTIMUM FILTER

As has been shown in Section 2 of this report, the weights for an optimum filter are given by (or proportional to):

$$W = M^{-1} S^* \quad (18)$$

$$\text{where } S^*(n) = e^{-j2\pi(\alpha \cos \psi + \beta)(n-1)} \quad (19)$$

Since the eigenvalues and eigenvectors of M will be required for the analysis of the transient behavior we obtained the optimum weights by a different computational procedure. We compute Q and Λ such that Λ is diagonal, $Q^{*T}Q = I$, and

$$Q^{-1} M Q = \Lambda \quad (20)$$

$$W = Q \Lambda^{-1} Q^{*T} S^* = M^{-1} S^* \quad (21)$$

Note that since Λ is diagonal, the computation of Λ^{-1} is trivial.

3.8 FILTER RESPONSE

$$S(f) = \left| \sum_{n=1}^N e^{j2\pi f(n-1)} W(n) \right|^2 \quad (22)$$

The spectral response is normalized to 0 dB at $f = \gamma$ which is the observed doppler frequency of a target with a normalized radial velocity β relative to ground.

3.9 OPTIMUM S/C RATIO

The optimum S/C Ratio has been shown to be^f

$$S/C = S^T M^{-1} S^* \quad (23)$$

Again since certain routines and items will be needed for the transient analyses, we used the equivalent computational formula

$$\begin{aligned} S/C &= \frac{w_T^* s^* s_T w}{w_T^* \Lambda w} = \frac{s_T \Lambda^{-1} s^* s_T \Lambda^{-1} s^*}{s_T \Lambda^{-1} \Lambda \Lambda^{-1} s^*} \\ &= s_T \Lambda^{-1} s^* = s_T Q \Lambda^{-1} Q^{-1} s^* = S_T M^{-1} S^* \end{aligned}$$

where $W = Qw$
 $S^* = Q s^*$

(24)

3.10 LOOP NOISE FACTOR

It has been shown[#] (when the loop noise is small) that the total noise in the filter output is increased by the following factor due to control loop noise. This equation is derived in Appendix C.

$$C = 1 + \frac{G\Delta t}{2\tau} T_r \quad (25)$$

where G = control loop gain

Δt = time between independent samples

τ = control loop time constant

T_r = Trace of the covariance matrix (Trace (M))

3.11 MEAN TRANSIENT WEIGHTS

It has been shown that the mean transient transformed weights are given by[#]

$$w_n(t) = \left(w_{no} - \frac{s_n^*}{\lambda_n + 1/G} \right) e^{-(\lambda_n + 1/G) \frac{Gt}{\tau}} + \frac{s_n^*}{(\lambda_n + 1/G)}$$

where w_{no} = initial transformed weights w

$W = Qw$

$S^* = Q s^*$

λ_n = elements of Λ

(26)

[#] See Ref. 2.

We define $\eta = C - 1 = \frac{G(\Delta t)T_r}{2\tau}$ as the loop noise factor. Then the mean transient weights are

$$w_n(i) = \left(w_{no} - \frac{s_n^*}{\lambda_n + 1/G} \right) e^{-(\lambda_n + 1/G) \frac{2n}{T_r} i} + \frac{s_n^*}{\lambda_n + 1/G} \quad (27)$$

where i = the number of independent samples, spaced Δt apart

G = control loop gain (determined by allowable steady-state degradation from optimum performance)

T_r = trace of covariance matrix (total clutter power in all N pulses)

η = loop noise factor (was shown to be 0.1)

3.12 MEAN TRANSIENT RESPONSE

We have calculated the mean transient response using

$$S/C = \frac{w_T^* S^* S_T w}{w_T^* \Lambda w}$$

where w are the mean transient transformed weights. This neglects the effect of loop noise on the S/C ratio, however, loop noise is by design (choice of noise factor) quite small so the above approximation is close. As shown in Appendix C, the 2nd order transient moment of the weights is required to determine this loop noise, which can be determined by an

iterative procedure. For the steady-state a direct solution has been found (i.e., the noise factor) but no simple solution for the transient loop noise has yet been found.

APPENDIX B

GENERAL EFFECT OF ENVELOPE NORMALIZATION IN ADAPTIVE ARRAY CONTROL LOOPS

G. W. Lank

INTRODUCTION

The properties of an adaptive array antenna, including transient response rate and control loop noise, depend on the intensity of the external noise field. The dependence can be reduced by a general envelope normalization. This can be done without degrading the performance of the adaptive array. Special cases of the normalization are envelope limiting, considered in [4], and one-bit digitization of the real and imaginary parts of the signal from which the envelopes are formed, considered in [5].

Another important special case is one-bit digitization of the imaginary part of the signal from which the envelopes are formed while the real part is set to zero.

DISCUSSION

Adaptive array antennas have been discussed in [1], [2], and [3] by, respectively, Widrow, Applebaum, and Brennan, et al. In [4], by Brennan and Reed, it is shown that envelope limiting in the control loops reduces the effects of varying noise intensity without degrading array performance. In [5], by Lank and Brennan, this is also shown to be true when one-bit digitization of the real and imaginary parts of the signal from which the

envelope is obtained is performed instead of envelope limiting. It will be shown that the results of [4] and [5] are special cases of a general envelope normalization to be defined.

Another important special case of the general result is to digitize to one bit the imaginary part of the signal from which the envelope is obtained while setting the real part to zero. This eliminates one-half the multiplications in the control loop (as well as eliminating the storage of the real part of the signal from which the envelope is formed in some adaptive systems).

The loops considered are those analyzed in [3] and [4].

Let v_m = the complex video input to the m^{th} array element, v_m^* = the complex conjugate of v_m , and $f(v_m^*)$ = the function of the envelope applied to the control loops.

As a direct consequence of the results of [3], the average value of the transient response of the loops as well as the steady-state RMS noise are only dependent on the covariance matrix

$$A_{mn} = E[f(v_m^*)v_n] \quad (1)$$

This is true, assuming the loop time constants are long compared to the correlation times of v_n and the steady-state RMS noise is small.

Let

$$v_m = R_m e^{j\phi_m} \quad (2)$$

Then assume

$$f(v_m^*) = f(R_m e^{-j\phi_m}) = g(e^{-j\phi_m}) \quad (3)$$

Thus (3) assumes that the function of the envelope applied to the loops is only a function of ϕ_m . Hence it is a general normalization in that $f(v_m^*)$ is independent of R_m .

References [4] and [5] can be considered special cases of (3). In [4],

$$f(v_m^*) = g(e^{-j\phi_m}) = e^{-j\phi_m} \quad (4)$$

while in [5],

$$f(v_m^*) = g(e^{-j\phi_m}) = \begin{cases} 1-j, & 0 \leq \phi_m < \pi/2 \\ -1-j, & \pi/2 \leq \phi_m < \pi \\ -1+j, & \pi \leq \phi_m < 3\pi/2 \\ 1+j, & 3\pi/2 \leq \phi_m < 2\pi \end{cases} \quad (5)$$

As in [4] and [5], we shall calculate the covariance matrix in (1) for the case where v_n is a zero mean complex stationary Gaussian process.

The joint probability density of R_m, ϕ_m, R_n, ϕ_n is given as in [4] by

$$p(R_m, R_n, \phi_m, \phi_n) = \frac{R_m R_n}{4\pi^2 \sigma^4 (1-\rho^2)} \exp \left\{ -\frac{R_m^2 + R_n^2 - 2\rho R_m R_n \cos(\phi_n - \phi_m - \psi)}{2\sigma^2 (1-\rho^2)} \right\} \quad (6)$$

where

$$\sigma^2 = \frac{1}{2} E\{|v_m|^2\} = \frac{1}{2} E\{|v_n|^2\}; \quad E\{v_m^* v_n\} = 2\sigma^2 \rho e^{i\psi} = M_{mn}$$

$$E\{v_m v_n\} = 0$$

From the above, the elements of the covariance matrix A are

$$A_{mn} = \int_0^{2\pi} d\phi_m \int_0^\infty dR_m \int_0^\infty dR_n \int_0^{2\pi} d\phi_n \mathcal{E} \left(e^{-j\phi_m} \right) R_n e^{j\phi_n} p(R_m, R_n, \phi_m, \phi_n) \quad (7)$$

Let $\beta = \phi_n - \phi_m - \psi$ in (7). Then, using (6) and the periodicity of the cosine function, (7) becomes

$$A_{mn} = \frac{1}{2\pi} \int_0^{2\pi} \mu_{mn} \mathcal{E} \left(e^{-j\phi_m} \right) e^{j\phi_m} d\phi_m \quad (8)$$

where

$$\mu_{mn} = \int_0^\infty dR_m \int_0^\infty dR_n \int_0^{2\pi} d\beta \frac{R_m^2 R_n^2}{2\pi\sigma^4(1-\rho^2)} \exp \left\{ -\frac{R_m^2 + R_n^2 - 2\rho R_m R_n \cos\beta}{2\sigma^2(1-\rho^2)} + j(\beta+\psi) \right\} \quad (9)$$

In [4], μ_{mn} is obtained (see Eqs. (8) to (13) inclusive of [4]), as

$$\mu_{mn} = \sqrt{\frac{\pi}{8}} \frac{M_{mn}}{\sigma} \quad (10)$$

Thus, substituting (10) into (8), one obtains

$$A_{mn} = \frac{M_{mn}}{\sigma\sqrt{32\pi}} \int_0^{2\pi} \mathcal{E} \left(e^{-j\phi_m} \right) e^{j\phi_m} d\phi_m \quad (11)$$

As in [4] and [5], the elements of the covariance matrix A differ from the elements of M only by a common factor which is proportional to $1/\sigma$. Thus

the transient response will be independent of σ and the performance will not be degraded as a result of a general envelope normalization as specified by $f(v_m^*)$ in (3).

If the particular cases of (4) and (5) are substituted into (11) for $g(e^{-j\phi_m})$, then the results in [4] and [5] for A_{mn} are obtained.

Consider the following case:

$$f(v_m^*) = g(e^{-j\phi_m}) = \begin{cases} -j, & 0 \leq \phi_m < \pi \\ & \text{i.e., } \text{Im } v_m^* \geq 0 \\ j, & \pi \leq \phi_m < 2\pi \\ & \text{i.e., } \text{Im } v_m^* < 0 \end{cases} \quad (12)$$

Substituting (12) into (11), one has

$$A_{mn} = \frac{1}{\sqrt{2\pi}} \frac{M_{mn}}{\sigma} \quad (13)$$

Equation (12) corresponds to digitizing the imaginary part of v_m^* to one bit while setting the real part of v_m^* to zero.

References for Appendix B

1. B. Widrow, et al., "Adaptive Antenna Systems," Proc. IEEE, Vol. 55, December 1967, pp. 2143-2159.
2. S. P. Applebaum, "Adaptive Arrays," Syracuse Univ. Res. Corp., Syracuse, N.Y., SPL-709, June 1964.
3. L. E. Brennan, E. Pugh, and I. S. Reed, "Control-Loop Noise in Adaptive Array Antennas," IEEE Trans. AES, Vol. AES-7, March 1971, pp. 254-262.
4. L. E. Brennan and I. S. Reed, "Effect of Envelope Limiting in Adaptive Array Control Loops," IEEE Trans. AES, Vol. AES-7, July 1971, pp. 698-700.
5. G. W. Lank and L. E. Brennan, "Effect of Single Bit Digitization in Adaptive Array Control Loop," IEEE Trans. AES, to be published.

APPENDIX C

MEAN STEADY STATE OUTPUT CLUTTER - APPLEBAUM ARRAY

In an adaptive filter or array, the weights are a stochastic process. Expressions for the steady state mean and covariance of the weights are derived. From these an explicit relationship for the mean steady state output clutter is calculated. An iterative solution to the mean transient output clutter is inherent in the method.

1.0 System Description

1.1 Schematic

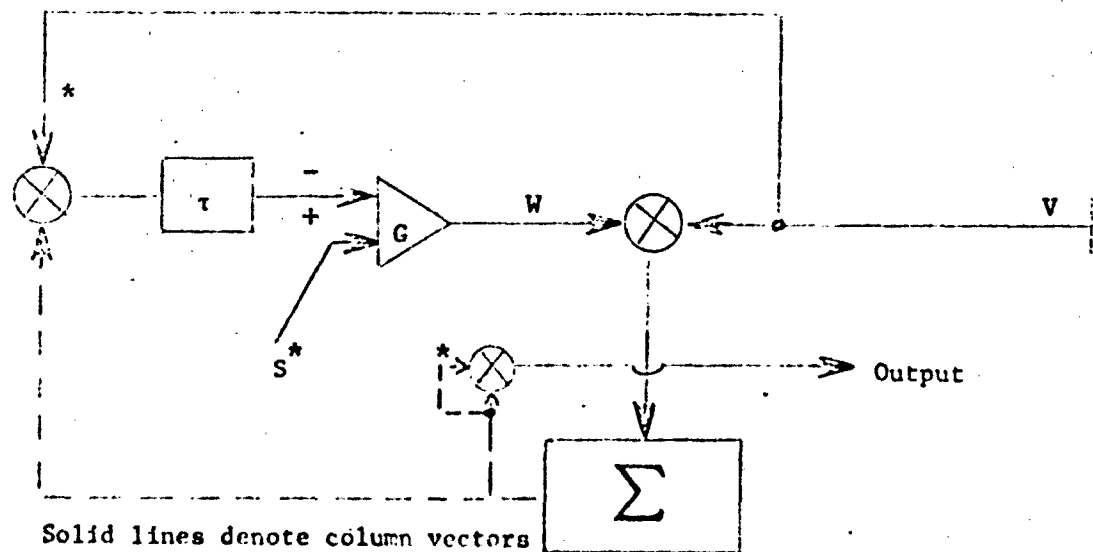


Fig. 1 - Applebaum Array (Filter)

1.2 Equations

$$\frac{\tau}{G} \dot{W} + [V^*V^T + I/G]W = S^* \quad (1)$$

V (when no signal is present) is a vector of zero mean complex Gaussian stationary random variables with covariance

$$E V^* V^T = M. \quad (2)$$

where E denotes the expectation or average.

$$\text{Output} = W^{T*} V^* V^T W \quad (3)$$

Note that $E W^{T*} V^* V^T W \neq E W^{T*} E V^* V^T E W$ unless the time constant of the integrator, τ , is chosen sufficiently large.

2.0 Difference Equation

Let Δt = time between samples of V , then (1) becomes

$$W_{t+\Delta t} = \frac{G\Delta t}{\tau} \left[S^* - (V_t^* V_t^T + I/G) W_t \right] + W_t \quad (5)$$

3.0 Steady-state mean weights

Taking the expectation of (5), noting that since W_t is determined by V_u $u < t - \Delta t$ it is statistically independent of V_t ,

$$\bar{W}_{t+\Delta t} = \frac{G\Delta t}{\tau} \left[S^* - (M+I/G)\bar{W}_t \right] + \bar{W}_t. \quad (6)$$

In the steady state $\bar{W}_{t+\Delta t} = \bar{W}_t = \bar{W}$ hence

$$(M + I/G)\bar{W} = S^*$$

$$\boxed{\bar{W} = (M+I/G)^{-1} S^*} \quad \text{For convergence:} \quad \frac{G\Delta t}{2\tau} (\lambda_i + I/G) < 1. \quad (7)$$

4.0 Output Clutter related to weight statistics

From (3) Output = $W^{T*} V^* V^T W$

$$= \sum_{i,j} W_{i1}^* V_{i1}^* V_{j1} W_{j1} = \sum_{i,j} V_{i1}^* V_{j1} W_{j1} W_{i1}^* \quad (8)$$

Thus

$$E \text{ output} = \sum_{i,j} M_{ij} Z_{ji} \quad (9)$$

where

$$Z = E W W^{T*}. \quad (10)$$

hence

$$\boxed{E \text{ output} = \text{Trace} (MZ) = \text{Trace}[E V^* V^T E W W^{T*}]} \quad (11)$$

Now let P be the diagonalizing rotation for the positive definite matrix M, i.e.

$$P M P^{-1} = \Lambda \quad (12)$$

The trace is invariant to rotations hence

$$E(\text{Output}) = \text{Trace}(P M P^{-1} P Z P^{-1}) = \text{Trace}(\Lambda P Z P^{-1}) \quad (13)$$

5.0 Steady state output

From (5)

$$\begin{aligned} W_{t+\Delta t} W_{t+\Delta t}^{*} &= \frac{G\Delta t}{\tau} \left\{ \frac{G\Delta t}{\tau} \left[S^* S^T + (V^* V^T + I/G) W_t W_t^{*T} (V^* V^T + I/G) \right. \right. \\ &\quad \left. \left. - S^* W_t^{*T} (V^* V^T + I/G) - (V^* V^T + I/G) W_t S^T \right] \right. \\ &\quad \left. + S^* W_t^{*T} - (V^* V^T + I/G) W_t W_t^{*T} \right. \\ &\quad \left. + W_t S^T - W_t W_t^{*T} (V^* V^T + I/G) \right\} + W_t W_t^{*T} \quad (14) \end{aligned}$$

Taking expectations, again noting that W_t is independent of V_t , and using the relationship (see Section 7 of this appendix)

$$\begin{aligned} EV^* V^T W_t W_t^{*T} V^* V^T &= M Z_t M + M \text{Trace}(Z_t M) \\ Z_{t+\Delta t} &= EW_{t+\Delta t} W_{t+\Delta t}^{*T} = \frac{G\Delta t}{\tau} \left\{ \frac{G\Delta t}{\tau} \left[S^* S^T + M Z_t M + M \text{Trace}(Z_t M) + Z_t / G^2 \right. \right. \\ &\quad \left. \left. + Z_t M / G + M Z_t / G \right. \right. \\ &\quad \left. \left. - S^* \bar{W}_t^{*T} (M + I/G) - (M + I/G) \bar{W}_t S^T \right] \right. \\ &\quad \left. + S^* \bar{W}_t^{*T} - (M + I/G) Z_t + \bar{W}_t S^T - Z_t (M + I/G) \right\} \quad (15) \\ &\quad + Z_t \end{aligned}$$

In the steady state $Z_{t+\Delta t} = Z_t$ and \bar{W}_t is given by (7). Hence

$$\begin{aligned} \frac{G\Delta t}{\tau} \left[S^* S^T + MZM + M \text{Trace}(ZM) + Z/G^2 + ZM/G + MZ/G \right. \\ \left. - S^* S^T - S^* S^T \right] \\ + S^* S^T (M+I/G)^{-1} + (M+I/G)^{-1} S^* S^T \\ - (M+I/G)Z - Z(M+I/G) = 0 \end{aligned} \quad (16)$$

Next diagonalize as in (12) and (13). Let $z = PZP^{-1}$

$$s^* = PS^* \quad (17)$$

Equation 16 has the following form after transformation

$$\begin{aligned} \frac{G\Delta t}{\tau} \left[\Lambda z \Lambda + z/G^2 + z\Lambda/G + \Lambda z/G \right] - (\Lambda+I/G)z - z(\Lambda+I/G) \\ = \frac{G\Delta t}{\tau} \left[s^* s^T - \Lambda \text{Trace}(\Lambda z) \right] - s^* s^T (\Lambda+I/G)^{-1} - (\Lambda+I/G)^{-1} s^* s^T \end{aligned} \quad (18)$$

Taking the i,i component of this matrix equation we obtain

$$z_{ii} = s_{i1}^* s_{i1} / (\lambda_i + 1/G)^2 + \frac{\frac{G\Delta t}{2\tau} \text{Trace}(\Lambda z) \lambda_i / (\lambda_i + 1/G)}{1 - \frac{G\Delta t}{2\tau} (\lambda_i + 1/G)} \quad (19)$$

$$\text{Trace}(\Lambda z) = \sum_i \lambda_i z_{ii} = \sum_i \frac{\lambda_i^* s_i s_i}{(\lambda_i + 1/G)^2} + \frac{G\Delta t}{2\tau} \text{Trace}(\Lambda z) \frac{\lambda_i^2 / (\lambda_i + 1/G)}{1 - \frac{G\Delta t}{2\tau} (\lambda_i + 1/G)} \quad (20)$$

$$E \text{ Output} = \text{Trace}(\Lambda z) = \sum_i \frac{\lambda_i^* s_i s_i}{(\lambda_i + 1/G)^2} \left/ 1 - \sum_i \frac{\lambda_i^2 / (\lambda_i + 1/G)}{\frac{2\tau}{G\Delta t} - (\lambda_i + 1/G)} \right. \quad (21)$$

It is easily shown that

$$\sum_i \frac{\lambda_i^* s_i s_i}{(\lambda_i + 1/G)^2} = \bar{W}^T M \bar{W} \quad (22)$$

Hence

$$E(\text{Output}) = \bar{W}^T M \bar{W} \left/ 1 - \sum_i \frac{\lambda_i^2 / (\lambda_i + 1/G)}{\frac{2\tau}{G\Delta t} - (\lambda_i + 1/G)} \right. \quad (23)$$

6.0 Relationship to previous result

Suppose $\frac{G\Delta t}{2\tau} \sum_i \lambda_i \ll 1$ and $G \gg \frac{1}{\lambda_{\min}}$

Then Equation 23 becomes

$$\begin{aligned} E(\text{output}) &= \bar{W}^T M \bar{W} \left/ \left(1 - \frac{G\Delta t}{2\tau} \sum_i \frac{\lambda_i}{1 - \frac{G\Delta t}{2\tau} \lambda_i} \right) \right. \\ &= \bar{W}^T M \bar{W} \left(1 + \frac{G\Delta t}{2\tau} \sum_i \lambda_i \right) \end{aligned} \quad (24)$$

which is the result obtained in Reference 1.

7.0 Derivation of $E V^* V^T W W^{T*} V^* V^T$

The following expression was used in Equation 15.

$$A_{ij} = E \sum_{m,k} V_i^* V_m W_m W_k^* V_k^* V_j$$

$$A_{ij} = \sum_{m,k} E V_i^* V_m V_k^* V_j E W_m W_k^* \quad \text{since } V \text{ and } W \text{ are independent.}$$

$$\text{Using Reference [2]} \quad E V_i^* V_m V_k^* V_j = E V_i^* V_m E V_k^* V_j + E V_i^* V_j E V_m V_k^*.$$

Thus

$$A_{ij} = \sum_{m,k} M_{im} M_{kj} Z_{mk} + \sum_{m,k} M_{ij} M_{km} Z_{mk}$$

$$= (M Z M)_{ij} + M_{ij} \text{Trace } M Z$$

or

$$A = M Z M + M \text{Trace } (Z M) \quad (25)$$

References for Appendix C

- [1] Brennan, Pugh, Reed/"Control Loop Noise in Adaptive Array Antennas"/
IEEE Transactions, AES, March 1971.
- [2] I. S. Reed/"On a Moment Theorem for Complex Gaussian Processes"/
IEEE Transactions IT-8, April 1962.

UNCLASSIFIED

Security Classification

DOCUMENT CONTROL DATA - R & D

Security classification of title, body of abstract and indexing annotation must be entered when the overall report is classified

1. ORIGINATING ACTIVITY (Corporate author) Technology Service Corporation 225 Santa Monica Boulevard Santa Monica, California 90401		2a. REPORT SECURITY CLASSIFICATION UNCLASSIFIED	
3. REPORT TITLE "ADAPTIVE FILTERING IN ANTI RADAR"		2b. GROUP	
4. DESCRIPTIVE NOTES (Type of report and inclusive dates) FINAL		DISTRIBUTION LIMITED TO U.S. GOVERNMENT AGENCIES ONLY; <input type="checkbox"/> FOREIGN INFORMATION <input type="checkbox"/> PROPRIETARY INFORMATION <input checked="" type="checkbox"/> TEST AND EVALUATION <input type="checkbox"/> CONTINUOUS PERFORMANCE EVALUATION	
5. AUTHOR(S) (First name, middle initial, last name) Ivan P. Bettlik, Lawrence E. Brennan, Gerald W. Lank		DATE: 11-7-72 OTHER REQUESTS FOR THIS DOCUMENT MUST BE REFERRED TO COMMANDER, NAVAL AIR SYSTEMS COMMAND, AIR-50174	
6. REPORT DATE 29 September 1972		7a. TOTAL NO. OF PAGES	7b. NO. OF REFS 8
8. CONTRACT OR GRANT NO. N00019-72-C-0164		9a. ORIGINATOR'S REPORT NUMBER(S) TSC-PD-083-2	
b. PROJECT NO.		9b. OTHER REPORT NO(S) (Any other numbers that may be assigned this report)	
c.		d.	
9. DISTRIBUTION STATEMENT			
11. SUPPLEMENTARY NOTES		12. SPONSORING MILITARY ACTIVITY Naval Air Systems Command Washington, D.C. 20360	

13. ABSTRACT

Adaptive filtering is a technique for optimizing the doppler filter response in an MTI (moving target indication) radar. In airborne MTI radars, the clutter spectrum is continually changing and varies with scan angle, antenna pattern, and angular distribution of the clutter intensity. Rain backscatter, if present, has a doppler spectrum which depends on local wind velocity and wind shear. An adaptive filter senses each of these effects and adaptively controls the filter weights to maximize the signal-to-clutter ratio in the filter output. Curves are presented in this report which illustrate the performance of adaptive filters in ANTI radar. The steady-state and transient response of adaptive filters, and performance in rain, are included. Methods of simplifying adaptive filter control loops are discussed.

FORM 1473

UNCLASSIFIED
Security Classification

Summary of Conclusions

AMTI (airborne moving target indication)

Security Classification

END

DATE
FILMED

11-72